Application of Electrospray Ionization Mass Spectrometry to Study Protein-Ligand Interactions and Enzyme Kinetics

by

Reza Rezaei Darestani

A thesis submitted in partial fulfillment of the requirements for the degree of

Master of Science

Department of Chemistry

University of Alberta

Abstract

This thesis describes the development and application of electrospray ionization mass spectrometry (ESI-MS) to study the noncovalent protein-ligand interactions and also investigate the kinetic of enzymatic reactions.

The rate of glycolipids cleavage by the human neuraminidase 3 (hNEU3) was studied using time-resolved ESI-MS assay. The ESI-MS method was validated by comparing the relative hydrolysis rates of soluble glycolipids obtained from ESI-MS aasay with fluorescence-based assay. The kinetic analysis revealed that picodiscs present a better presentation of glycolipids for enzymatic studies.

A catch-and-released electrospray ionization mass spectrometry (CaR-ESI-MS) assay was employed to screen a series of anti-cancer drugs against target protein. The bound ligands were then identified and relatively quantified using collision-induced dissociation (CID). The assay was capable of observing specific interactions between anti-cancer drugs and protein of interest.

Preface

Part of chapter 2, related to enzymatic studies of glycolipids incorporated in picodiscs and nanodiscs, was published recently: Leney, A. C., Rezaei Darestan, R., Li, J., Nikjah, N., Kitova, E. N., Zou, C., Cairo, C. W., Xiong, Z. J., Privé, G. G., Klassen, J. S. *Analytical Chemistry* DOI: 10.1021/acs.analchem.5b00170, April 9, 2015.

In this paper, my supervisor, Dr. Klassen, J. S., and Leney, A. C. designed the project and wrote the paper with input from Cairo, C. W. and Privé, G. G. I performed and analyzed all the enzyme kinetic measurements on picodiscs and nanodiscs using ESI-MS assay. Xiong, Z. J. prepared the SapA protein and Zou, C. prepared hNEU3 sample. Leney, A. C. made the picodiscs with assistance from Li, J. who prepared the nanodiscs. Leney, A. C. also perfomed all MS experiments on protein-glycolipid interactions. Nikjah, S. determined the anti-GD2 antibody-soluble GD2 ligand binding affinity. Kitova, E. N. assisted with MS experiments. Privé, G. G. provided helful advice on SapA disc preparation.

A version of Chapter 3 is being prepared for submission for publication as Rezaei Darestani, R., Winter, P., Kitova, E. N., Tuszynski, J. A., and Klassen, J. S., entitled "Screening Anti-Cancer Drugs against Tubulin using Catch-and-Release Electrospray Mass Spectrometry". My supervisor, Dr. Klassen, conceived the idea of using the CaR-ESI-MS assay in screening the colchicine analogs against tubulin. I performed all the MS experiments including proof-of-concepts experiments and screened the library of colchicinoids against target protein. Our

collaborators, Winter, P. and Tuszynski, J. A., provided the tubulin and all the analogs for this works. The paper was written by Klassen. J. S. and me with input from Winter, P., Kitova, E. N., Tuszynski, J. A.

Table of Contents

List of Figures

List of Tables

List of Abbreviations

4MU-NA	2´-(4-methylumbelliferyl)-α-D-N-acetylneuraminic acid
Ab	Abundance of gas phase ions
CaR	Catch-and-release
CEM	Chain ejection model
CID	Collision induced dissociation
CRM	Charge residue model
Da	Dalton
DC	Direct current
DESI	Desorption electrospray ionization
DTIMS	Drift time ion mobility spectrometry
ECD	Electron capture dissociation
ELISA	Enzyme-linked immunosorbent assay
ESI	Electrospray ionization
ESI-MS	Electrospray ionization mass spectrometry
FPLC	Fast performance liquid chromatography
Gal	Galactose
GalNAc	N-acetyl galactosamine
GSL	Glycosphingolipid
Glc	Glucose
GlcNAc	N-acetyl glucosamine
H	Hydrogen

H-bound	Hydrogen bound
HPLC	High performance liquid chromatography
IEM	Ion ejection model
IMS	Ion mobility separation
IS	Internal standard
ITC	Isothermal titration calorimetry
K_a	Association constant
K_d	Dissociation constant
K_{eq}	Equilibrium constant
K_m	Michaelis constant
k_{rel}	Relative reaction rate
L	Ligand
LC	Liquid chromatography
m/z	Mass-to-charge ratio
MS	Mass spectrometry
MSP	Membrane scaffold protein
MW	Molecular weight
MWCO	Molecular weight cutoff
nanoESI	Nanoflow electrospray ionization
N	Nitrogen
ND	Nanodisc
Neu5Ac	N-acetyl neuraminidase
NMR	Nuclear magnetic resonance

NEU	Neuraminidase
hNEU3	Human neuraminidase 3
PD	Picodisc
PL	Protein-ligand complex
POPC	1-palmitoyl-2-oleoyl-sn-glycero-3-phosphocholine
P_{ref}	Reference protein
R	Abundance ratio
RF	Response factor
RF	Radiofrequency
SA	Sialic acid
SPR	Surface plasmon resonance spectroscopy
TLC	Thin layer chromatography
TOF	Time-of-flight
T-wave	Travelling wave
TWIMS	Travelling wave ion mobility separartion
V_{max}	Maximum rate at saturating substrate concentration
V_0	Initial reaction rate
µL	Microliter
µM	Micromolar
mM	Milimolar

Chapter 1

Study of Non-Covalent Protein-Ligand Complexes by Electrospray Ionization Mass Spectrometry

1.1 Introduction

Protein-ligand interactions play significant roles in many important biological processes, including the immune response, cell signaling, intracellular communications, and for therapeutic intervention in drug discovery.[1-5] To identify and quantify the interactions of non-covalent biological complexes, a number of analytical techniques have been used, each with particular strengths and weaknesses. Isothermal titration calorimetry (ITC), surface plasmon resonance (SPR) spectroscopy, enzyme-linked immunosorbent assays (ELISA), and nuclear magnetic resonance (NMR) spectroscopy are among the most widely used methods for measuring the association constants (K_a).

ITC is generally considered as the "gold standard" technique for quantifying the binding thermochemistry in solution. This technique is also the only assay that directly provides a measurement of the change in enthalpy (ΔH) associated with the formation of a complex.[6-8] One of the major issues associated with conventional ITC is that usually requires large amounts (~mg) of pure protein and ligand for each analysis. However, new ITC technologies, such as nano-ITC, have improved sensitivity and require lower sample amounts.[9]

Surface plasmon resonance (SPR) spectroscopy represents another widely used method for evaluating both the association and dissociation rate constants[10, 11] and the affinities[12-14] of protein-ligand interactions. SPR affords high sensitivity, and requires a very small amount of sample (~ng). A potential limitation of SPR is the immobilization of one binding partner (usually the ligand) on a sensor chip while the other binding partner is flowed over the sensor surface. The immobilization may affect the nature of the binding interaction. Indeed, there are examples where the ITC and SPR yield divergent binding data for the same protein-ligand interaction.[15]

Enzyme linked immunosorbent assay (ELISA) is an extensively used tool for quantifying protein-ligand interactions with fairly high sensitivity and good reproducibility.[16] While there are several different ways of implementing ELISA, the typical setup involves the immobilization of ligands to the surface of microplate, which are then incubated with solutions containing the protein. The protein is often linked to an enzyme, and in the final step the enzyme's substrate is added. This process produces a detectable signal that can be properly quantified. However, the relatively large immobilization surface area can lead to nonspecific binding and increase background. Moreover, ELISA relies upon enzyme-mediated amplification of signal to achieve reasonable sensitivity, which can limit its application.

Nuclear magnetic resonance (NMR) spectroscopy is another solution based method for characterizing the structure of biological molecules and complexes, and for quantifying the strength of the interactions.[17-20] In particular, transferred

NOSY NMR assay could estimate the dissociation kinetics of proteins with small molecules.[21] The saturation transfer difference (STD)-NMR has been employed to study protein-carbohydrate interactions for library screening.[22-25] However, NMR is unable to study the binding of large proteins (larger than 40 kDa), in addition to requiring large amounts of sample (typically ~mg) and being a time consuming assay.

X-ray crystallography, as a most widely used technique, represents three dimensional structure information of protein-ligand complex.[26-28] However, crystallization of all biomolecules and their complexes is not feasible, which brought a limitation for X-ray crystallography. Moreover, the obtained results from this method are not able to provide direct measurement of the non-covalent interactions.[29]

Spectroscopic approaches (e.g. dichroism or fluorescence-based methods) are commonly used to characterize the interactions of macromolecular complexes with high sensitivity.[30-33] However, the methods require a chromophore or fluorophore, which change the nature of the reactions being investigated and influence the binding of protein-ligand in some cases.[34]

Recently, electrospray ionization mass spectrometry (ESI-MS) has emerged as a promising tool for identifying and quantifying noncovalent protein-ligand interactions in solution.[35-39] The ESI-MS measurements can be categorized as either “direct” or “indirect” in nature. The direct ESI-MS assay, which is the focus of this thesis, is based on the detection of free and bound protein or ligand ions by ESI-MS leading to the determination of the association constant (K_a) from

the abundance ratio of the bound and unbound protein ions. While indirect ESI-MS utilize biochemical and chromatographic methods for preparation of the desired components and ESI-MS as a detector. Compared with other techniques, the ESI-MS assay benefits from a number of advantages such as speed (1–2 min/measurement), sensitivity (~10 pmol for nanoflow ESI-MS), simplicity (immobilization and label free), and specificity (ability of measuring binding stoichiometry and multiple binding equilibriums directly). Besides its wide applications on quantifying noncovalent interactions, ESI-MS has been used to measure the kinetics of chemical and biochemical reactions.[38, 40-54] A detail description of the implementation of ESI-MS assay along with some of the limitations will be discussed more in section 1.2 and 1.3.

1.1.1 Enzyme kinetics

In addition to recognition role of proteins for specific ligands mentioned above, in some cases proteins act as enzymes to do a change in a particular ligand named substrate. The enzymatic reactions play a crucial role not only in the regulation of all processes of life,[55] but also their roles as biocatalysts in industrial processes or as targets in drug discovery are becoming increasingly important.[55] Therefore, it is necessary to establish rapid and sensitive methods for enzymatic studies. In the enzymatic reactions, the kinetic of reaction is measured by monitoring the formation of enzymatic products or the depletion of substrates. The enzyme kinetics can be affected by few factors, such as temperature, pH, the interaction between enzyme and substrate as well as the presence of inhibitors. Spectroscopic

and radiochemical assays are widely used to measure the enzyme kinetics.[56, 57] In spectroscopic assays, a synthetic substrate with a chromophore is used to measure enzymatic activity. The rate of the enzymatic reactions is monitored by measuring the change in emission (in fluorometric assay) or absorption (in spectrophotometric assay) of light. In radiochemical assay, a radiolabeled substrate is used to monitor the change in radiation intensities which is related to product formation. Although these assays are well established and widely employed, there are several limitations. The critical drawback in both spectroscopic and radiochemical assays is that these assays depend on chromogenic and radioactive substrates. These chromogenic substrates have their own limitations due to preparation which needs labor-intensive, multistep synthesis. Moreover, the modification by chromogenic agents can alter enzyme kinetics in a spectroscopic assay.[58] A radioactive-labeled substrate is more preferred due to the fact that it possesses similar recognition properties to an original substrate, and they usually exhibit identical enzymatic kinetics. However, the use of radioisotopes has a number of disadvantages, including the requirement of expensive radiolabeled ligands and associated issues related to handling, disposal and detection.

Recently, ESI-MS has been employed as a label-free, non-radioactive assay to study enzymatic reactions.[59-65] The ESI-MS is independent from the spectroscopic properties of the analyte molecules, no modification is required since the identity of reactants and products and possibly intermediates can usually be established directly from the measured *m/z*.[41, 66] Another advantage of ESI-MS

is the possibility of monitoring multiple reactions simultaneously, a feature not associated with most kinetic assays.[55] The rates of reaction can be determined by ESI-MS from one of two general strategies: on-line (real-time) monitoring of the reaction mixture, and off-line analysis, usually following a quench step that stops the reaction. The main advantage of on-line technique over the off-line is that it allows the direct analysis of the time-dependent distribution of reactants, intermediates and products. However, real-time ESI-MS kinetic measurements are restricted mostly to relatively slow reactions with timescales greater than min, due to minimum acquisition time in mass spectrometers. Interestingly, there are some examples of relatively fast kinetic measurements that could monitor the reaction time in the ms to s range.[40, 41, 43, 45, 47, 48] To do the fast kinetic measurements, the use of rapid mixing systems, such as continuous-flow,[40, 41, 43, 45] rapid quenched-flow apparatus[47] or stopped-flow,[47, 48] is necessary. The off-line approach is easier and more flexible in terms of experimental conditions compared to on-line technique.

The vast majority of enzyme studies are carried out in the steady-state regime, which yields the macroscopic Michaelis parameters k_{cat}, K_m. These parameters are useful in defining enzyme function.[67] To obtain these parameters, the formation of product needs to be monitored over time, but the rate of product formation starts to decline at longer incubations times (Figure 1.1a). The decrease in enzyme activity comes from several factors, including substrate depletion, product inhibition, pH change, and enzyme denaturation.[56, 57] However, these factors have minimal effects at the early time periods, and thus initial rates (v_0)

are used for the enzyme kinetic studies. The v_0 values can be extracted from the plot of product concentration against reaction time by drawing the initial linear portion of the curve (Figure 1.1a).

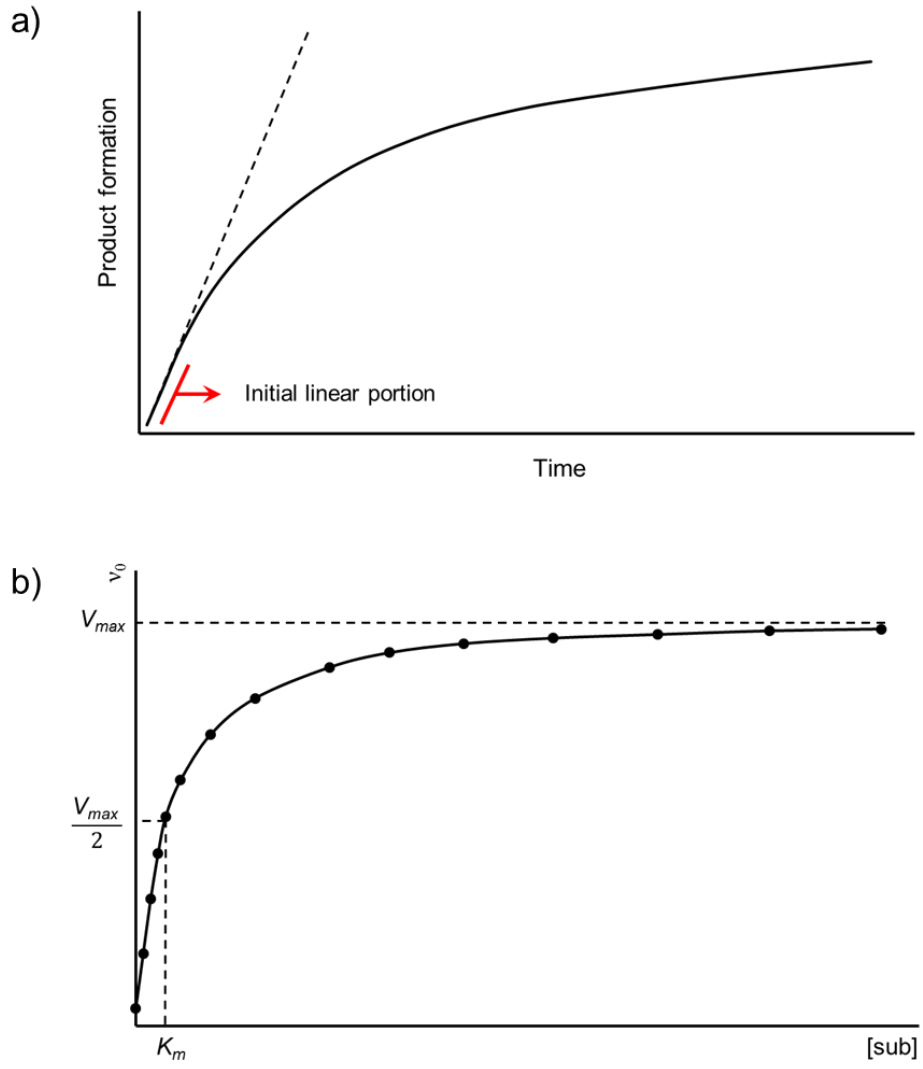

Figure 1.1. Schematic diagrams of **(a)** a representative progress curve of enzymatic reaction and **(b)** a representative Michaelis-Menten plot.

In the next step of enzyme kinetic studies, the v_0 value can be measured over a range of substrate concentration. As shown in Figure 1.1b, the plot of v_0 against substrate concentration displays saturation kinetics, due to the limited number of

active sites in enzymes, which are fully occupied by excess substrate. Reaction rate as a function of substrate concentration often follows the Michaelis-Menten equation, eq 1.1:

$$v_0 = \frac{V_{\max}[S]}{K_m + [S]} \tag{1.1}$$

where V_{max} is the maximum rate when the reaction is saturated by substrate concentration, [S] is the substrate concentration and K_m is the Michealis constant representing the concentration of substrate when v_0 is half of the V_{max} value (Figure 1.1b).

Before describing the strategies of ESI-MS assays for protein-ligand interactions and enzyme kinetics in detail, it is necessary to first review the basic principles of ESI as given below.

1.2 Electrospray ionization mass spectrometry

1.2.1 Electrospray ionization

ESI is a soft ionization technique that allows biological molecules and their non-covalent complexes to be transferred from solution to the gas phase as intact ions at the atmospheric pressure (Figure 1.2).[68] For the first time in 1991, Henion and co-workers detected a non-covalent biological complex by ESI-MS.[69] Since then, ESI-MS has been used widely to identify and quantify variety of non-covalent biological complexes, including antibody-antigen,[69] enzyme-substrate/inhibitor,[70] multiprotein,[42, 43, 71] and DNA-ligand complexes.[72, 73]

As described by Kebarle and coworkers,[74] the mechanism of ESI process involves three major steps:

a) Production of charged droplets at the ESI capillary tip.

b) Shrinkage of the charged droplets due to the solvent evaporation.

c) Production of the gas-phase ions from these droplets.

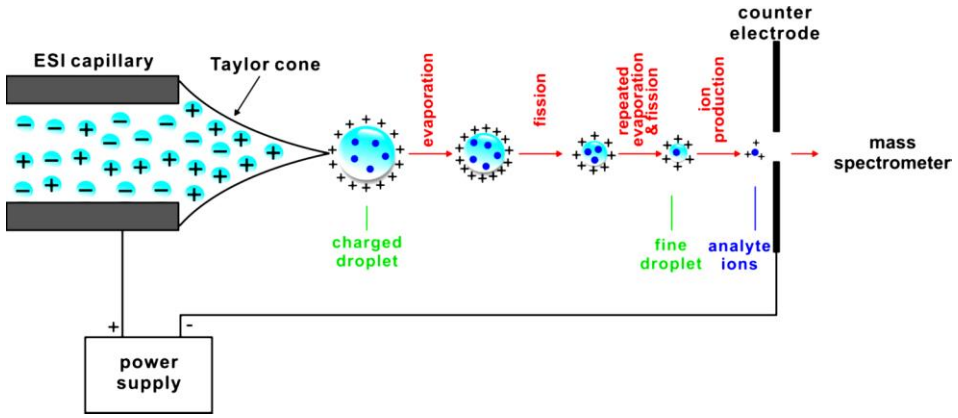

Figure 1.2. Schematic representation of ESI process operated in positive ion mode, adapted from reference 76.

As Shown in Figure 1.2, high positive voltage was applied to the capillary inducing charge separation of electrolytes in solution. As a result, the positive ions drift towards liquid surface and form a liquid cone referred to as a Taylor cone[75]– a stable liquid cone exists with competing forces between downfield forces generated by electric field and resistance by surface tension of the liquid. Under sufficiently high field, the liquid cone becomes unstable and emits a fine jet from the cone tip,[75] which breaks up into small charged droplets due to the repulsion between the charges. The initial ESI droplets usually have radii in the

micrometer range.[74] Solvent evaporation leads to droplet shrinkage at the spray needle and an increase of electric field normal to the surface of the droplet.[74] The energy required for the solvent evaporation is provided by the thermal energy of the ambient gas, air at atmospheric pressure in most cases. As the droplets get smaller, the charge density on the shrinking droplets increases until the Rayleigh limit, the point at which the Coulombic repulsion of the surface charges is equal to the surface tension of the droplets.[76] These droplets undergo Rayleigh fission, eventually forming small highly charged offspring droplets. Repeated evaporation/fission events ultimately yield the final generation of ESI droplets with radii of a few nanometers. The production of gas-phase ions from these droplets follows one of three proposed mechanisms: IEM, CRM, and CEM.[74, 77-80]

i) The ion evaporation model (IEM) was proposed by Iribarne and Thomson in 1976 (Figure 1.3a). This model assumes ion emission directly from very small and highly charged droplets. The escape of the ion to gas phase is initiated by elastic deformation of the droplet, facilitated by the repulsion between the ions and charges on the surface of droplet. This model is believed to operate for small (in)organic ions.

ii) Dole and coworkers proposed the charged residue model (CRM). This model (Figure 1.3b) assumes that the droplets undergo many fission events and finally produces very small droplets containing a single analyte molecule. CRM model also describe the formation of gas phase macromolecule ions based on the observations that the charge acquired by a macromolecule during ESI is strongly related to the size of the molecule.

Recently Gross and co-workers[81] proposed a modification of CRM in which CRM is preceded by IEM. This mechanism is expected to operate when salt additives (buffers) such as ammonium acetate or triethylacetate are present in millimolar concentrations in the solution that is electrosprayed.

iii) The chain ejection model (CEM) was introduced recently by Konermann and coworkers (Figure 1.3c).[82, 83] This model applies to unfolded proteins where the side chains of unfolded proteins are disordered. This mechanism suggests that the side chains migrate to the droplet surface to minimize solvent interactions with the hydrophobic regions. One chain terminus was then sent out into the gas phase. This process is followed by stepwise sequential ejection of the remaining protein residues. The ions produced by CEM model carry more charges compared to the ions of folded protein generated by CRM model.

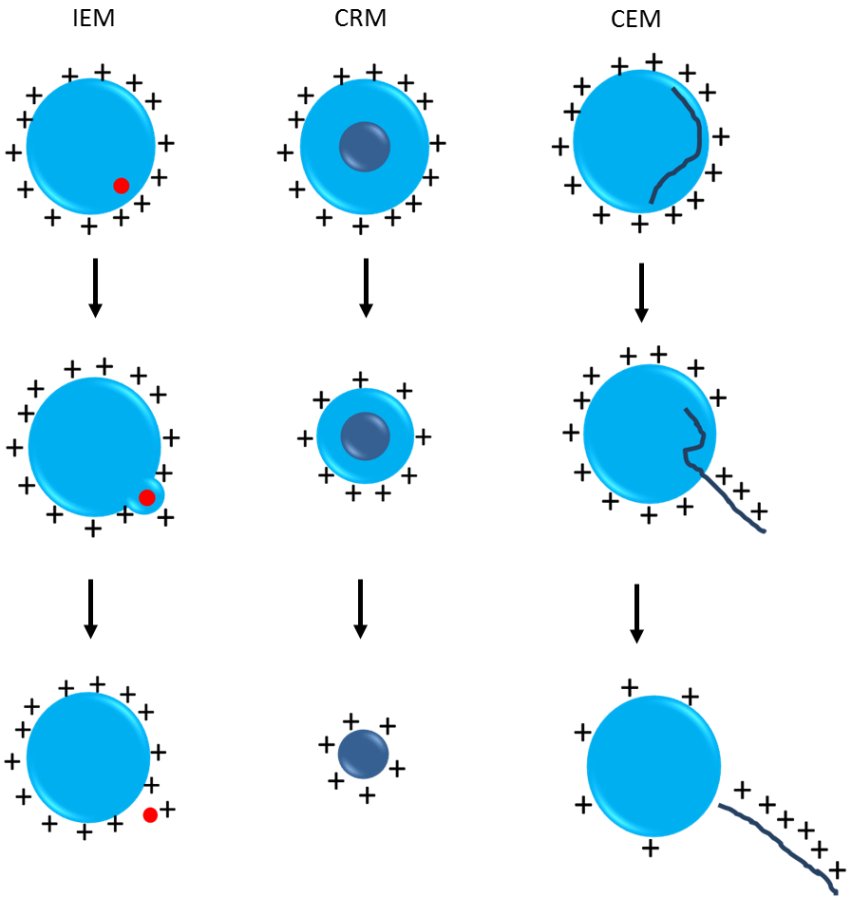

Figure 1.3. Different ESI models proposed for the formation of gas-phase ions. **(a)** IEM: small ion ejection from a highly charged nanodroplet. **(b)** CRM: Release of a folded protein into the gas-phase. **(c)** CEM: Ejection of disordered macromolecule. Figure is adapt from reference 80.

In this work, gaseous ions were produced by nanoESI whose mechanism is the same as that of ESI. The only difference comes from using a narrow glass tip in nanoESI, which operates at lower solution flow rates (10-50 nL/min) and correspondingly emits smaller droplets than conventional ESI (1-10 µL/min).[84] Smaller droplets possess the advantage of higher surface-to-volume ratio, making

a larger proportion of analyte molecules available for desorption. In addition, nanoESI readily allows the transfer of non-covalent complexes from buffered aqueous solutions to the gas phase and, therefore, can be directly performed on complex solutions that more closely resemble physiological conditions. Furthermore, nanoESI can minimize nonspecific aggregation happening during the ESI process as there are fewer analyte molecules per droplets.[85, 86] These features of nanoESI make it an appropriate method for investigating noncovalent complexes directly by MS.

1.2.2 MS instrumentation

In this work, all experiments were carried out using Synapt G2-S quadrupole-ion mobility separation-time-of-flight (Q-IMS-TOF) mass spectrometer (Waters UK Ltd., Manchester, UK), (Figure 1.4), equipped with a nanoESI source. The Waters Synapt G2-S nanoESI-quadrupole-IMS-TOF mass spectrometer was used in this study for its wide mass range, high sensitivity, and high IMS efficiency which enables differentiating samples based on size, shape, and charge, as well as mass.

Briefly, fine droplets were produced by nanoESI at atmospheric pressure from buffered aqueous solutions containing analytes. Small droplets first pass through the source sampling orifice and then enter into the mass spectrometer through a "Z-spray source", which minimizes the transfer of neutral molecules and enhances the signal-to-noise ratio. StepWave transfer optic then focuses the ions, and the resulting gaseous ions are transmitted through a quadrupole mass filter to the ion mobility section of the instrument (Triwave). The mobility

separated ions are then detected by an orthogonal acceleration TOF mass analyzer (QuanTOF^{TM}) equipped with a high field pusher and a dual-stage reflection. A brief overview of three main parts of the Synapt mass spectrometer is given below.

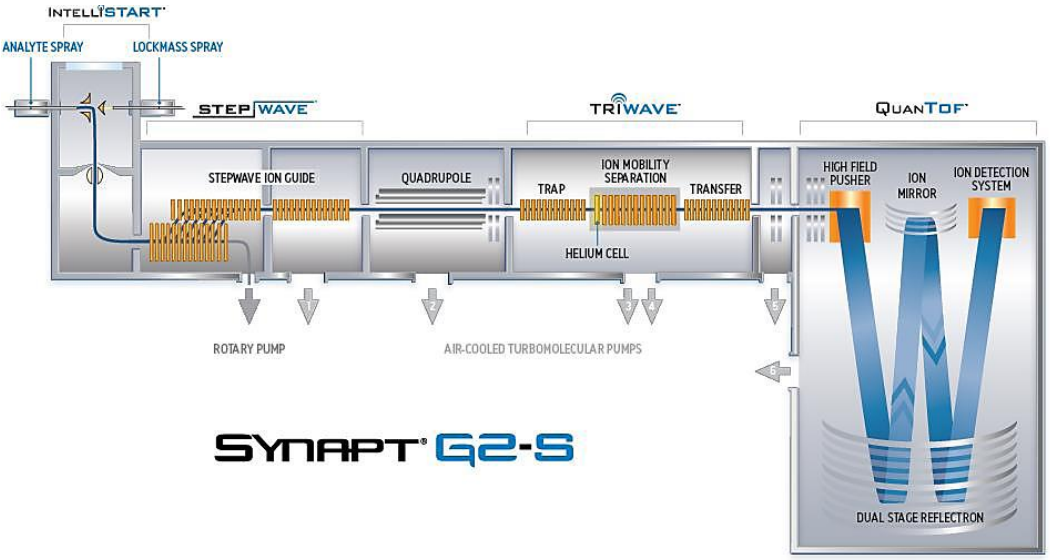

Figure 1.4. A schematic diagram of the Synapt G2-S Q-IMS-TOF mass spectrometer, adapted from Waters user's manual.

1.2.2.1 Quadrupole mass filter

The quadrupole consists of four cylindrical metal rods that are accurately positioned in a radial array and diametrically opposed rods are paired. Each of the rods carries both a direct current (DC) potential and a raiofrequency (RF) potential, with opposing rods being held at identical potentials and polarity, and adjacent rods being identical in potential, but opposite in polarity. The quadrupole

in Synapt mass spectrometer contains two parts: a quadrupole prefilter followed by a quadrupole mass filter (Figure 1.5). The prefilter raises the absolute sensitivity by minimizing the effects of fringing fields at the entrance to the quadrupole.[87]

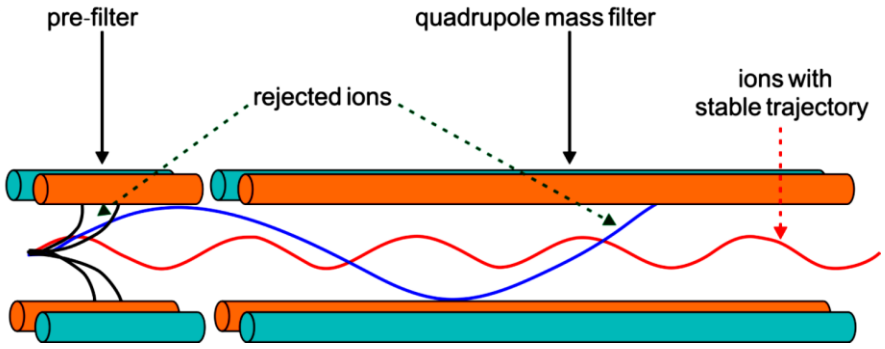

Figure 1.5. A schematic diagram of the quadrupole in the Waters Synapt G2-S mass spectrometer.

1.2.2.2 Travelling-wave ion guides

Shown in Figure 1.6a is a Triwave section of the Waters Synapt G2-S mass spectrometer. Travelling-wave technology is employed for the StepWave ion guide as well as Trap, Ion Mobility and Transfer cells of Synapt G2S mass spectrometer. These travelling-wave devices are used to guide (trap, focus, release, fragment and separate) ions. Each ion guide comprises a series of planar electrodes arranged orthogonally to the ion transmission axis,[88] as shown in Figure 1.6b. Opposite phases of a RF voltage are applied to adjacent electrodes and provide a radially confining effective potential barrier. The presence of background gas can slow down or stop the ion axial motion through the ion guide

due to the presence of axial traps generated by the ring geometry. When a DC voltage is applied to a pair of adjacent rings, a potential barrier is produced and ions within this region cannot cross. The DC voltage is subsequently applied to the next sets of electrodes downstream at regular time intervals providing a continuous sequence of "travelling waves". The ions are driven away from the potential barriers generated by the travelling waves and consequently are propelled through the device with the waves, minimizing their transit time. Ions can pass through the travelling-wave region with fast speed, which allows high data acquisition rates while the sensitivity is maintained. Additionally, the ion mobility separation can be applied in the travelling-wave region, which is explained in the next section.

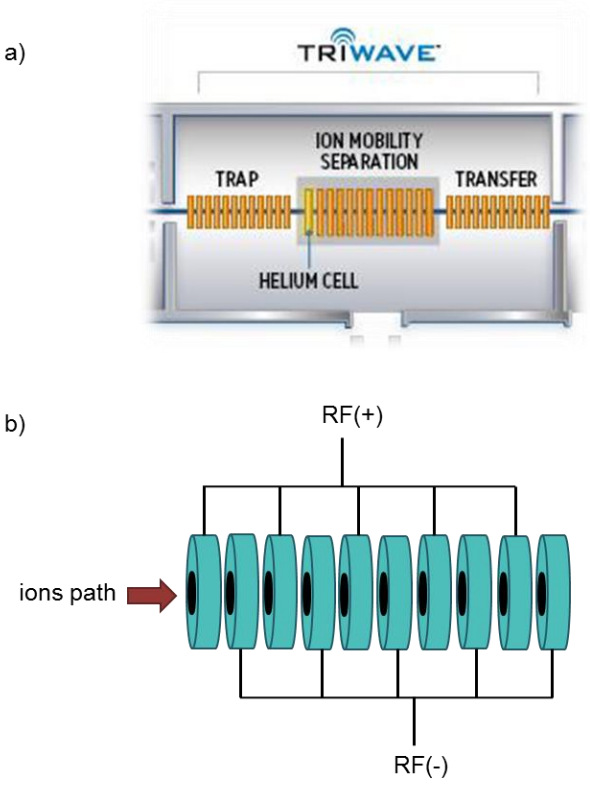

Figure 1.6. (a) A schematic diagram of the IMS section of the Synapt G2-S, containing three travelling wave ion guides labelled as trap, ion mobility separation, and transfer. **(b)** A stacked ring ion guide.

1.2.2.3 Ion mobility separation

IMS is a gas phase electrophoretic technique for studying shape and conformation in protein and protein complexes. IMS separates ions on the basis of their mass, charge and collision cross section (i.e., size and shape).[89-91] Briefly, a pulse of ions is injected into a drift region with a combination of an electric field that moves the ions towards the drift region and a buffer gas, which is a known inert gas. Under the influence of a static electric field, ions experience electrostatic force pulling them through the region; this force is countered by a number of collisions between ions and the buffer gas that impede its progress towards the detector. Therefore, large ions with greater collision cross sections experience more collisions than smaller ions and thereby require longer time to migrate through the drift cell. The distinct velocity of ions depends on the electric field strength and the mobility of an ion (K), which is determined by eq 1.2:[89]

$$K = \frac{d}{t_d \cdot E} \qquad (1.2)$$

where td is the time for an ion traversing the drift cell (i.e., arrival time) of length d; E is the electric field gradient.

There are several types of ion mobility instrumentation that are currently used with mass spectrometry, drift-time ion mobility spectrometry (DTIMS),[92]

differential-mobility spectrometry (DMS), which is also called field-asymmetric waveform ion mobility spectrometry (FAIMS),[93] trapped ion mobility spectrometry (TIMS) and traveling-wave ion mobility spectrometry (TWIMS).[94-96] The detail of TWIMS, which is used in this thesis, is outlined briefly below.

In Synapt G2S mass spectrometer, IMS cell is filled with nitrogen gas and a high electric field is applied to one segment of IMS cell. Ion migration starts in pulses through the mobility cell and ions separates based on their mobilities. Ions with high mobility are able to "surf" the waves and are transported through the IMS cell more quickly while lower-mobility ions slip behind the waves more often and travel more slowly. A particular advantage of the TWIMS device over most drift tubes is that through the use of ion accumulation and radial ion confinement, the sensitivity of the mass spectrometer is not compromised when operating in mobility mode.[88, 96]

1.2.2.4 Time of Flight (TOF)

TOF mass analyzers measure the flight time that take for ions to move through a field-free region (flight tube) between the source and the detector.[88] Mass-to-charge (m/z) values are determined by measuring that travelling time according to eq 1.3:

$$m/z = t^2 \frac{2eV_s}{L^2} \qquad (1.3)$$

where m is the mass of the ion, z is the charge state of the ion, e is the elementary charge, *Vs* is the acceleration potential, t is the flight time and L is the length of

the flight tube. This equation shows that *m/z* can be calculated from a measurement of t. From this equation, ions with smaller *m/z* will move faster and reach the detector earlier.

There are two types of TOF analyzers: linear TOF analyzer and reflectron TOF analyzer. The weakness of linear TOF analyzer is that due to initial energy distribution, ions of the same *m/z* may reach the detector at different times that could result in peak broadening and poor resolution. In Waters Synapt G2-S mass spectrometer, a reflectron TOF analyzer is used to improve the resolution. Coupling TOF mass analyzer with ESI requires the use of orthogonal acceleration technique. Continuous ions from the ionization source are parceled into packets and filled in the orthogonal accelerator. The pusher is then introduces ions into the orthogonally situated flight tube. The reflectron TOF analyzer compensates the energy distribution of ions by using successive sets of electric grids of increasing potential which deflects the ions and reverses their flight direction sending them back through the flight tube. While ions are travelling in the flight tube, the orthogonal accelerator is refilled with new packet of ions. Depending on their kinetic energy, ions of the same *m/z* will penetrate the field at different depths; ions with more kinetic energy and hence with faster velocity will penetrate the field more deeply than ions with lower kinetic energy. Consequently, the fast and slow ions are focused at the detector and the energy distribution of the ions is compensated. Of particular note, Waters Synapt G2S instrument can be operated under either single stage reflectron mode ("V mode") or dual stage reflectron

mode ("W mode"). The net effect is improved mass resolution typically in the range of 10,000 – 20,000 with minimal losses in sensitivity.

After introducing the review of the basic principles and instrumentations of ESI-MS, a more detailed introduction of ESI-MS binding assays for studying noncovalent protein-ligand interactions is given in the following section.

1.3 MS-based methods for quantifying interactions of non-covalent complexes

1.3.1 *Direct* ESI-MS assay

The focus of *direct* ESI-MS binding assay is on the direct detection of free and ligand-bound protein ions by ESI-MS. For a solution containing protein P, and ligand L, the equilibrium (association) constant (K_a) is expressed using eq 1.5:

$$P + L \rightleftharpoons PL \tag{1.4}$$

$$K_a = \frac{[PL]_{eq}}{[P]_{eq}\,[L]_{eq}} \tag{1.5}$$

where [PL], [P] and [L] are the equilibrium concentrations of protein-ligand complex, free protein and ligand in solution, respectively. These equilibrium concentrations can be calculated from the initial concentrations of P and L in solution, $[P]_0$ and $[L]_0$ and the concentration ratio of PL and P at equilibrium (eq 1.6-1.8). It is assumed that the ratio (*R*) of the total abundance (*Ab*) of PL and P ions are equal to the ratio of concentrations of PL and P in the solution at equilibrium.[97]

$$\frac{[PL]_{eq}}{[P]_{eq}} = \frac{\sum Ab(PL)}{\sum Ab(P)} = R \qquad (1.6)$$

$$[P]_0 = [P]_{eq} + [PL]_{eq} \qquad (1.7a)$$

$$[L]_0 = [L]_{eq} + [PL]_{eq} \qquad (1.7b)$$

$$[PL]_{eq} = \frac{R\,[P]_0}{1+R} \qquad (1.8)$$

Then K_a value for the 1:1 protein-ligand complex is determined from the ratio R, $[P]_0$ and $[L]_0$ eq 1.9:

$$K_a = \frac{R}{[L]_0 - \frac{R}{1+R}[P]_0} \qquad (1.9)$$

Normally, the affinity measurements are performed at a number of different concentrations or from a titration experiment, wherein $[L]_0$ is fixed but $[P]_0$ is varied. In this case, K_a can be measured using a nonlinear regression analysis of the experimentally determined concentrations using an internal standard:[98]

$$[L] = \frac{K_a[L]_0 - K_a[P]_0 - 1 + \sqrt{(1+K_a[P]_0 - K_a[L]_0)^2 + 4K_a[L]_0}}{2K_a} \qquad (1.10)$$

1.3.2 Catch-and-release (CaR)-ESI-MS assay

The CaR-ESI-MS approach holds tremendous promise for screening libraries of ligands against target proteins to rapidly identify and quantify specific interactions.[99-101] This assay has a number of attractive features, including its simplicity, speed, low sample consumption, and unique ability to directly probe

binding stoichiometry and affinity. The assay involves direct ESI-MS analysis of the target protein(s) in the presence of a mixture of ligands to detect specific protein−ligand complexes. In many instances, the identity of ligands ("caught" by the protein) can be found from the molecular weight (MW) of the corresponding protein−ligand complex, as determined from the ESI mass spectrum. In cases where MW cannot be accurately determined (due to the size or heterogeneity of the protein), the ligands are "released" as ions from the protein using collision-induced dissociation (CID), followed by accurate mass analysis alone or in combination with ion mobility separation (IMS) or another stage of CID.

Of the known ion activation and dissociation techniques, only collision-induced dissociation (CID), which is the most common ion activation method, is used for the purpose of this study.

In Synapt G2-S, CID can be performed in the Trap and Transfer regions by applying a DC voltage (collision energy) to the selected ions of interest. The Trap and/or Transfer cells are also filled with neutral background gases (e.g. Argon). During the collision if sufficient internal energy is accumulated, a portion of the ion's kinetic energy is converted into internal energy, resulting in the subsequent fragmentation. The internal energy of ions can be increased by several factors, such as increasing the number of collisions between ions and gas and increasing time of collision in the cell. CID is a "slow-heating" process, where energy randomization is faster than the decomposition. Therefore, the energy will be distributed among all the internal modes of ion, which allows preferential decomposition at the weakest sites.[102] This feature makes CID a useful technique

to investigate gas phase dissociation of non-covalent protein complexes, since non-covalent interactions are usually broken prior to covalent bond cleavage. In the present work, MS combined with CID was used to identify the bound ligand and deliver compositional information of the protein-ligand complex based on the dissociation products and dissociation pathways upon collision. Examples of CID applied for studying protein-ligand bindings can be found in Chapter 2 and 3 of this thesis.

1.3.3 Potential pitfalls

In the ESI-MS binding measurements, free and ligand-bound proteins are transferred to the gas phase from the solution by ESI. Therefore, physical or chemical processes during ESI and in the gas phase that alter the ratio (*R*) will lead to incorrect K_a values. Four common sources of error associated with the ESI-MS measurements are: (i) non-uniform response factors, (ii) in-source dissociation, and (iii) nonspecific ligand–protein binding. Each of these problems and the available strategies to minimizing their effects are discussed below.

1.3.3.1 Non-uniform response factors

In ESI-MS binding assay, the abundances of each species is related to the solution concentrations by their response factors (*RF*), which account for the ionization and detection efficiencies, as defined in eq 1.11:

$$\frac{[\mathrm{PL}]_{\mathrm{eq}}}{[\mathrm{P}]_{\mathrm{eq}}} = \frac{Ab(\mathrm{PL}) / RF_{\mathrm{PL}}}{Ab(\mathrm{P}) / RF_{\mathrm{P}}} = RF_{\mathrm{P/PL}} \frac{Ab(\mathrm{PL})}{Ab(\mathrm{P})} \qquad (1.11)$$

where RF_P and RF_{PL} are the response factors for P and PL, respectively, and $RF_{P/PL}$ is the relative response factor. Generally, *RF* reflects the ionization and detection efficiencies of each protein species, which depends on the size, structure and surface properties of protein and protein-ligand complex, as well as solution conditions and the instrumental parameters used for the measurements. An essential assumption in the eq 1.11 is that the *RF* values for P and PL ions are equal ($RF \sim 1$). This could be a valid assumption when L is small compared to P and therefore, the size and surface properties of P and PL are similar.

1.3.3.2 In-source dissociation

Gaseous protein-ligand complex ions may undergo collision-induced dissociation and alter the relative abundance of PL and P ions.[37] This change will necessarily reduce the magnitude of K_a for a 1:1 P–L complex. In the extreme case, where no PL ions survive to detection, in-source dissociation results in a false negative. The configuration of the ESI source, the choice of instrumental parameters as well as the gas-phase stability of the complex being investigated influence the extent of in-source dissociation. In some cases, the in-source dissociation can be identified from the change in *R* resulting from changes in ion source parameters, such as voltage differences in high pressure regions.

1.3.3.3 Nonspecific ligand–protein binding

Nonspecific ligand binding during the ESI process is another pitfall of ESI-MS assay, which happens as a consequence of the charge residue model (CRM) when free L binds nonspecifically to P and PL due to concentration effects, resulting false positive. According to the CRM model (Figure 1.7), the initial ESI droplets undergo solvent evaporation until they reach to Rayleigh limit, followed by fission and releasing several small multiply charged nanodroplets, which contain no analyte or one or more analyte. Consequently, the observation of gaseous ions corresponding to a particular PL complex does not, by itself, establish the presence of that interaction in solution. Observation of the change in the magnitude of K_a with changes in ligand concentration is a sign of having nonspecific ligand binding. If a nanodroplet contains two or more analyte molecules, nonspecific interaction appears as the droplets starts solvent evaporation. Interestingly, these nonspecific complexes exhibit a Poisson-like distribution, which suggests nonspecific ligand binding is a random process. Nonspecific binding of L to P and PL obscures the true binding stoichiometry in solution and introduces error into the K_a values measured by ESI-MS.

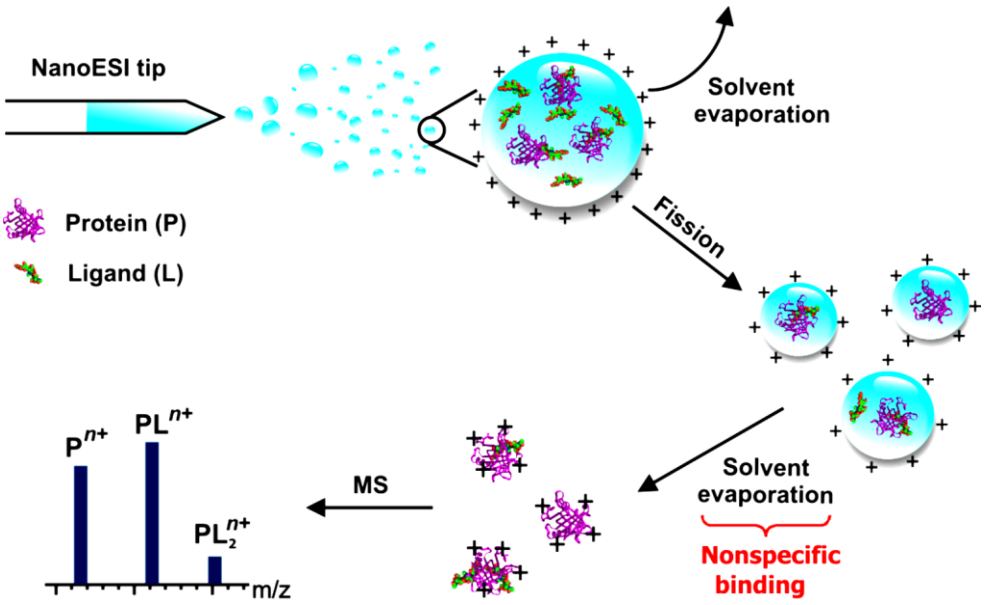

Figure 1.7. Cartoon of the nonspecific protein-ligand interactions during the ESI process. Figure is adapted from reference 39.

The extent of nonspecific binding declines with free ligand concentration in solution as well as the size of the ESI droplet.[36] In cases with strong protein-ligand binding ($K_a > 10^6$ M^{-1}), nonspecific complex formation is minimum, since nearly all of the ligand molecules are bound to the protein in solution. In contrast, nonspecific complex formation is often unavoidable for weak protein-ligand interactions ($K_a < 10^4$ M^{-1}), as high initial concentrations of ligand (≥50 μM) are necessary to produce detectable level of complex signals and, most of ligand molecules are unbound in solution at equilibrium.

A number of strategies have been developed to identify the occurrence of nonspecific interactions of ESI-MS, such as the reporter molecule method,[103] nonspecific probe method[104] and reference protein method.[37]

The reference protein method, used in chapter 3, is the most straightforward approach that allows the correction of ESI mass spectra quantitatively. This method involved the addition of a reference protein (P_{ref}) that does not bind to the protein and ligand of interest specifically. The occurrence of nonspecific protein-ligand binding can be monitored by the appearance of ions corresponding to nonspecific complexes of P_{ref} and L in mass spectrum. The fractions of P_{ref} involved in nonspecific binding with L are used to quantitatively correct the nonspecific complexes of the target protein P to L. However, we only used the reference protein assay qualitatively in chapter 3 to confirm the absence of nonspecific bindings in our protein-ligands interactions.

1.4 The present work

The work described in this thesis focuses on the studying of ESI process and the application of direct ESI-MS assay to study noncovalent protein-ligand interactions.

The work described in chapter 2 focuses on the application of ESI-MS technique to study the enzymatic reaction of sialic acid-containing glycosphingolipids (gangliosides) in different lipid environments. Glycolipids, in general, are insoluble in water due to their hydrophobic chain and to study protein-glycolipid interactions, they should be solubilized in aqueous solution. According to the recent advances for the integration of a variety of model lipid bilayers, those can be incorporated into nanodiscs (ND), picodiscs (PD) or as a micelle. In this study, time-resolved ESI-MS assay was used to monitor the

reaction of human neuraminidase enzyme (hNEU3) with gangliosides, including GM3, GM2, and GM1. The findings suggest that picodiscs, consistent with their hypothesized role in glycolipid degradation, allow for a more native-like presentation of glycolipids for enzymatic studies compared to nanodiscs and micelle.

Chapter 3 describes the first report on the screening of anti-cancer drugs against tubulin using ESI-MS assay. In this study, catch-and-release (CaR)-ESI-MS assay was employed to discriminate the relative binding affinity of 7 colchicine analogues for a specific binding site on tubulin. Proof-of-concept experiments were performed on two anti-cancer drugs with two different binding sites to test the reliability of this assay on the tubulin-drugs interactions. Bound-ligands were released in Trap region by applying the optimum voltage. Moreover, ion mobility separation (IMS) followed by second CID in Transfer was used to prove the complete dissociation of complex ions. Screening reveals that **L3** was released more than other drugs, and thus it has the highest affinity in this series of anti-cancer drugs.

1.5 Literature cited

1. Cleveland, D. W.; Mao, Y.; Sullivan, K. F. *Cell* **2003**, *112*, 407-421.

2. Igakura, T.; Stinchcombe, J. C.; Goon, P. K. C.; Taylor, G. P.; Weber, J. N.; Griffiths, G. M.; Tanaka, Y.; Osame, M.; Bangham, C. R. M. *Science* **2003**, 1713-1715.

3. Waldron, K. J.; Robinson, N. J. *Nature Reviews Microbiology* **2009**, *7*, 25-35.

4. Berg, J. M. *Annual Review of Biophysics and Biophysical Chemistry* **1990**, *19*, 405-421.

5. Anderson, B. F.; Baker, H. M.; Dodson, E. J.; Norris, G. E.; Rumball, S. V.; Waters, J. M.; Baker, E. N., *Proceedings of the National Academy of Sciences* **1987**, *84*, 1769-1773.

6. Saboury, A. A. *Journal of the Iranian Chemical Society* **2006**, *3*, 1-21.

7. Wilcox, D. E. *Inorganica Chimica Acta* **2008**, *361*, 857-867.

8. Velázquez Campoy, A.; Freire, E. *Biophysical Chemistry* **2005**, *115*, 115-124.

9. Utsuno, K.; UludaA, H. *Biophysical Journal* **2010**, *99*, 201-207.

10. Daghestani, H. N.; Day, B. W. *Sensors* **2010**, *10*, 9630-9646.

11. De Crescenzo, G.; Boucher, C.; Durocher, Y.; Jolicoeur, M. *Cellular and Molecular Bioengineering* **2008**, *1*, 204-215.

12. Karlsson, R. *Journal of Molecular Recognition* **2004**, *17*, 151-161.

13. Schuck, P. *Annual Review of Biophysics And Biomolecular Structure* **1997**, *26*, 541-566.

14. Homola, J. *Analytical & Bioanalytical Chemistry* **2003**, *377*, 528-539.

15. Loo, J. A. *Mass Spectrometry Reviews* **1997**, *16*, 1-23.

16. Fangel, J. U.; Pedersen, H. L.; Vidal-Melgosa, S.; Ahl, L. I.; Salmean, A. A.; Egelund, J.; Rydahl, M. G.; Clausen, M. H.; Willats, W. G. T. *Methods In Molecular Biology* **2012**, *918*, 351-362.

17. Wishart, D. *Current Pharmaceutical Biotechnology* **2005**, *6*, 105-120.

18. Angulo, J.; Rademacher, C.; Biet, T.; Benie, A. J.; Blume, A.; Peters, H.; Palcic, M.; Parra, F.; Peters, T. *Methods in Enzymology* **2006**, *416*, 12-30.

19. Shuker, S. B.; Hajduk, P. J.; Meadows, R. P.; Fesik, S. W., *Science* **1996**, 274, 1531-1534.

20. Zech, S. G.; Olejniczak, E.; Hajduk, P.; Mack, J.; McDermot, A. E. *Journal of the American Chemical Society* **2004**, *126*, 13948-13953.

21. Gizachew, D.; Dratz, E. *Chemical Biology and Drug Design* **2011**, *78*, 14-24.

22. Mayer, M.; Meyer, B. *Angewandte Chemie-International edition* **1999**, *38*, 1784-1788.

23. Mayer, M.; Meyer, B. *Journal of the American Chemical Society* **2001**, *123*, 6108-6117.

24. Haselhorst, T.; Lamerz, A.-C.; Itzstein, M. v. Methods in Molecular Biology, Glycomics: Methods and Protocols **2009**, *534*, pp 375-386.

25. Viegas, A.; Manso, J.; Nobrega, F. L.; Cabrita, E. J. *Journal of Chemical Education* **2011**, *88*, 990-994.

26. Palmer, R. A.; Niwa, H. *Biochemical Society Transactions* **2003**, *31*, 973-979.

27. Greco, A.; Ho, J. G. S.; Lin, S.-J.; Palcic, M. M.; Rupnik, M.; Ng, K. K. S. *Nature Structural and Molecular Biology* **2006**, *13*, 460-461.

28. Jason, G. S. H.; Antonio, G.; Maja, R.; Kenneth, K. S. N.; Levitt, M., *Proceeding of the National Academy of Sciences* **2005**, 18373-18378.

29. Staunton, D.; Owen, J.; Campbell, I. D. *Accounts of Chemical Research* **2003**, *36*, 207-214.

30. Bizzarri, A. R.; Cannistraro, S. *Journal of Physical Chemistry B* **2009**, *113*, 16449-16464.

31. Hill, J. J.; Royer, C. A. *Methods In Enzymology* **1997**, *278*, 390-416.

32. Malnasi-Csizmadia, A.; Pearson, D. S.; Kovacs, M.; Woolley, R. J.; Geeves, M. A.; Bagshaw, C. R. *Biochemistry* **2001**, 12727-12737.

33. Srisa-Art, M.; Dyson, E. C.; deMello, A. J.; Edel, J. B. *Analytical Chemistry* **2008**, 7063-7069.

34. Bao, J.; Krylova, S. M.; Wilson, D. J.; Reinstein, O.; Johnson, P. E.; Krylov, S. N. *Chembiochem: A European Journal Of Chemical Biology* **2011**, *12*, 2551-2554.

35. Kitova, E. N.; Bundle, D. R.; Klassen, J. S. *Journal of the American Chemical Society* **2002**, 5902-5913.

36. Wang, W. J.; Kitova, E. N.; Klassen, J. S. *Analytical Chemistry* **2005**, *77*, 3060-3071.

37. Sun, J.; Kitova, E. N.; Wang, W.; Klassen, J. S. *Analytical Chemistry* **2006**, *78*, 3010-3018.

38. Liu, L.; Bagal, D.; Kitova, E. N.; Schnier, P. D.; Klassen, J. S. *Journal of the American Chemical Society* **2009**, *131*, 15980-15981.

39. Kitova, E. N.; El-Hawiet, A.; Schnier, P. D.; Klassen, J. S. *Journal of the American Society for Mass Spectrometry* **2012**, *23*, 431-441.

40. Konermann, L.; Collings, B. A.; Douglas, D. J. *Biochemistry* **1997**, *36*, 5554-5559.

41. Lee, V. W.; Chen, Y. L.; Konermann, L. *Analytical Chemistry* **1999**, *71*, 4154-4159.

42. Sobott, F.; Benesch, J. L. P.; Vierling, E.; Robinson, C. V. *Journal of Biological Chemistry* **2002**, *277*, 38921-38929.

43. Simmons, D. A.; Wilson, D. J.; Lajoie, G. A.; Doherty-Kirby, A.; Konermann, L. *Biochemistry* **2004**, *43*, 14792-14801.

44. Deng, G.; Sanyal, G. *Journal of Pharmaceutical And Biomedical Analysis* **2006**, *40*, 528-538.

45. Pan, J.; Rintala-Dempsey, A. C.; Li, Y.; Shaw, G. S.; Konermann, L. *Biochemistry* **2006**, *45*, 3005-3013.

46. Sharon, M.; Robinson, C. V. *Annual Review of Biochemistry* **2007**, *76*, 167-193.

47. Clarke, D. J.; Stokes, A. A.; Langridge-Smith, P.; Mackay, C. L. *Analytical Chemistry* **2010**, *82*, 1897-1904.

48. Robbins, M. D.; Yoon, O. K.; Barbula, G. K.; Zare, R. N. *Analytical Chemistry* **2010**, *82*, 8650-8657.

49. Miao, Z.; Chen, H.; Liu, P.; Liu, Y. *Analytical Chemistry* **2011**, *83*, 3994-3997.

50. Pacholarz, K. J.; Garlish, R. A.; Taylor, R. J.; Barran, P. E. *Chemical Society Reviews* **2012**, *41*, 4335-4355.

51. Kitova, E. N.; Bundle, D. R.; Klassen, J. S. *Angewandte Chemie-International Edition* **2004**, *43*, 4183-4186.

52. Shoemaker, G. K.; Kitova, E. N.; Palcic, M. M.; Klassen, J. S. *Journal Of The American Chemical Society* **2007**, *129*, 8674-8675.

53. Kitova, E. N.; Mikyung, S.; Roy, P.-N.; Klassen, J. S. *Journal of the American Chemical Society* **2008**, *130*, 1214-1226.

54. Liu, L.; Michelsen, K.; Kitova, E. N.; Schnier, P. D.; Klassen, J. S. *Journal Of The American Chemical Society* **2010**, *132*, 17658-17660.

55. Liesener, A.; Karst, U. *Analytical & Bioanalytical Chemistry* **2005**, *382*, 1451-1464.

56. Eisenthal, R.; Danson, M. J., Enzyme assays: a practical approach. Oxford, OX ; New York : Oxford University Press, **2002**. 2nd ed.: **2002**.

57. Harris, T. K.; Keshwani, M. M. Guide to Protein Purification, 2nd ed.: **2009**, *463*, 57-71.

58. Wallenfels, K. *Methods in Enzymology* **1962**, *5*, 212-219.

59. Zechel, D. L.; Konermann, L.; Withers, S. G.; Douglas, D. J. *Biochemistry* **1998**, *37*, 7664-7669.

60. Bothner, B.; Chavez, R.; Wei, J.; Strupp, C.; Phung, Q.; Schneemann, A.; Siuzdak, G. *The Journal of Biological Chemistry* **2000**, *275*, 13455-13459.

61. Ge, X.; Sirich, T. L.; Beyer, M. K.; Desaire, H.; Leary, J. A. *Analytical Chemistry* **2001**, *73*, 5078-5082.

62. Gao, H.; Petzold, C. J.; Leavell, M. D.; Leary, J. A. *Journal of the American Society for Mass Spectrometry* **2003**, *14*, 916-924.

63. Gao, H.; Leary, J. A. *Analytical Biochemistry* **2004**, *329*, 269-275.

64. Pi, N.; Hoang, M. B.; Gao, H.; Mougous, J. D.; Bertozzi, C. R.; Leary, J. A. *Analytical Biochemistry* **2005**, *341*, 94-104.

65. Danan, L. M.; Yu, Z.; Ludden, P. J.; Jia, W.; Moore, K. L.; Leary, J. A. *Journal of the American Society for Mass Spectrometry* **2010**, *21*, 1633-1642.

66. Soya, N.; Fang, Y.; Palcic, M. M.; Klassen, J. S. *Glycobiology* **2011**, *21*, 547-552.

67. Rob, T.; Wilson, D. J. *European Journal of Mass Spectrometry* **2012**, *18*, 205-214.

68. Covey, T. R.; Thomson, B. A.; Schneider, B. B. *Mass spectrometry reviews* **2009,** *28*, 870-897.

69. Ganem, B.; Li, Y. T.; Henion, J. D. *Journal of the American Chemical Society* **1991**, *113*, 6294-6296.

70. Drummond, J. T.; Loo, R. R. O.; Matthews, R. G. *Biochemistry* **1993**, 9282.

71. Deroo, S.; Hyung, S. J.; Marcoux, J.; Gordiyenko, Y.; Koripella, R. K.; Sanyal, S.; Robinson, C. V. *Chemical Biology* **2012**, *7*, 1120-1127.

72. Rosu, F.; Gabelica, V.; Shin-ya, K.; De Pauw, E. *Chemical Communications* **2003**, 2702-2703.

73. Gabelica, V.; Rosu, F.; De Pauw, E. *Analytical Chemistry* **2009**, *81*, 6708-6715.

74. Kebarle, P.; Verkerk, U. H. *Mass spectrometry reviews* **2009**, *28*, 898-917.

75. Wu, X. Y.; Oleschuk, R. D.; Cann, N. M. *Analyst* **2012**, *137*, 4150-4161.

76. Rayleigh, L. *Philosophical Magazine Series 5* **1882**, *14*, 184-187.

77. Fenn, J. B. *Angewandte Chemie-International Edition* **2003**, *42*, 3871-3894.

78. Cech, N. B.; Enke, C. G. *Mass Spectrometry Reviews* **2001**, *20*, 362-387.

79. Nguyen, S.; Fenn, J. B., *Proceedings of the National Academy of Sciences* **2007**, *23*, 1111-1117.

80. Konermann, L.; Ahadi, E.; Rodriguez, A. D.; Vahidi, S. *Analytical Chemistry* **2013**, *85*, 2-9.

81. Hogan, C. J., Jr.; Carroll, J. A.; Rohrs, H. W.; Biswas, P.; Gross, M. L. *Journal of the American Chemical Society* **2009,** *81*, 369-377.

82. Ahadi, E.; Konermann, L. *Journal of Physical Chemistry B* **2012**, *116*, 104-112.

83. Konermann, L.; Rodriguez, A. D.; Jiangjiang, L. *Analytical Chemistry* **2012**, *84*, 6798-6804.

84. Wilm, M.; Mann, M. *Analytical Chemistry* **1996**, 1-10.

85. Karas, M.; Bahr, U.; Dülcks, T. *Analytical Chemistry* **2000**, *366*, 669-676.

86. Juraschek, R.; Dulcks, T.; Karas, M. *Journal of the American Chemical Society for Mass Spectrometry* **1999**, *10*, 300-308.

87. Hoffmann, E. d.; Stroobant, V., Mass spectrometry: Principles and Applications. Chichester, England; Hoboken, NJ : J. Wiley, **2007**. 3rd ed. Edmond de Hoffmann, Vincent Stroobant.: **2007**.

88. Pringle, S. D.; Giles, K.; Wildgoose, J. L.; Williams, J. P.; Slade, S. E.; Thalassinos, K.; Bateman, R. H.; Bowers, M. T.; Scrivens, J. H. *International Journal of Mass Spectrometry* **2007**, *261*, 1-12.

89. Karasek, F. W. *Analytical Chemistry* **1974**, *46*, 710-710.

90. McCullough, B. J.; Kalapothakis, J.; Eastwood, H.; Kemper, P.; MacMillan, D.; Taylor, K.; Dorin, J.; Barran, P. E. *Analytical Chemistry* **2008**, *80*, 6336-6344.

91. Armenta, S.; Alcala, M.; Blanco, M. *Analytica Chimica Acta* **2011**, *703*, 114-123.

92. Cohen, M. J.; Karasek, F. W. *Journal of Chromatographic Science* **1970**, *8*, 330-337.

93. Buryakov, I. A.; Krylov, E. V.; Nazarov, E. G.; Rasulev, U. K. *International Journal of Mass Spectrometry and Ion Processes* **1993**, *128*, 143-148.

94. Shvartsburg, A. A.; Smith, R. D. *Analytical Chemistry* **2008**, 9689-9697.

95. Wildgoose, J.; McKenna, T.; Hughes, C.; Giles, K.; Pringle, S.; Campuzano, I.; Langridge, J.; Bateman, R. H. *Molecular and Cellular Proteomics* **2006**, *5*, S14-S14.

96. Ruotolo, B. T.; Benesch, J. L. P.; Sandercock, A. M.; Hyung, S.-J.; Robinson, C. V. *Nature Protocols* **2008**, *3*, 1139-1152.

97. Wang, W.; Kitova, E. N.; Klassen, J. S. *Methods In Enzymology* **2003**, *362*, 376-397.

98. Wortmann, A.; Rossi, F.; Lelais, G.; Zenobi, R. *Journal of Mass Spectrometry* **2005**, *40*, 777-784.

99. Abzalimov, R. R.; Dubin, P. L.; Kaltashov, I. A. *Analytical Chemistry* **2007**, *97*, 6055-6063.

100. Cederkvist, F.; Zamfir, A. D.; Bahrke, S.; Eijsink, V. G. H.; Sorlie, M.; Peter-Katalinic, J.; Peter, M. G. *Angewandte Chemie-International Edition* **2006,** *45*, 2429-2434.

101. El-Hawiet, A.; Shoemaker, G. K.; Daneshfar, R.; Kitova, E. N.; Klassen, J. S. *Analytical Chemistry* **2012,** *84*, 50-58.

102. Wyttenbach, T.; Bowers, M. T. *Annual Review of Physical Chemistry* **2007**, *58*, 511-33.

103. Sun, N.; Sun, J.; Kitova, E. N.; Klassen, J. S. *Journal Of The American Society For Mass Spectrometry* **2009**, *20*, 1242-1250.

104. Kitova, E. N.; Soya, N.; Klassen, J. S. *Analytical Chemistry* **2011**, *83*, 5160-5167.

Chapter 2

Enzymatic Studies of Glycolipids by Electrospray Ionization Mass Spectrometry (ESI-MS)[†]

2.1 Introduction

Glycosphingolipids are a major class of glycolipids present in both higher and lower eukaryotic organisms.[1] They consist of a ceramide moiety linked to an oligosaccharide.[1, 2] Gangliosides are sialic acid containing glycosphingolipids that are found in high abundance in the nervous system where they play roles in cell structure and signaling.[3-5] Sialic acid (SA) is a monosaccharide composed of nine carbon backbone and is involved in a surprising variety of biological processes including cell-cell interaction,[6, 7] viral and bacterial modulation of recognition,[8-10] inflammation,[11, 12] and cancers.[13, 14] The level of gangliosides in cells needs to be carefully controlled. Indeed, recent studies into lipid profiling and quantification of cellular lipids has revealed differing levels of gangliosides between healthy and disease states.[15] For example, GM1 levels are decreased in Alzheimer's disease,[16] Huntingtons disease,[17] and Parkinsons disease patients[18] whereas elevated levels of GD2 have been observed in breast cancer patients[19, 20] and serum from multiple sclerosis patients.[21] The ganglioside regulation is controlled by the removal of sialic acid catalyzed by neuraminidase enzyme.

[†] Part of this chapter has been published: Leney, A. C., Rezaei Darestani, R., Li. J., Nikjah, N., Kitova, E. N., Zou, C., Cairo, C. W., Xiong, Z. J., Privé, G. G., Klassen, J. S. *Analytical Chemistry*, **2015**, *87*, 4402-4408.

Therefore, enzymatic studies of gangliosides, which could give more insight about their method of actions, are needed.

Human neuraminidase enzymes (hNEU) are critical regulators of gangliosides, including diabetes, cancer, and cell adhesion.[22, 23] There are four known isoenzymes of NEU, known as NEU1-4, with a range of specificities.[24] The NEU3 isoenzyme, known as a plasma membrane-associated sialidase, increases the attention as the up-regulation of NEU3 has been observed in various carcinomas.[25-28] NUE3 exhibits a preference for glycolipids over glycoproteins. It was found that NEU3 has a substantial preference to cleave Neu5Ac (sialic acid) of gangliosides possessing both α(2,3) (e.g., GM3, GD1a, and GT1b) and α(2,8) (e.g., GD3, GD1b, and GT1b).[29-31] However, several gangliosides with α(2,3) linkage, such as GM1 and GM2, are known as poor substrates, when the linkage is placed at internal sites.[29, 32, 33]

Glycolipids, due to their amphipathic nature, can be readily immobilized on hydrophobic surfaces and their interactions with water-soluble carbohydrate binding proteins (lectins, antibodies and carbohydrate processing enzymes) can be probed using a variety of techniques, including enzyme-linked immunosorbent assays (ELISA), surface plasmon resonance (SPR) spectroscopy and thin layer chromatography (TLC) overlay.[34] Additionally, the use of glycolipid and neo-glycolipid microarrays enables the high-throughput screening of libraries of glycolipids.[35-39] These techniques can be applied to both natural and derivatized glycolipids and their application has led to the discovery of a number of protein-glycolipid receptors.[40, 41] These aforementioned methods, however, all employ an

artificial presentation of glycolipids and binding may be influenced by the nature of the coupling (immobilization) to the surface, ligand density, the loss of mobility of the glycolipid and effects related to the spatial orientation of the carbohydrate residues in the immobilized glycans.[40] Additionally, any required chemical modification of the protein or glycolipid, may influence the binding properties.[35, 42]

Because the removal of glycolipids from a lipid environment is expected to influence the nature of protein interactions, extensive research efforts are being directed towards the development of assays that allow protein-glycolipid binding to be studied under conditions where the glycolipid is maintained in a membrane environment.[43] To this end, the integration of a variety of model lipid bilayers with conventional biophysical binding assays has been reported. For example, protein binding to glycosphinglolipids incorporated into supported phospholipid membranes, micelles (or glycomicelles) and liposomes (or glycoliposomes), has been studied using diverse spectroscopic methods (e.g., fluorescence, nuclear magnetic resonance (NMR) and SPR) and microscopy (e.g., atomic force and total internal reflection fluorescence microscopy) techniques.[43-49] Recently, it was shown that the incorporation of glycosphinglolipids into synthetic phospholipid bilayers called nanodiscs (ND)[50-52] enable protein-glycolipid binding to be studied in aqueous solution using a variety of analytical methods, including SPR spectroscopy,[53] electrospray ionization-mass spectrometry (ESI-MS)[54, 55] and silicon photonic sensors.[56] While the use of these model lipid bilayers allow for the study of protein-glycolipid interactions in a membrane environment, there are

challenges to accurately establishing and precisely controlling the size and composition of the bilayers.[43]

Here, we report on a new glycolipid presentation strategy, which represents a significant contribution in the challenging area of protein-glycolipid interactions (in the area of enzyme kinetic studies). The method exploits a naturally occurring lysosomal sphingolipid activator protein, saposin A (SapA), as a new and highly versatile approach for solubilizing glycolipids, while maintaining them in a lipid environment. SapA is a small (~9 kDa) alpha helical protein that binds to cellular lipids, including glycolipids, and transports them to lysosomal hydrolases for degradation as a small, soluble protein-lipid complex (~3 nm).[57, 58] This lipid-transporting macromolecular complex, herein termed a picodisc (PD), provides an ideal presentation environment for glycolipid hydrolysis. Indeed, saposins are essential to normal processing of lipids in the lysosome, and their disfunction can result in lysosomal storage diseases.[59]

In this study, we report the application of on-line electrospray ionization mass spectrometry (ESI-MS)-based assay to study the kinetics of hNEU3 enzyme with gangliosides (GM1, GM2, and GM3) in picodiscs and compare the results with nanodiscs and micelles. The reliability of our ESI-MS enzyme kinetic method has been tested by comparing the enzyme kinetics of new synthetic soluble glycolipids obtained from ESI-MS with fluorescence-based assay.

2.2 Materials and methods

2.2.1 Proteins and ligands

Saposin A (SapA) was provided by our collaborator Prof. G. Privé [University of Toronto, ON].[58] Purified human NEU3 as a maltose-binding protein (MBP)-fusion protein (MBP-NEU3) used in this study were provided by Dr. Christopher Cairo (University of Alberta). Briefly, the human hNEU3 (92 kDa) was expressed in BL21 (DE3) pLysS *Escherichia coli* cells as a MBP-fusion protein (pMAL-c2x vector). The protein was purified using an amylose affinity column (New England Biolabs) and its activity confirmed by through enzymatic reactions with a fluorogenic substrate, 2′-(4-methylumbelliferyl)-α-D-N-acetylneuraminic acid, as previously described.[60] The enzyme was stored in buffer containing 20 mM MOPs, 10 mM maltose, 10% glycerol, 0.3 M NaCl at -80 °C and buffer exchanged into 50 mM ammonium acetate pH 6.8 immediately prior to ESI-MS analysis.

1-palmitoyl-2-oleoyl-sn-glycero-3-phosphocholine (POPC) was purchased from Avanti Polar Lipids Inc. (Alabaster, AL). The gangliosides GM1 (1545.8 Da, 1573.9 Da) GM2 (1383.7 Da, 1411.7 Da) and GM3 (1180.5 Da) were purchased from Enzo Life Science (Farmingdale, NY). The structures of the gangliosides are given in Figure 2.1a.

Neu5Ac sialoside (**S1,** 744.8 Da), Neu5Gc sialoside (**S2,** 760.8 Da), Neu9Ac (**S3,** 786.8 Da), and one internal standard (**IS**, 334.1 Da) were synthesized and provided by Dr. Christopher Cairo for further investigation (Figure 2.1). Leucine Enkephalin as the second internal standard (**IS2**, 555.6 Da)

was purchased from Waters, USA. Structures of substrates (**S1**, **S2**, and **S3**) and internal standards (**IS** and **IS2**) are shown in Figure 2.1b.

a)

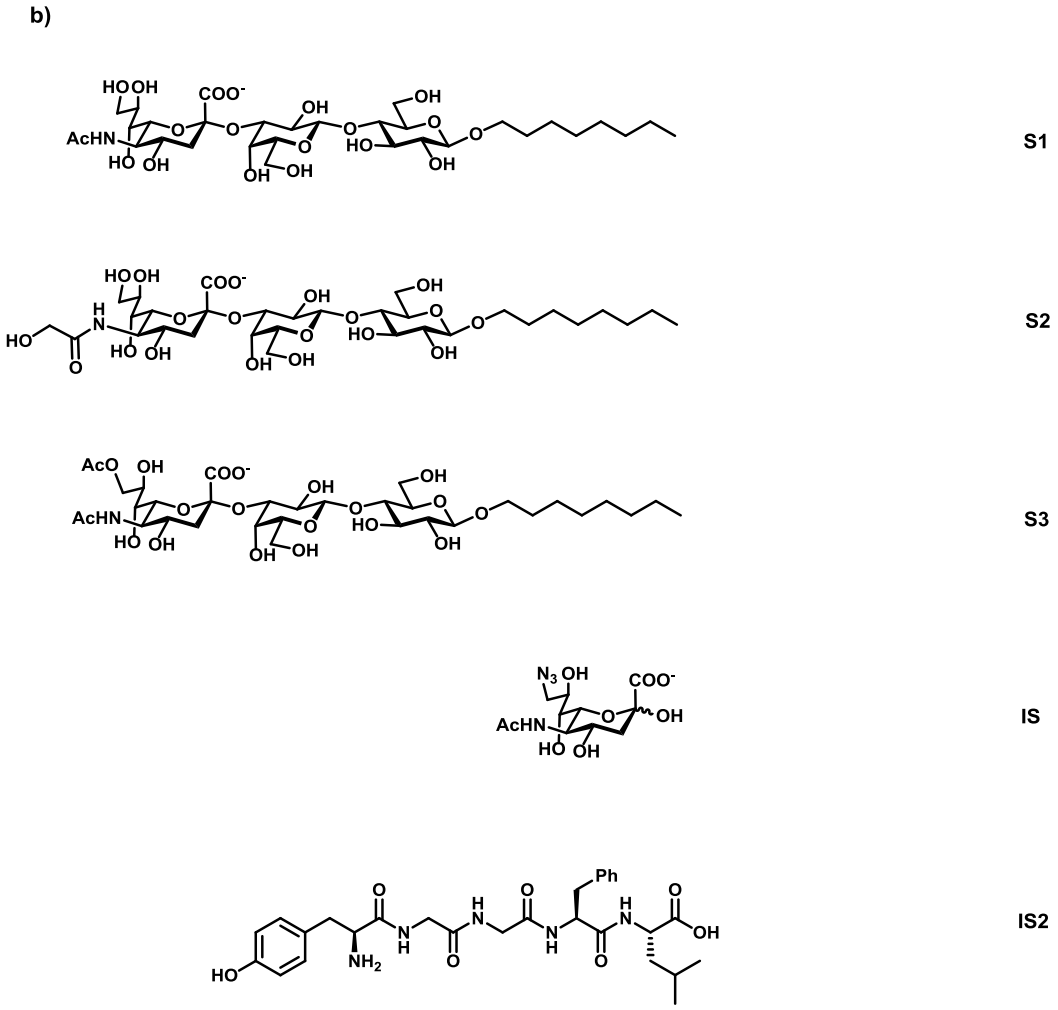

Figure 2.1. Structures of **(a)** gangliosides (GM1, GM2, GM3) and lipid (POPC), (b) soluble glycolipids (**S1**, **S2**, **S3**) and the internal standards (**IS** and **IS2**) used in the enzyme kinetics studies.

2.2.2 Incorporation of glycolipids into picodiscs

Picodiscs containing the scaffold protein, SapA, and the lipid, POPC, were chosen based on their previous characterization.[58] Picodiscs were prepared by mixing POPC and the glycolipid(s) of interest (dissolved in chloroform:methanol (2:1)) in a 1:4 ratio of glycolipid-to-POPC and the mixture dried under nitrogen gas to

form a lipid film. Liposomes containing POPC and glycolipid were then formed by diluting the lipid film in 50 mM sodium acetate and 150 mM NaCl (pH 4.8) followed by a combination of sonication and freeze/thaw cycles. Picodisc formation was then initiated by the addition of SapA protein at 1:10 molar ratio of SapA to total lipid followed by incubation at 37 °C for 45 min. Finally, the picodiscs were purified using a Superdex 75 10/300 size-exclusion column (GE Healthcare Bio-Science, Uppsala, Sweden), equilibrated in 50 mM sodium acetate and 150 mM NaCl (pH 4.8). Control size-exclusion chromatography experiments in which liposomes containing POPC alone, POPC+GM1, POPC+GM2, POPC+GM3, or SapA protein alone were individually injected onto the Superdex 75 10/300 column were carried out. Immediately prior to ESI-MS analysis, the picodiscs were concentrated and buffer exchanged into 200 mM ammonium acetate (pH 4.8 for the enzymatic studies). The concentrations of glycolipid picodiscs were established from the concentration of SapA monomer, which was determined by the absorbance at 280 nm using an extinction coefficient of 8855 M^{-1} cm^{-1}, and assuming a 1:1 ratio of ganglioside:SapA monomer.

2.2.3 Incorporation of glycolipids into nanodiscs

Nanodiscs containing POPC and glycolipids were prepared as previously described.[54, 55] Briefly, POPC (dissolved in chloroform: methanol at a 2:1 ratio) with GM1, GM2, or GM3 were mixed together in a 99:1 ratio for %1 NDs or in a 95:5 for %5 NDs. The sample was dried under nitrogen and placed in a vacuum desiccator overnight to form a POPC lipid film. The membrane scaffold protein

MSP1E1 was added to the lipid film at a molar ratio of 100:1 ratio of lipid to MSP1E1. The mixture was sonicated for 15 min in buffer containing 20 mM TrisHCl, 0.5 mM EDTA, 100 mM NaCl, and 25 mM sodium cholate at pH 7.4. After incubation for 15 min at 4 °C, the self-assembly process was initiated by adding pre-washed bio-beads (Bio-Rad Laboratories Ltd., Canada) and incubating for 3 h on an orbital shaker at 4 °C to remove all detergent. Finally, nanodiscs were purified using a Superdex 200 10/300 size exclusion column (GE Healthcare Bio-Science, Uppsala, Sweden) equilibrated in 200 mM ammonium acetate at pH 6.8. Nanodiscs were concentrated to approximately 20 μM and stored at -80 °C.

2.2.4 Preparation of micelles

A known amount of GM3 (dissolved in chloroform: methanol at a 2:1 ratio) was transferred to a 1 mL glass vial containing 50 μL methanol by syringe. The syringe was washed carefully with the methanol in vial to completely transfer the ganglioside. The solvent was then evaporated under nitrogen gas to form a lipid film of ganglioside and placed in a vacuum desiccator overnight to form a dry lipid film. The film was resuspended in 50 μL of ammonium acetate buffer (200 mM, pH 6.8) by sonicating for 30 min at room temperature. The final concentration of GM3 micelle (~500 μM) was calculated based on the initial amount of added GM3 and the final volume of stock solution. The stock solution was stored at 4 °C.

To prepare GM3 micelles containing different ratios of POPC to GM3, a range of POPC concentrations was added to initial amounts of GM3 as

[POPC]:[GM3] equals to 0 (only GM3), 30, 60, and 100. The rest of procedure remained the same as mentioned above.

2.2.5 Electrospray ionization mass spectrometry analysis

All ESI-MS measurements were carried out using a Synapt G2S instrument (Waters, Manchester, UK) equipped with a nano-ESI source. Negative ion mode was used for all the ESI-MS measurements involving ganglioside picodiscs (owing to the ease of detecting the deprotonated ganglioside ions). Borosilicate capillaries (1.0 mm o.d., 0.68 mm i.d.) were pulled in-house using a P-1000 micropipette puller (Sutter Instuments, Novato, CA). A platinum wire was inserted into the nanoESI tip and a capillary voltage of 0.8 kV (negative ion mode) or 1.0 kV (positive ion mode) was applied. For all experiments, a source temperature of 60 °C was used. For ESI-MS analysis of picodiscs, an argon gas flow of 2 mL min^{-1} was used with the Trap and Transfer collision energies set to 5 and 2 V, respectively. Energy was applied in-source (sampling cone voltage increased from 5 to 150 V) to dissociate the gaseous picodisc ions. Where necessary, the collision energy in the Trap region was increased using a Trap gas flow of 5 mL min^{-1} to detect the released ganglioside ions. For protein-glycolipid detection, optimization of the cone voltage was required for each sample; values used ranged from 30 to 150 V. To release glycolipids from the protein-complexes, the *m/z* region corresponding to the complex ions of interest was selected and subjected to CID in the Trap region using a collision energy of 50-100 V. The released ligands were identified based on the measured *m/z* of the corresponding

ions. Where overlap between picodisc and protein-glycolipid complex occurred in the mass spectrum, CID was performed in the Transfer region using IMS to separate the protein-glycolipid complex from picodisc prior to CID. All data were processed using Mass Lynx software v.4.1 (Waters, Manchester, UK).

2.2.6 Enzymatic studies of gangliosides

Enzymatic studies were performed by rapid manual mixing of hNEU3 (0.0002 units) with picodiscs (5–30 μM ganglioside), nanodiscs (1–30 μM ganglioside), or glycomicelles (30–300 μM) in 100 mM ammonium acetate (pH 4.8). A 5 μL sample was then immediately injected into a nanoESI tip for time-resolved ESI-MS measurements, with data points measured at reaction times ranging from 5 to 30 min. To monitor the formation of sialic acid (SA) due to enzyme activity, GM3, GM2, and GM1 picodiscs, nanodiscs, or GM3 micelle were incubated, separately, with hNEU3. An internal standard, 5-acetamido-9-azido-3,5,9-trideoxy-D-glycero-D-galacto-2-nonulosonic acid (IS), synthesized as described by Cairo and co-workers,[61] was added at a concentration of 2 μM. The ion abundance (Ab) ratio of SA-to-IS was monitored as a function of reaction time (eq 1); each data point was calculated using summed ion abundances measured over a ± 0.1 min interval centered at the reaction time of interest. The ESI and instrumental voltages were: capillary 0.8–1.0 kV, cone 10 V and source offset 50 V.

$$SA/IS = Ab(SA)/Ab(IS) \quad (1)$$

Control experiments, in which no enzyme was added to the picodiscs, nanodiscs, and micelles containing gangliosides, were carried out to confirm that any SA detected was due to hydrolysis and not formed in the gas phase as a result of fragmentation of the GM3 or GM2 or GM1.

To monitor the depletion of substrates from the picodiscs/nanodiscs, GM2 picodiscs/nanodiscs and GM3 picodiscs/nanodiscs were mixed in a 1:1 ratio. The Ab ratios of GM2 and GM3 ions, relative to SapA ions (at charge states -4 and -5) (eqs 2 and 3), released from the picodiscs by CID were measured over time. To dissociate the gas-phase picodisc/nanodisc ions, sampling cone voltages of 110 and 150 V, respectively, and Trap collision energies of 50 and 150 V, respectively, were used; the Trap gas flow rate was 8 mL min^{-1}. All other instrumental parameters were the same as those used for the SA detection measurements. In all cases, the pH of the solution prior to the addition of enzyme and after the enzymatic reaction was directly measured to confirm no pH change had occurred.

$$GM2/SapA = Ab(GM2)/Ab(SapA) \quad (2)$$

$$GM3/SapA = Ab(GM3)/Ab(SapA) \quad (3)$$

2.2.7 Enzymatic studies of soluble substrates

Enzymatic studies of soluble glycolipids were performed in the same condition as described in section 2.2.5. The initial attempt was aimed to track the substrate depletion or product formation of each substrate separately. However, these studies were also doable when we have mixture of three substrates, since the

enzymatic hydrolysis of substrates were resulted in products (**PS1** 308.1 *m/z*, **PS2** 324.2 *m/z*, and **PS3** 350.1 *m/z*) with unique molecular weights, in comparison to the gangliosides that form identical monosaccharide product (**SA** 308.1 *m/z*). The main advantage of having mixture of substrates is the consistency in all experimental circumstances related to response factor. Thus, the ion abundance (Ab) ratio of substrates (SX)-to-IS or products (PSX)-to-IS was monitored as a function of reaction time (eq 4, 5):

$$SX/IS = Ab(SX)/Ab(IS) \quad (4)$$

$$PSX/IS = Ab(PSX)/Ab(IS) \quad (5)$$

2.3 Results and Discussion

2.3.1 Validating the ESI-MS kinetic assay

To validate our ESI-MS kinetic assay, two sets of experiments were designed. In the first experiment, the hydrolysis of a fluorogenic substrate, 4-methylumbelliferyl α-D-N-acetylneuraminic acid (4MU-NA), has been monitored to compare the steady-state kinetic parameters (K_m, V_{max}) from our ESI-MS assay with previously reported values. The kinetic parameters of 4MU-NA were determined by acquiring the initial rates of hydrolysis (v_0) over a range of substrate concentrations (10 – 300 μM) in ammonium acetate (100 mM) at pH 4.8 and 22 °C (Figure 2.2). As shown in Figure 2.2, the Michaelis Menten constant (K_m) of 30 ± 5 μM and V_{max} of 0.333 ± 0.015 μM min^{-1} was obtained from our experimental ESI-MS at 22 °C, which is in reasonable agreement with previous

values (K_m = 39 ± 7 µM, V_{max} = 0.243 ± 0.0108 µM min^{-1} by quench-based ESI-MS assay, and K_m = 45 ± 3 µM, V_{max} = 0.314 ± 0.006 µM min^{-1} by fluorescence-based assay at 37 °C).[61]

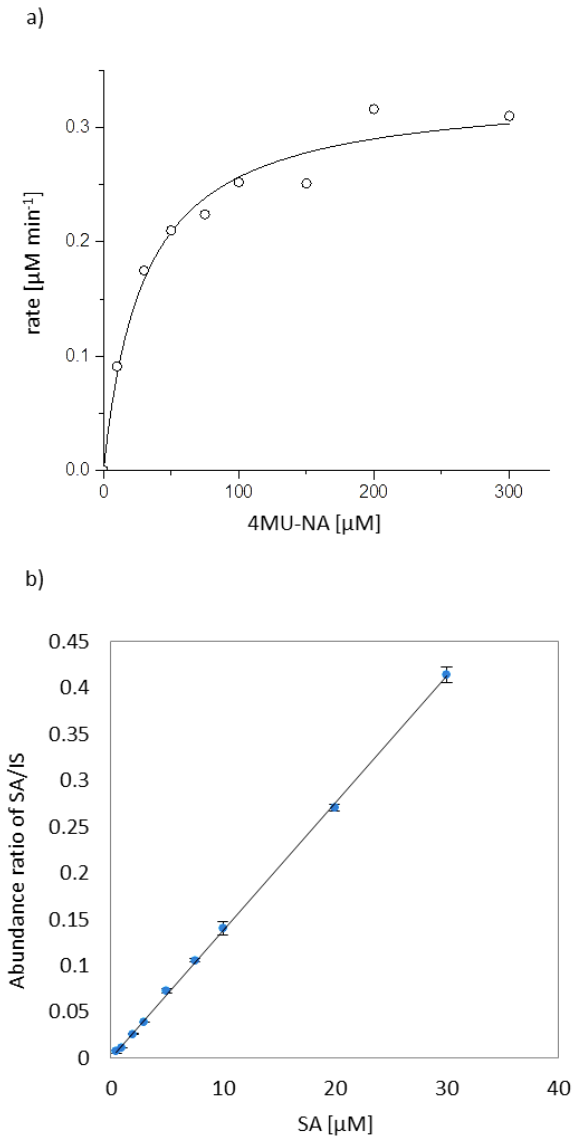

Figure 2.2. (a) The steady-state kinetic of 4MU-NA hydrolysis by hNEU3 measured by ESI-MS assay in ammonium acetate (200 mM) solution at 22 °C and pH 4.8. **(b)** The calibration curve of sialic acid for ESI-MS assay in ammonium acetate (100 mM) solution at 22 °C and pH 4.8.

For further validation of ESI-MS kinetic assay, another set of enzyme kinetic reactions has been performed. In these experiments, the hydrolysis of three soluble glycolipid substrates, **S1**, **S2**, and **S3** (Figure 2.3), was monitored over time by ESI-MS assay and then compared with solution assay using fluorescence spectroscopy.

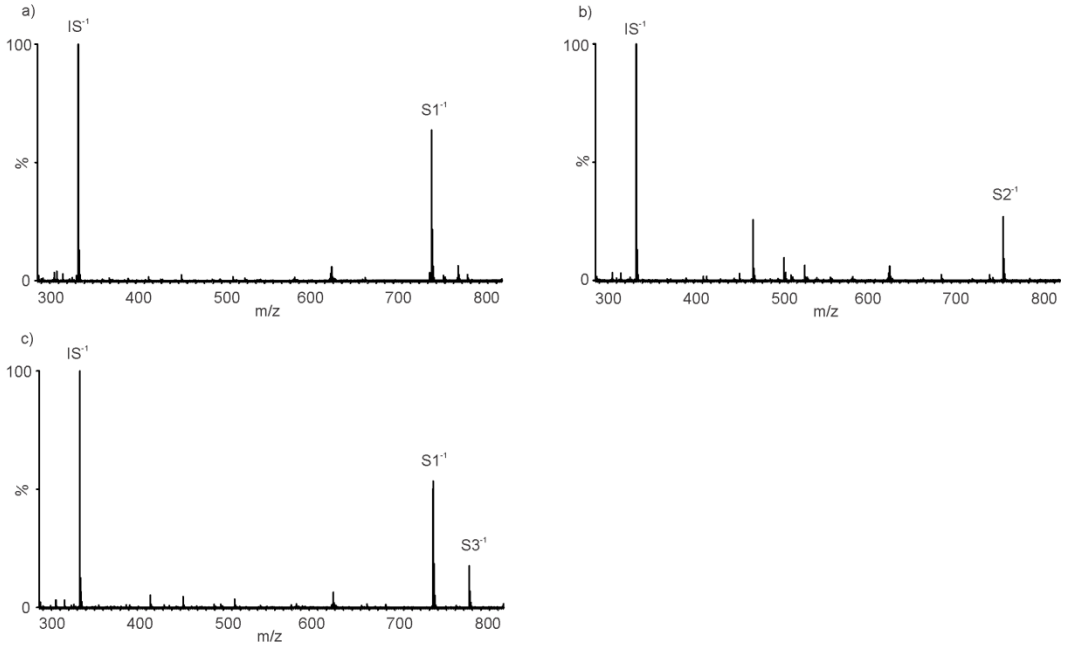

Figure 2.3. ESI mass spectra of soluble substrates (100 μM) acquired in negative ion mode in the absence of hNEU3 in ammonium acetate buffer (200 mM) **(a) S1, (b) S2,** and **(c) S3** at pH 4.8 and 22°C.

The hydrolysis of substrates was initially monitored in separate experiments where each substrate was mixed with hNEU3 and monitored over time. The assay was then repeated in a mixture of three substrates to overcome

any pitfall due to gas phase ionization. The activities of three substrates were differentiated through the use of k_{rel} obtained from the normalization of initial velocity (v_0) of product formation or substrate depletion to the highest value (Table 2.1). The use of a k_{rel} analysis has been used in a variety of enzymatic systems, including hNEUs.[32, 62-64]

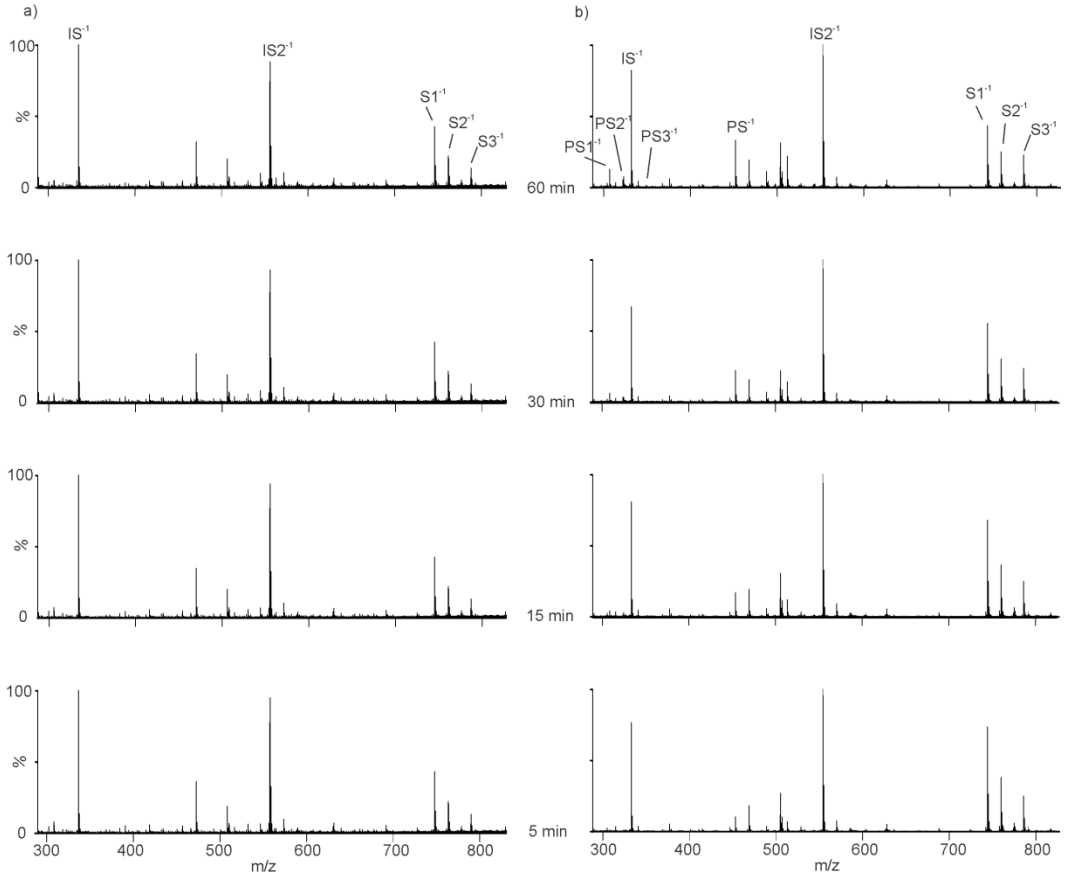

Figure 2.4. ESI mass spectra of soluble substrates (**S1**, **S2**, and **S3**) (100 μM) **(a)** in the absence of hNEU3, and **(b)** in the presence of hNEU3 (0.0002 units) acquired in negative ion mode for 60 min at pH 4.8 and 22 °C. $PS1^{-1}$, $PS2^{-1}$, and $PS3^{-1}$ are the monosaccharide products cleaved from S1, S2, and S3 respectively; and PS^{-1} is the common product resulted from three substrates.

The control experiments have been performed on the absence of enzyme to confirm that the change in abundance of substrates or products is not due to the fragmentation in the gas phase (Figure 2.4a). As shown in Table 2.1, comparing the results obtained form ESI-MS assay, either separate or mixture of substrates, with solution assay suggests that **S1** has the faster kinetics of hydrolysis, while **S3** is the slowest. Importantly, the hydrolysis rates obtained from analysis of substrates depletion represents the same trend as the analysis of product formation.

Table 2.1. Relative rate of hydrolysis of soluble substrates (**S1, S2,** and **S3,** 100 μM) with hNEU3 (0.0002 units) in ammonium acetate solution (200 mM) by ESI-MS kinetic assay obtained in negative ion mode at pH 4.8 and 22°C.

	ESI-MS				Solution assay	
	Mixture of subs.		Separate subs.		Separate subs.	
	v_0 (abn min^{-1})	k_{rel}	v_0 (abn min^{-1})	k_{rel}	v_0 (abn min^{-1})	k_{rel}
S1	0.0140 ± 0.0014	1.0 ± 0.0	0.0162 ± 0.0005	1.0 ± 0.0	-	-
S2	0.0051 ± 0.0009	0.37 ± 0.07	0.1025 ± 0.0020	0.63 ± 0.11	-	-
S3	0.0035 ± 0.0003	0.25 ± 0.02	0.0027 ± 0.0009	0.17 ± 0.06	-	-
PS1	0.0035 ± 0.0006	1.0	0.0048 ± 0.0001	1.0	-	1.0
PS2	0.0015 ± 0.0002	0.44 ± 0.08	0.0020 ± 0.0003	0.42 ± 0.07	-	0.54 ± 0.26
PS3	0.0004 ± 0.0002	0.11 ± 0.03	0.0003 ± 0.0001	0.06 ± 0.03	-	0.55 ± 0.07

However, the k_{rel} of **S3** from solution assay does not match with ESI-MS assay and the reason could arise from the impurity of **S3** containing **S1** (Figure

2.3c). Consequently, the k_{rel} obtained for **S3** from solution assay is the result of hydrolysis of not only **S3** but also **S1**. Notably, ESI-MS assay is able to monitor the kinetic of several substrates simultaneously if each substrate has unique molecular weight. Thus, ESI-MS kinetic assay can explain the high rate of **S3** hydrolysis from solution assay, and the reported k_{rel} from ESI-MS assay is only related to **S3** cleavage.

In addition to the internal standard (**IS)** used in all enzymatic studies, another internal standard (**IS2**, 555.6 Da) was also used to monitor the abundance ratio of substrates reduction or products formation over **IS2** as well as **IS**, and to measure the v_0 and k_{rel} (Table 2.2).

Table 2.2. Relative rate of substrates hydrolysis (**S1**, **S2**, and **S3)** (50 and 100 µM) with hNEU3 in ammonium acetate (200 mM) solution obtained from monitoring the rate of hydrolysis relative to **IS** or **IS2** using ESI-MS assay acquired in negative ion mode at pH 4.8 and 22°C.

	IS				IS2	
	Mixture of subs 50 µM		Mixture of subs 100 µM		Mixture of subs 100 µM	
	v_0 (abn min^{-1})	k_{rel}	v_0 (abn min^{-1})	k_{rel}	v_0 (abn min^{-1})	k_{rel}
S1	0.0067 ± 0.0009	1.0 ± 0.0	0.0074 ± 0.0005	1.0 ± 0.0	0.0056 ± 0.0002	1.0 ± 0.0
S2	0.0032 ± 0.0006	0.48 ± 0.08	0.0036 ± 0.0001	0.48 ± 0.02	0.0026 ± 0.0001	0.47 ± 0.01
S3	0.0009 ± 0.0002	0.14 ± 0.02	0.0011 ± 0.0002	0.15 ± 0.02	0.007 ± 0.0001	0.12 ± 0.01
PS1	0.0015 ± 0.0002	1.0 ± 0.0	0.0023 ± 0.0002	1.0 ± 0.0	0.0020 ± 0.0002	1.0 ± 0.0
PS2	0.0008 ± 0.0001	0.56 ± 0.08	0.0013 ± 0.0003	0.59 ± 0.07	0.0012 ± 0.0003	0.58 ± 0.05
PS3	0.0002 ± 0.0001	0.11 ± 0.06	0.0002 ± 0.0001	0.09 ± 0.01	0.0002 ± 0.0001	0.10 ± 0.03

As shown in Table 2.2, using another internal standard (IS2) is giving similar relative kinetic values (k_{rel}). The consistencies in relative rates obtained from IS and IS2 suggest that our ESI-MS assay is not a standard-dependent method. Moreover, the relative rate of hydrolysis did not change by altering the substrates concentration as it was expected. These finding suggest that the relative rate of substrates hydrolysis is: **S1** > **S2** > **S3**, and confirm that our ESI-MS kinetic assay is a reliable assay for kinetic studies.

2.3.2 Incorporation of glycolipids into picodiscs

Glycolipid-containing picodiscs were formed *in vitro* through incubation of POPC liposomes containing glycolipid with SapA protein. Consistent with previous results obtained for galactosylceramide-containing picodiscs, size exclusion chromatography suggested the presence of a 35 kDa complex.[58] Given that a 1:1 ratio of ganglioside:SapA monomer was used to prepare the picodiscs and the discs are believed to contain two SapA,[58] it is assumed that each picodisc contains two glycolipids. ESI-MS analysis of aqueous solutions of picodiscs failed to detect the presence of free glycolipid (data not shown).

Moreover, collision-induced dissociation (CID) performed on the gaseous picodisc ions revealed the loss of deprotonated glycolipid in all cases (Figure 2.5). Together, these results confirm the successful incorporation of glycolipids into the discs.

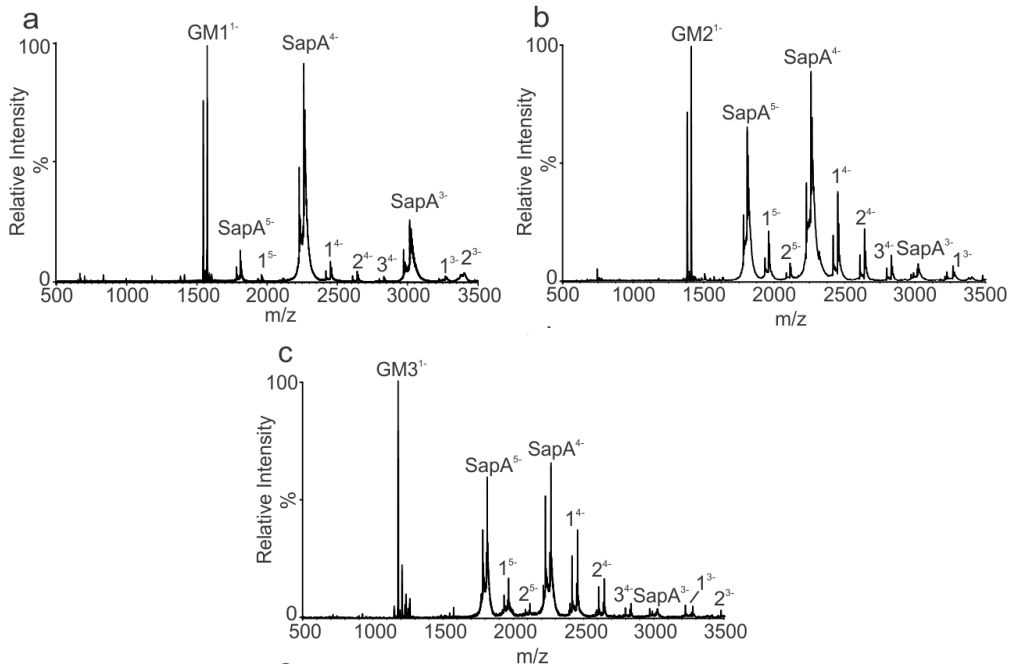

Figure 2.5. CID mass spectra of glycolipid picodisc ions produced by ESI performed on aqueous ammonium acetate solutions (200 mM, pH 6.8): **(a)** GM1 picodisc, **(b)** GM2 picodisc, **(c)** GM3 picodisc. CID was carried out in the Trap region using collision energies of 30 to 100 V. Peaks labelled 1, 2 and 3 correspond to SapA-POPC complexes with 1, 2 and 3 POPC molecules bound, respectively. The mass spectra in **(a)** – **(d)** were acquired in negative ion mode.

2.3. Picodiscs present glycolipids for enzymatic processing

Validation of picodiscs as a means of presenting glycolipids for enzymatic studies in aqueous solution was carried out using reactions involving NEU3, and ganglioside substrates GM2 and GM3.[24] hNEU3 can cleave sialic acid (SA) from GM2 and GM3 and is known to be more active against GM3.[65] Picodiscs containing either GM2 or GM3 were incubated with hNEU3 in 200 mM

ammonium acetate (pH 4.8 and 22 °C) and the abundance of the singly deprotonated ion of SA was monitored in real-time with ESI-MS and compared to an internal standard (IS) (Figure 2.1). As expected based on the greater activity of NEU3 for GM3, as compared with GM2, SA release by NEU3 was readily observed with the GM3 picodiscs (Figure 2.6a), whereas little free SA was observed in the case of the GM2 picodiscs (Figure 2.6b). Although SA is generated by enzyme cleavage of both GM2 and GM3, it is possible to monitor the rate of desialylation of both gangliosides, simultaneously, by dissociating the picodisc ions in the gas phase using CID. Analysis of NEU3 with picodiscs containing an equimolar mixture of GM2 and GM3 in ESI-CID-MS measurements allowed the relative abundances of the GM2 and GM3 substrates to be monitored over time (Figure 2.6c). Consistent with the results obtained for the formation of SA in picodiscs with a single ganglioside, the abundance of GM3 decreased with reaction time relative to GM2. Comparison of the relative abundances of intact GM2 and GM3 (monitored as the abundance ratios of GMX to released SapA ions) with those measured for SA from the individual GM2 or GM3 picodiscs (monitored as the abundance ratio of SA/IS) shows that the decrease in substrate abundance correlates with the increase in SA formation (Figure 2.6d).

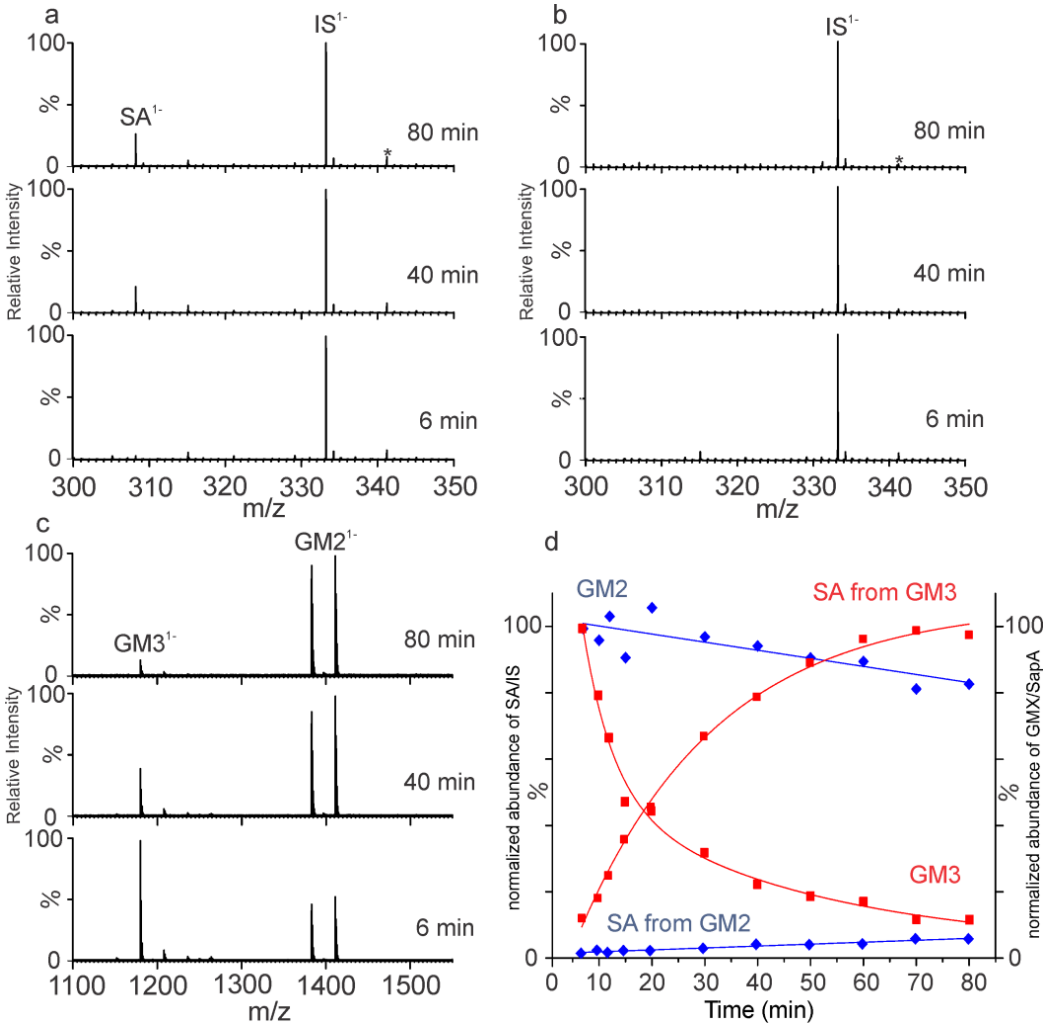

Figure 2.6. Enzymatic hydrolysis of gangliosides. Time-resolved ESI-MS analysis of 200 mM aqueous ammonium acetate solutions (pH 4.8, 22 °C) containing NEU3 and **(a)** GM3 picodiscs (10 μM ganglioside) or **(b)** GM2 picodiscs (10 μM ganglioside), with 2 μM internal standard (**IS**). Signal corresponding to maltose, which is present in the NEU3 stock solution, indicated by *. **(c)** Time-resolved ESI-CID-MS of picodisc ions produced from a 1:1 mixture of GM2 and GM3 picodiscs (10 μM ganglioside) in a 200 mM aqueous ammonium acetate solution (pH 4.8, 22 °C) with NEU3. **(d)** Plots of SA:IS abundance ratios measured for GM2 picodiscs (blue) and GM3 picodiscs (red),

and GMX/SapA (where GMX = GM2 or GM3) abundance ratios measured for a 1:1 mixture of GM2 and GM3 picodiscs.

Control experiments, performed in the absence of NEU3, showed that the abundance ratio of GM3 and GM2 ions remains constant over this time period and confirm that the picodiscs remain intact (Figure 2.7).

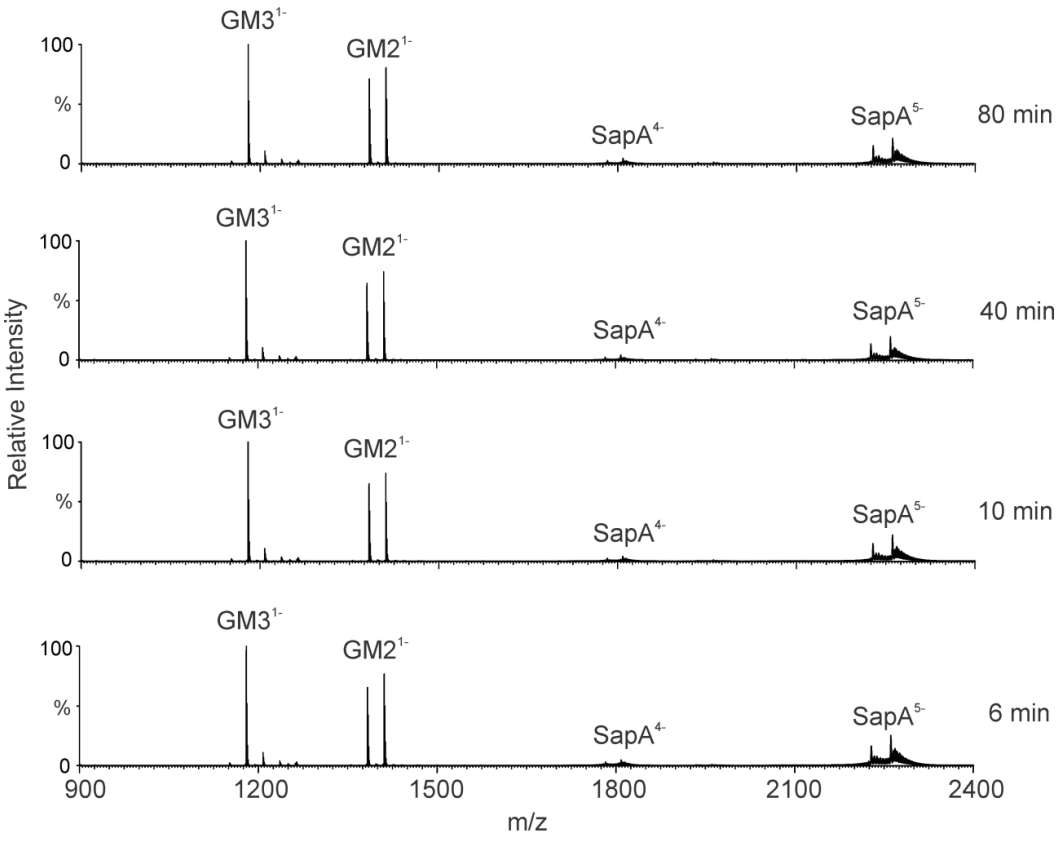

Figure 2.7. CID mass spectra of GM2 picodiscs and GM3 picodiscs produced by ESI performed in negative ion mode on aqueous ammonium acetate solutions (200 mM, pH 4.8) at 6, 10, 40 and 80 min after mixing. CID was carried out in the Trap region using a collision energy of 50 V.

Notably, when incorporated into a nanodisc containing POPC, GM3 exhibits no measurable reactivity with NEU3 under similar experimental conditions (Figure 2.8).

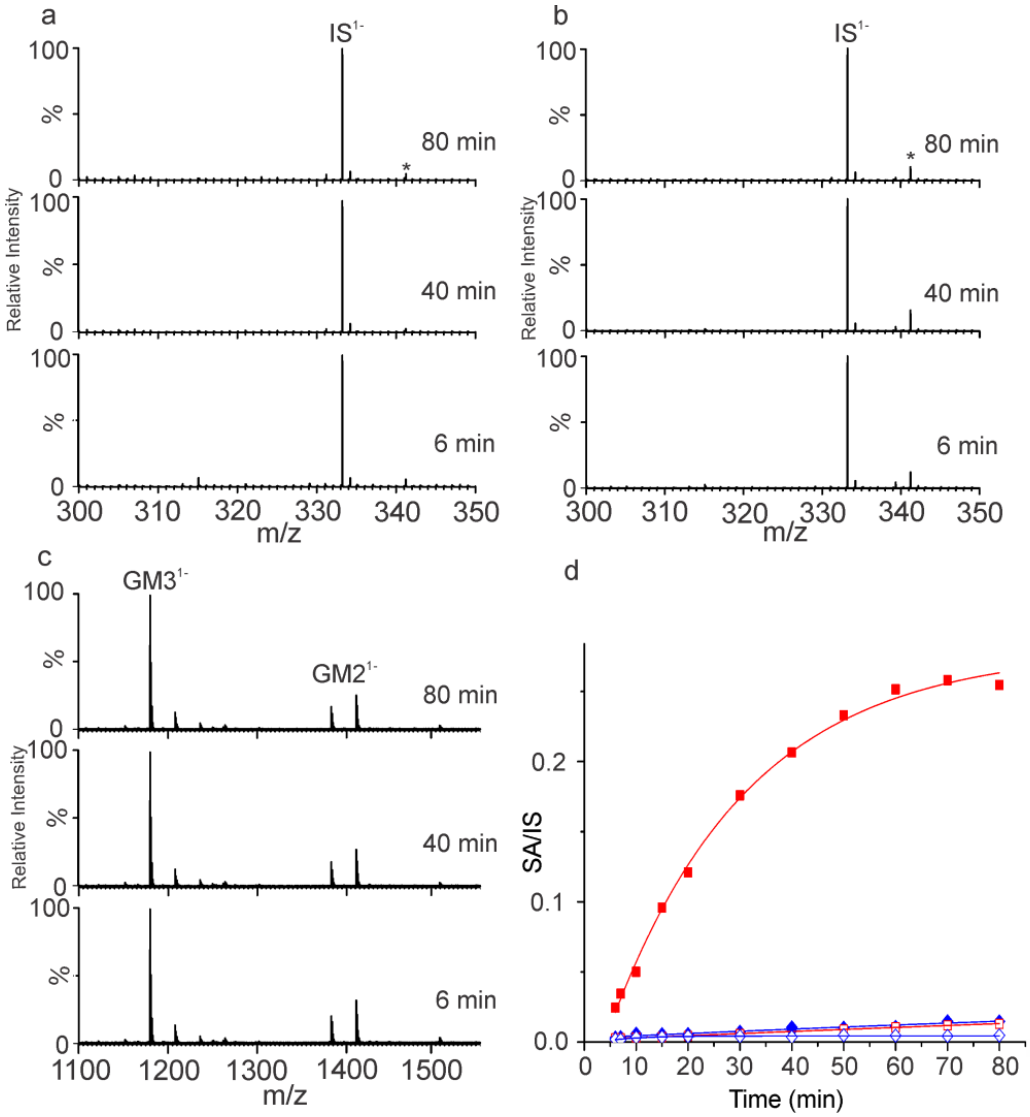

Figure 2.8. Enzymatic hydrolysis of gangliosides in picodiscs and nanodiscs. Time-resolved ESI-MS (negative ion mode) analysis of 200 mM aqueous ammonium acetate solution (pH 4.8, 22 °C) containing NEU3 and **(a)** GM3 nanodiscs (10 μM ganglioside) or **(b)** GM2 nanodiscs (10 μM ganglioside), and 2

μM internal standard (IS). Signal corresponding to maltose, which is present in the hNeu3 stock solution, indicated by *. **(c)** Time-resolved ESI-CID-MS of nanodisc ions produced from a 1:1 mixture of GM2 and GM3 nanodiscs (10 μM ganglioside) in a 200 mM aqueous ammonium acetate solution (pH 4.8, 22 °C) with NEU3. **(d)** Plots of SA:IS abundance ratios measured for GM3 picodiscs (solid red square) and GM2 picodiscs (solid blue diamond), GM3 nanodiscs (hollow red square), GM2 nanodiscs (hollow blue diamond).

The initial results of sialic acid cleavage of GM3 and GM2 picodiscs/nanodiscs represent that picodiscs provide a better environments for hydrolysis. Moreover, as it was expected, GM3 shows faster cleavage compared to GM2. To expand these findings, we decided to look at the relative rates of GM3-picodiscs and -nanodiscs hydrolysis in a range of concentrations (5 - 30 μM GM3-picodiscs and 1 - 30 μM GM3- 1% and 5% nanodiscs) and include the hydrolysis rates of GM1 in both picodiscs and nanodiscs. As shaown in Table 2.3, the hydrolysis rate of GM3-picodiscs with hNEU3 (0.0002 units) at pH 4.8 and 22 °C rises by increasing the concentration. Consequently, the kinetic parameters of K_m = 33.3 ± 13.5 μM and V_{max} = 1.11± 0.28 μM min^{-1} were obtained for GM3-picodiscs. However, no considerable change in the relative rates of GM3-nanodiscs was observed. Including the rates of GM1 hydrolysis also suggests that the GM3 cleavage by hNEU3 is the fastest, while the GM1 is the slowest, as previously described.[61]

Further investigations on the hydrolysis rates of gangliosides could be achieved by comparing the obtained results from picodiscs and nanodiscs with a native presentation of lipid molecules in aqueous solution, named micelles. Micelles are spherical lipid molecules in aqueous solutions that contain both hydrophobic regions (inner side of sphere) and hydrophilic regions (surface of sphere). The comparison is beneficial since micelles do not contain any other solubilizing agents compared to picodiscs and nanodiscs (such as SapA and MSP proteins). For this aim, the hydrolysis of GM3-micelles with a range of GM3 concentrations (30 - 300 μM) were monitored over time using ESI-MS assay in the same conditions as picodiscs and nanodiscs (Table 2.3).

Table 2.3. Rates of gangliosides, presented in different environments, hydrolysis by hNEU3 in ammonium acetate (200 mM) solution obtained by ESI-MS assay at pH 4.8 and 22 °C.

platform	Ganglioside [μM]	v_0 (μM min^{-1})	k_{rel}
GM3-PD	5	0.098 ± 0.003	0.192 ± 0.014
GM3-PD	10	0.285 ± 0.007	0.557 ± 0.010
GM3-PD	15	0.337 ± 0.001	0.661 ± 0.025
GM3-PD	20	0.439 ± 0.001	0.861 ± 0.037
GM3-PD	30	0.511 ± 0.022	1.000 ± 0.0
GM2-PD	30	0.0103 ± 0.0006	0.020 ± 0.001
GM1-PD	30	0.00054 ± 0.00005	0.0011 ± 0.0001
GM3-%1 ND	1	0.00053 ± 0.00006	0.00104 ± 0.00007
GM3-%1 ND	2	0.00106 ± 0.00006	0.0021 ± 0.0002
GM3-%1 ND	4	0.00153 ± 0.00015	0.0030 ± 0.0003
GM3-%1 ND	6	0.00153 ± 0.00006	0.0030 ± 0.0002
GM3-%1 ND	10	0.0016 ± 0.0002	0.0031 ± 0.0004
GM3-%1 ND	30	0.00157 ± 0.00011	0.0031 ± 0.0003
GM2-%1 ND	30	0.00024 ± 0.00001	0.00047 ± 0.00002
GM1-%1 ND	30	0.00012 ± 0.00003	0.00023 ± 0.00007
GM3-%5 ND	30	0.0021 ± 0.0002	0.0041 ± 0.0004
GM2-%5 ND	30	0.00024 ± 0.00001	0.00047 ± 0.00005
GM1-%5 ND	30	0.00012 ± 0.00001	0.00021 ± 0.00001
GM3-micelle	30	0.1553 ± 0.0179	0.305 ± 0.041
GM3-micelle	50	0.1507 ± 0.0185	-
GM3-micelle	75	0.390 ± 0.008	-
GM3-micelle	100	0.975 ± 0.023	-
GM3-micelle	150	0.886 ± 0.098	-
GM3-micelle	200	1.255 ± 0.0736	-
GM3-micelle	300	1.221 ± 0.0446	-

From the Table 2.3, it can be observed that the relative rates of GM3 hydrolysis, taken as most active gangliosides in hydrolysis with hNEU3, in picodiscs (k_{rel} of 1) is faster than micelles (k_{rel} of 0.305 ± 0.041), 1% nanodiscs (k_{rel} of 0.0031 ± 0.0003), and 5% nanodiscs (k_{rel} of 0.0041 ± 0.0004). It can be concluded that picodisc presentation provides a better environment for glycolipids hydrolysis rather than micelle and nanodisc.

Since the ratio of ganglioside to lipid is different in picodiscs and nanodiscs, the question is if the amount of POPC (lipid) in those platforms is affecting the rate of hydrolysis? To answer this question, a series of experiments has been designed on micelles, known as native presentations of gangliosides in aqueous solution, with different ratios of POPC:GM3 to check the effect of POPC in those presentations. All micelles were incubated with hNEU3 in the same condition as before and the obtained k_{rel} was then plotted against the [POPC]:[GM3]. If POPC is the main source of the difference in hydrolysis rate, we should observe this in the micelles with different ratios of POPC:GM3.

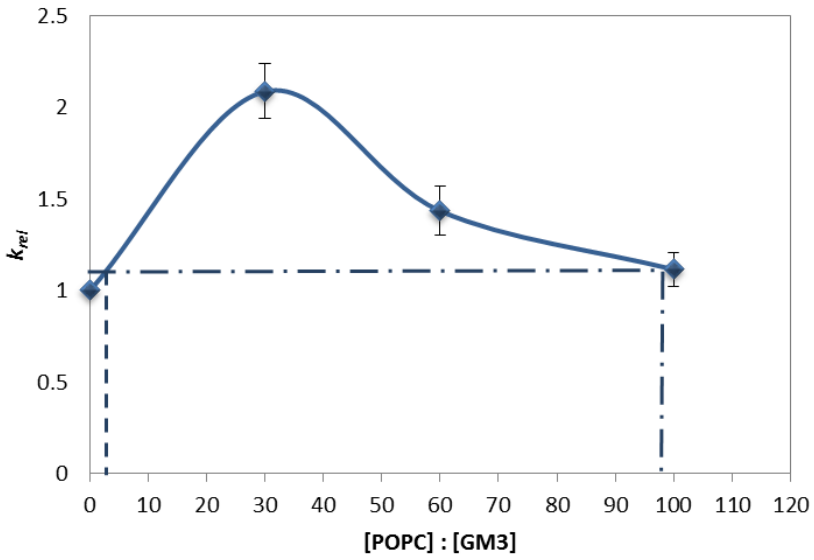

Figure 2.9. Relative hydrolysis rate of GM3-micelles containing different ratios of POPC/GM3 with hNEU3 in ammonium acetate (100 mM) solution at pH 4.8 and 22 °C.

Shown in Figure 2.9 represents the k_{rel} of micelles in a range of POPC:GM3 concentration. k_{rel} reaches the maximum when the POPC is 30 times more than GM3 in micelle. Based on the Table 2.3, the rate of hydrolysis in GM3-PD (30 μM) is almost 300 times greater than that of GM3-%1 ND. If the POPC is affecting this difference, same rate difference should be observed for GM3-micelles when the ratio of [POPC]:[GM3] are 4 (similar ratio in picodisc) and 99 (similar ratio in %1 nanodisc). However, as shown in Figure 2.9, the k_{rel} in both cases are almost equal (k_{rel} of 1.1). These results suggest that POPC ratio in picodiscs and nanodiscs cannot be the cause of difference in the rate of hydrolysis.

These findings suggest that picodiscs, consistent with their hypothesized role in glycolipid degradation, allow for a better presentation of glycolipids for enzymatic studies compared to model lipid bilayers. The use of picodiscs in ESI-MS analysis requires no synthetic modification of the glycolipid and should require less material than TLC-based assays. Taken together, these results illustrate the tremendous opportunity afforded by glycolipid-loaded picodiscs, combined with real-time ESI-MS analysis, for studying the enzymatic degradation of glycolipids, which are key regulators in diabetes, cancer, and cellular adhesion.[22]

2.4 Conclusions

In summary, we have developed a powerful new method, which combines picodiscs and native ESI-MS, for enzymatic studies *in vitro*. The proof-of-concept experiments with soluble glycolipids and 4MU-NA tested the reliability of ESI-MS assay for enzyme kinetic studies. The results of time-resolved measurements of enzyme-catalyzed hydrolysis of glycolipids substrates demonstrate that picodiscs provide a better environment for hydrolysis of glycolipids in aqueous solution compared to nanodiscs and micelles.

2.5 Literature cited

1. Hakomori, S. I. *Annual Review of Biochemistry* **1981,** *50*, 733-764.

2. Hakomori, S. I. *Journal of Biological Chemistry* **1990,** *265*, 18713-18716.

3. Cohen, M.; Varki, A. *Omics-a Journal of Integrative Biology* **2010,** *14*, 455-464.

4. Byrne, B.; Donohoe, G. G.; O'Kennedy, R. *Drug Discovery Today* **2007,** *12*, 319-326.

5. Bieberich, E.; Liour, S. S.; Yu, R. K. *Sphingolipid Metabolism and Cell Signaling, Pt B* **2000,** *312*, 339-358.

6. Schauer, R. *Current Opinion in Structural Biology* **2009,** *19*, 507-514.

7. Lopez, P. H. H.; Schnaar, R. L. *Current Opinion in Structural Biology* **2009,** *19*, 549-557.

8. Sakarya, S.; Oncu, S. *Medical Science Monitor : International Medical Journal of Experimental and Clinical Research* **2003,** *9*, 76-82.

9. Suzuki, Y.; Ito, T.; Suzuki, T.; Holland, R. E.; Chambers, T. M.; Kiso, M.; Ishida, H.; Kawaoka, Y. *Journal of Virology* **2000,** *74*, 11825-11831.

10. Viswanathan, K.; Chandrasekaran, A.; Srinivasan, A.; Raman, R.; Sasisekharan, V.; Sasisekharan, R. *Glycoconjugate Journal* **2010,** *27*, 561-570.

11. Lasky, L. A. *Science* **1992,** *258*, 964-969.

12. Lowe, J. B. *Current Opinion in Cell Biology* **2003,** *15*, 531-538.

13. Mabry, E. W.; Carubelli, R. *Experientia* **1972,** *28*, 182-183.

14. Hakomori, S. *Proceedings of the National Academy of Sciences* **2002,** *99*, 10231-10233.

15. Rual, J. F.; Venkatesan, K.; Hao, T.; Hirozane-Kishikawa, T.; Dricot, A.; Li, N.; Berriz, G. F.; Gibbons, F. D.; Dreze, M.; Ayivi-Guedehoussou, N.; Klitgord, N.; Simon, C.; Boxem, M.; Milstein, S.; Rosenberg, J.; Goldberg, D. S.; Zhang, L. V.; Wong, S. L.; Franklin, G.; Li, S. M.; Albala, J. S.; Lim, J. H.; Fraughton, C.; Llamosas, E.; Cevik, S.; Bex, C.; Lamesch, P.; Sikorski, R. S.; Vandenhaute, J.; Zoghbi, H. Y.; Smolyar, A.; Bosak, S.; Sequerra, R.; Doucette-Stamm, L.; Cusick, M. E.; Hill, D. E.; Roth, F. P.; Vidal, M. *Nature* **2005,** *437*, 1173-1178.

16. Yanagisawa, K.; Odaka, A.; Suzuki, N.; Ihara, Y. *Nature Medicine* **1995,** *1*, 1062-1066.

17. Maglione, V.; Marchi, P.; Di Pardo, A.; Lingrell, S.; Horkey, M.; Tidmarsh, E.; Sipione, S. *Journal of Neuroscience* **2010,** *30*, 4072-4080.

18. Bembi, B.; Marsala, S. Z.; Sidransky, E.; Ciana, G.; Carrozzi, M.; Zorzon, M.; Martini, C.; Gioulis, M.; Pittis, M. G.; Capus, L. *Neurology* **2003,** *61*, 99-101.

19. Battula, V. L.; Shi, Y.; Evans, K. W.; Wang, R.-Y.; Spaeth, E. L.; Jacamo, R. O.; Guerra, R.; Sahin, A. A.; Marini, F. C.; Hortobagyi, G.; Mani, S. A.; Andreeff, M. *Journal of Clinical Investigation* **2012,** *122*, 2066-2078.

20. Marquina, G.; Waki, H.; Fernandez, L. E.; Kon, K.; Carr, A.; Valiente, O.; Perez, R.; Ando, S. *Cancer Research* **1996,** *56*, 5165-5171.

21. Pender, M. P.; Greer, J. M. *Current Allergy and Asthma Reports* **2007,** *7*, 285-292.

22. Miyagi, T.; Yamaguchi, K. *Glycobiology* **2012,** *22*, 880-896.

23. Taeko, M. *Trends in Glycoscience and Glycotechnology* **2010,** *22*, 162-172.

24. Cairo, C. W. *Medchemcomm* **2014,** *5*, 1067-1074.

25. Kakugawa, Y.; Wada, T.; Yamaguchi, K.; Yamanami, H.; Ouchi, K.; Sato, I.; Miyagi, T. *Proceedings of the National Academy of Sciences* **2002,** *99*, 10718-10723.

26. Miyagi, T.; Wada, T.; Yamaguchi, K.; Hata, K. *Glycoconjugate Journal* **2004,** *20*, 189-98.

27. Kato, K.; Shiga, K.; Yamaguchi, K.; Hata, K.; Kobayashi, T.; Miyazaki, K.; Saijo, S.; Miyagi, T. *Biochemical Journal* **2006,** *394*, 647-656.

28. Miyagi, T. *Proceedings of the Japan Academy Series B-Physical and Biological Sciences* **2008,** *84*, 407-418.

29. Wada, T.; Yoshikawa, Y.; Tokuyama, S.; Kuwabara, M.; Akita, H.; Miyagi, T. *Biochemical and Biophysical Research Communications* **1999,** *261*, 21-27.

30. Ha, K. T.; Lee, Y. C.; Cho, S. H.; Kim, J. K.; Kim, C. H. *Molecules and Cells* **2004,** *17*, 267-273.

31. Azuma, Y.; Sato, H.; Higai, K.; Matsumoto, K. *Biological & Pharmaceutical Bulletin* **2007,** *30*, 1680-1684.

32. Miyagi, T.; Wada, T.; Iwamatsu, A.; Hata, K.; Yoshikawa, Y.; Tokuyama, S.; Sawada, M. *Journal of Biological Chemistry* **1999,** *274*, 5004-5011.

33. Wang, Y.; Yamaguchi, K.; Shimada, Y.; Zhao, X. J.; Miyagi, T. *European Journal of Biochemistry* **2001,** *268*, 2201-2208.

34. Lopez, P. H. H.; Schnaar, R. L. *Methods in Enzymology* **2006,** *417*, 205-220.

35. Song, X.; Heimburg-Molinaro, J.; Cummings, R. D.; Smith, D. F. *Current Opinion in Chemical Biology* **2014,** *18*, 70-77.

36. Feizi, T. *Annals of the New York Academy of Sciences* **2013,** *1292*, 33-44.

37. Palma, A. S.; Feizi, T.; Childs, R. A.; Chai, W.; Liu, Y. *Current Opinion in Chemical Biology* **2014,** *18*, 87-94.

38. Rinaldi, S.; Schiavo, G.; Crocker, P. R.; Willison, H. J.; Brennan, K. M.; Goodyear, C. S.; O'Leary, C. *Glycobiology* **2009,** *19*, 789-796.

39. Arigi, E.; Blixt, O.; Buschard, K.; Clausen, H.; Levery, S. B. *Glycoconjugate Journal* **2012,** *29*, 1-12.

40. Grant, O. C.; Smith, H. M. K.; Firsova, D.; Fadda, E.; Woods, R. J. *Glycobiology* **2014,** *24*, 17-25.

41. Campanero-Rhodes, M. A.; Smith, A.; Wengang, C.; Sonnino, S.; Mauri, L.; Childs, R. A.; Yibing, Z.; Ewers, H.; Helenius, A.; Imberty, A.; Feizi, T. *Journal of Virology* **2007,** *81*, 3-3.

42. Stowell, S. R.; Leffler, H.; Smith, D. F.; Cummings, R. D.; Blixt, O.; Arthur, C. M.; Mehta, P.; Slanina, K. A. *Journal of Biological Chemistry* **2008,** *283*, 10109-10123.

43. Czogalla, A.; Grzybek, M.; Jones, W.; Coskun, Ü. *BBA - Molecular & Cell Biology of Lipids* **2014,** *1841*, 1049-1059.

44. Cho, H.; Wu, M.; Bilgin, B.; Walton, S. P.; Chan, C. *Proteomics* **2012,** *12*, 3273-3282.

45. Sanghera, N.; Correia, Bruno E. F. S.; Correia, Joana R. S.; Ludwig, C.; Agarwal, S.; Nakamura, Hironori K.; Kuwata, K.; Samain, E.; Gill, Andrew C.; Bonev, Boyan B.; Pinheiro, Teresa J. T. *Chemistry and Biology* **2011,** *18*, 1422-1431.

46. Shi, J.; Yang, T.; Kataoka, S.; Zhang, Y.; Diaz, A. J.; Cremer, P. S. *Journal of the American Chemical Society* **2007,** *129*, 5954-5961.

47. Rao, C. S.; Lin, X.; Pike, H. M.; Molotkovsky, J. G.; Brown, R. E. *Biochemistry* **2004,** *43*, 13805-13815.

48. Chen, W. C.; Kawasaki, N.; Nycholat, C. M.; Han, S.; Pilotte, J.; Crocker, P. R.; Paulson, J. C. *Public Library of Science One* **2012,** *7,* 1-9.

49. Jayaraman, N.; Maiti, K.; Naresh, K. *Chemical Society Reviews* **2013,** *42*, 4640-4656.

50. Nath, A.; Atkins, W. M.; Sligar, S. G. *Biochemistry* **2007,** *46*, 2059-2069.

51. Bayburt, T. H.; Sligar, S. G. *Febs Letters* **2010,** *584*, 1721-1727.

52. Denisov, I. G.; Grinkova, Y. V.; Lazarides, A. A.; Sligar, S. G. *Journal of the American Chemical Society* **2004,** *126*, 3477-3487.

53. Borch, J.; Torta, F.; Sligar, S. G.; Roepstorff, P. *Analytical Chemistry* **2008,** *80*, 6245-6252.

54. Zhang, Y.; Liu, L.; Daneshfar, R.; Kitova, E. N.; Li, C.; Jia, F.; Cairo, C. W.; Klassen, J. S. *Analytical Chemistry* **2012,** *84*, 7618-7621.

55. Leney, A. C.; Fan, X.; Kitova, E. N.; Klassen, J. S. *Analytical Chemistry* **2014,** *86*, 5271-5277.

56. Sloan, C. D. K.; Marty, M. T.; Sligar, S. G.; Bailey, R. C. *Analytical Chemistry* **2013,** *85*, 2970-2976.

57. Locatelli-Hoops, S.; Remmel, N.; Klingenstein, R.; Breiden, B.; Rossocha, M.; Schoeniger, M.; Koenigs, C.; Saenger, W.; Sandhoff, K. *Journal of Biological Chemistry* **2006,** *281*, 32451-32460.

58. Popovic, K.; Holyoake, J.; Pomes, R.; Prive, G. G. *Proceedings of the National Academy of Sciences of the United States of America* **2012,** *109*, 2908-2912.

59. Schulze, H.; Sandhoff, K. *Biochimica Et Biophysica Acta-Molecular and Cell Biology of Lipids* **2014,** *1841*, 799-810.

60. Albohy, A.; Li, M. D.; Zheng, R. B.; Zou, C.; Cairo, C. W. *Glycobiology* **2010,** *20*, 1127-1138.

61. Sandbhor, M. S.; Soya, N.; Albohy, A.; Zheng, R. B.; Cartmell, J.; Bundle, D. R.; Klassen, J. S.; Cairo, C. W. *Biochemistry* **2011,** *50*, 6753-6762.

62. Mehrotra, K. N.; Dauterman, W. C. *Journal of Neurochemistry* **1963,** *10*, 119-129.

63. Roberts, M. F.; Adamich, M.; Robson, R. J.; Dennis, E. A. *Biochemistry* **1979,** *18*, 3301-3308.

64. Sato, K.; Hanagata, G.; Kiso, M.; Hasegawa, A.; Suzuki, Y. *Glycobiology* **1998,** *8*, 527-532.

65. Li, S. C.; Li, Y. T.; Moriya, S.; Miyagi, T. *Biochemical Journal* **2001,** *360*, 233-237.

Chapter 3

Screening Anti-Cancer Drugs against Tubulin using Catch-and-Release Electrospray Ionization Mass Spectrometry[†]

3.1 Introduction

The αβ-tubulin heterodimers are the building blocks of microtubules (MTs),[1] which are long, hollow, cylindrical protein polymers and dynamic structural components of the cellular cytoskeleton.[2-5] Both the α and β subunits exist as different isotypes in many organisms, with dissimilar relative amounts, e.g. there are six isoforms of both α (αI-VI) and β (βI-VI) subunits in mammals, differing from each other in their amino acid sequences.[6, 7] Microtubules control cell shape and play important roles in mitosis, intracellular vesicle transport, organization, and positioning of membranous organelles.[8-10] The critical role of microtubules in cell division makes them an attractive target in cancer chemotherapy. Microtubule targeting agents (MTAs) modify the formation and function of MTs by altering microtubule dynamics.[11] These MTAs interact with tubulin so as to stabilize or destabilize the polymeric microtubules. In general, drugs that interact with microtubule are divided in two groups: (i) microtubule stabilizers, which include taxanes,[12] epothilones,[13] discodermolide,[14] and peloruside A,[15] or (ii) microtubules destabilizers, including colchicinoids,[16] vinca alkaloids,[17] dolastatin,[18] and hemiasterins.[19]

[†]Manuscript in preparation for *J. Am. Soc. Mass. Spectrum.*

Of the known MTAs, taxol, colchicine, and vinblastine are among the best characterized.[20] Colchicine binds at the interface of the α and β subunits,[21] while taxol and vinblastine bind to β subunit. Colchicine has been widely used to treat gout, familial Mediterrenian fever and auto-inflammatory diseases.[22, 23] It is an alkaloid found in *Colchium autmnale* and *Gloriosa superba* and is composed of three rings, a trimethoxy benzene ring (ring A), a methoxy tropone ring (ring C), and a seven-membered ring (ring B).[16] The administration of colchicine inhibits the cell division through two proposed mechanisms. In the first mechanism, referred to as the end poisoning mechanism, polymerization is inhibited through colchicine binding to the ends of the microtubules, thus preventing the microtubules growth by sterically blocking further addition of the tubulin dimers. The other mechanism focuses on colchicine binding-induced conformational changes in the tubulin dimers, which leads to disassembly of the microtubules.[9, 16, 24] However, the high concentrations of colchicine required to effectively kill cancer cells also adversely affects non-tumoral cells. Consequently, extensive research to design analogs of colchicine (e.g. combretastatin A4)[25] with improved binding (to MTs), thereby lowering the required therapeutic does, has been undertaken in recent years.[26]

As reported originally by Diaz and co-workers,[16, 27, 28] the association of colchicine to tubulin appears to be a two-step process – a fast, reversible step, followed by a slow, reversible step, eq 3.1:

$$T + C \underset{}{\overset{K_1}{\rightleftharpoons}} TC \underset{k_{-2}}{\overset{k_2}{\rightleftharpoons}} TC' \qquad (3.1)$$

where T, C, TC and TC' represent tubulin dimer, colchicine, and the non-covalent tubulin-colchicine complexes, respectively, and K_1 is the equilibrium constant of the fast reversible step and k_2 and k_{-2} are the rate constants of the forward and reverse reactions of the second step. It was originally proposed that colchicine binds to αβ-tubulin dimer initially through a single ring (ring C), corresponding to the fast step,[29, 30] followed by conformational changes in tubulin associated with insertion of ring A and B to give a higher affinity interaction.[29, 30] However, it was later suggested by Banerjee and *et al.* that the biphasic nature of the colchicine-tubulin binding kinetics is related to the differential binding of colchicine to the β-tubulin isotypes.[16, 31] For example, different k_2 values were measured for the four β-isotypes found in bovine brain: 132 ± 5 s^{-1} (αβII), 30 ± 2 s^{-1} (αβIII), and 236 ± 7 s^{-1} (αβI and αβIV).[31]

Currently, no general binding assay exists for tubulin interactions with colchicinoid drugs, as well as other classes of MTAs. The use of isothermal titration calorimetry (ITC), which represents the gold standard for quantifying protein-ligand interactions *in vitro*, is limited by the relatively long equilibration times required for these interactions (Figure 3.1). Radiolabeling assays have previously been used to study tubulin-colchicine binding. However, the radiolabeled compounds are expensive and require special handling, disposal and detection. Fluorescence assays have also been used to quantify colchicine binding to tubulin.[9, 32] The main advantage of this method is neither requires the labeling of drugs nor the separation of free colchicine from the complex.[9] However, some colchicine analogues (e.g. thiocolchicine) exhibit little or no fluorescence and can

not be studied using this approach.[9, 33] Therefore, there is a significant need for a general and robust assay to measure the affinities of colchicine analogues for tubulin.

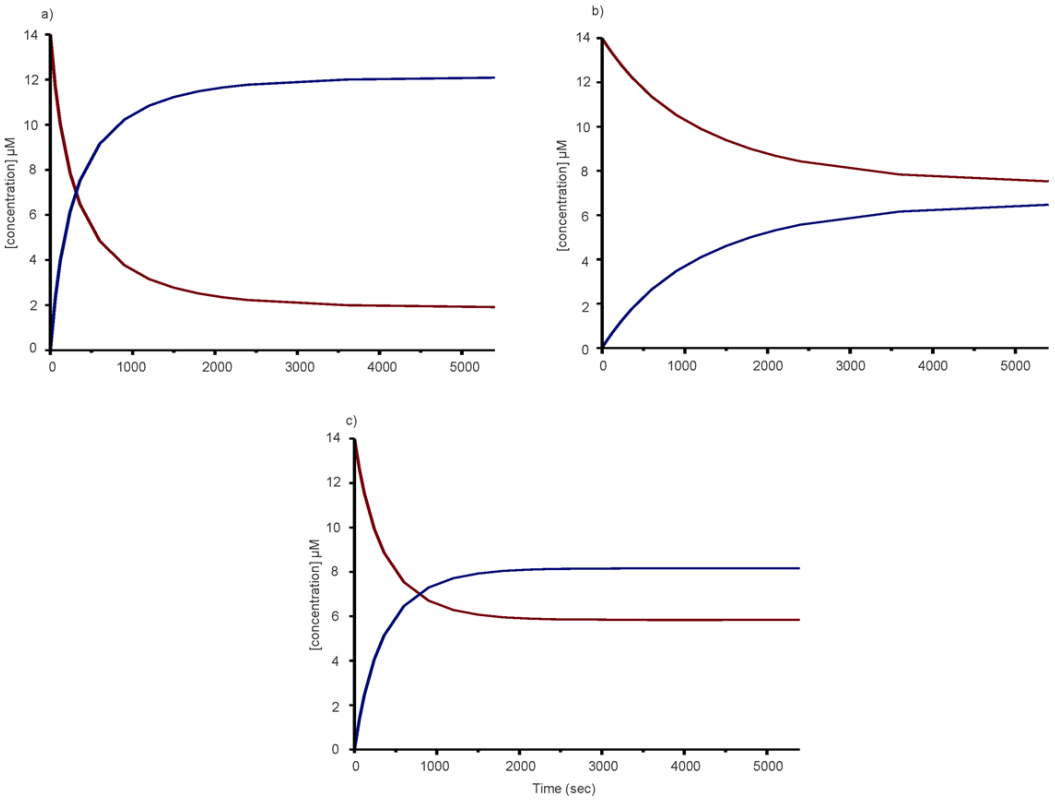

Figure 3.1. Calculated the time of reaching equilibrium for **(a)** αβII (k_2 of 132 ± 5 M^{-1} s^{-1}), **(b)** αβIII (k_2 of 30 ± 2 M^{-1} s^{-1}), and **(c)** αβIV (k_2 of 236 ± 5 M^{-1} s^{-1}) when tubulin (14 µM) is incubated with colchicine (14 µM). Blue and red lines correspond to tubulin-colchicine formation and reactants depletion, respectively.

Recently, the direct electrospray ionization mass spectrometry (ESI-MS) assay has emerged as a powerful tool for measuring the affinities of protein-ligand interactions *in vitro*.[34-37] The assay is based on direct measurement of the relative

abundances of the ligand-bound and free protein ions measured by ESI-MS. This assay has a number of strengths that make it a valuable technique for binding measurements including simplicity (no labeling or immobilization is required), speed (measurements can be completed within a few minutes) and low sample consumption (typically less than pmol per analysis). The ability to measure multiple binding equilibria simultaneously makes the ESI-MS assay well suited for screening libraries of compounds against target proteins.[38-40] Where direct detection of the protein-ligand complexes by ESI-MS is not possible, due to factors such as high molecular weight (MW) or protein heterogeneity, the catch-and-release (CaR) ESI-MS assay can be employed.[38, 41-43] In this assay, ligand binding is established by releasing (as ions) ligands bound to the protein in the gas phase using activation methods such as collision-induced dissociation (CID). Typically, ligands can be identified based on their measured MW; in some cases fragmentation of the released corresponding ligand ion or ion mobility separation (IMS) may be required for positive identification. The CaR-ESI-MS assay has been used to screen carbohydrate, peptide and small molecule libraries against target proteins.[38, 39, 44-46]

Here, we describe the application of the CaR-ESI-MS assay to investigate the binding of colchicinoid drugs to αβ-tubulin dimers extracted from porcine brain. Proof-of-concept experiments using positive (ligands with known affinities) and negative (non-binders) controls were performed to establish the reliability of the assay. The assay was then used to screen a small library of seven colchicinoid analogues to test their binding to tubulin and to rank their affinities.

3.2 Experimental

3.2.1 Proteins and ligands

αβ-tubulin dimer (MW ~110 kDa), extracted from porcine brain, was purchased from Cytoskeleton, Inc. (Denver, CO). Bovine Serum Albumin (BSA) was purchased from Sigma-Aldrich Canada (Oakville, Canada). A stock solution of αβ-tubulin dimer was prepared by dissolving a known mass of protein in 500 μL of aqueous ammonium acetate (50 mM, pH 6.8, at 4 °C) and concentrated to 5 mg mL^{-1} (~40 μM) by ultracentrifugation using a Vivaspin a 0.5 mL centrifugal filter (Sartius Stedim Biotech, Göttingen, Germany) with MW cutoff of 30 kDa. The stock solution was then separated into aliquots, which were snap frozen in liquid nitrogen and then stored at -80 °C until needed. The stock solution of BSA was prepared by dissolving a known mass of protein in deionized water, followed by buffer exchange into ammonium acetate (50 mM, pH 6.8) using a Vivaspin 0.5 mL centrifugal filter (Sartius Stedim Biotech, Göttingen, Germany) with MW cutoff of 10 kDa. The stock solution, with a final concentration of 500 μM, was then stored at 4 °C.

Colchicine (**L1**, MW 399.2 Da) and thiocolchicoside (**L8**, MW 563.6 Da) were purchased from Sigma-Aldrich Canada (Oakville, ON) and Abcam Inc. (Cambridge, UK), respectively. Vincristine sulfate (**L9**, MW 824.4 Da) was purchased from Sigma-Aldrich Canada (Oakville, ON). The colchicine analogues (**L2**, MW 415.1 Da; **L3**, MW 445.2 Da; **L4**, MW 510.2 Da; **L5**, MW 526.1 Da; **L6**, MW 554.2 Da; **L7**, MW 587.2 Da) were synthesized by ChemRoutes Corp. (Edmonton, Canada). The structures of **L1** – **L8** are given in Figure 3.2. The

purity of all ligands was determined to be >95% by liquid chromatography (LC)-MS (Agilent Eclipse plus C18 column, 250 mm × 4.6 mm, 5 µm particle size; mobile phase, water/acetonitrile (0.1% HCOOH) 80:20 to 5:95 over 5 min and held for 1.5 min; flow rate 0.5 mL/min). Stock solutions of 20 mM of each of **L1** – **L8** were prepared by dissolving the compound into DMSO and then diluting with deionized water and stored at -20 °C.

a)

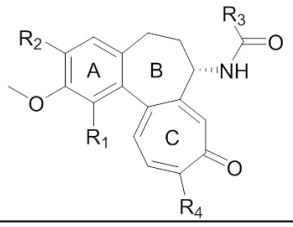

compound	MW	R1	R2	R3	R4
L1	399.2	$-OCH_3$	$-OCH_3$	$-CH_3$	$-OCH_3$
L2	415.1	$-OCH_3$	$-OCH_3$	$-CH_3$	$-SCH_3$
L3	445.2	$-OCH_3$	$-OCH_2CH_3$	$-OCH_3$	$-SCH_3$
L4	510.2	$-OCH_3$	$-OCH_3$	$-CH_2NHC(=O)CF_3$	$-OCH_3$
L5	526.1	$-OCH_3$	$-OCH_3$	$-CH_2NHC(=O)CF_3$	$-SCH_3$
L6	554.2	$-OCH_2CH_2OCH_3$	$-OCH_3$	$-CH_2NHC(=O)CF_3$	$-OCH_3$
L7	587.2	$-OCH_2$ *m*-Pyr	$-OCH_3$	$-CH_2NHC(=O)CF_3$	$-OCH_3$
L8	563.6	$-OCH_3$	$-OCH_6O_5$	$-CH_3$	$-SCH_3$

b)

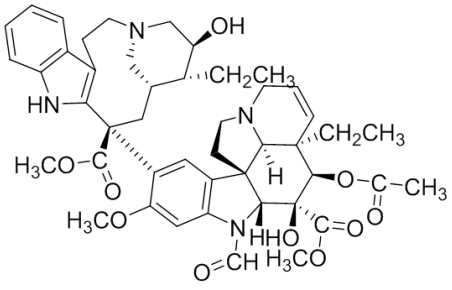

Figure 3.2. The structures of **(a)** colchicinoid drugs (**L1- L8**) and **(b)** vincristine (**L9**) used for CaR-ESI-MS assay..

3.2.2 Mass spectrometry

All of the ESI-MS measurements were carried out in positive ion mode using a Waters Synapt G2S quadrupole-ion mobility separation-time of flight (Q-IMS-TOF) mass spectrometer (Manchester, UK) equipped with a nanoflow (nanoESI) source. A P-1000 micropipette puller was used to produce nanoESI tips from borosilicate capillaries (1.0 mm o.d., 0.68 mm i.d.) (Sutter Instruments, Novato, CA). A voltage of ~1.3 kV was applied to platinum wire inserted into the nanoESI tip to carry out ESI. A source temperature of 60 °C and cone voltage 10 V were used for all measurements. Data acquisitions and processing were performed using MassLynx software (version 4.1).

3.2.3 CaR-ESI-MS Assay

To carry out CaR-ESI-MS, the quadrupole mass filter was set to pass ions with a range of *m/z* values; with a window of 2400 - 12500 *m/z* that was maximized at 4000 - 7000 *m/z*. Setting the quadrupole mass filter allows the ions, corresponding to the proteins (including tubulin dimer and tetramer and BSA) and complexes, to pass and reach Trap region. To set the quadrupole, the parameters were set at: mass 1, 2, and 3 at 3000, 4000, and 5000 *m/z*, respectively, with dwell times of 5% for mass 1 and 2, ramp time for *m/z* 3000 at 5% and for *m/z* 4000 at 85%. These ions were then subjected to CID in the Trap region using collision energies ranging from 2 to 140 V and the released ligand ions identified based on the measured *m/z*. Where indicated, and following CID in the Trap region, the tubulin ions were subjected to another stage of CID in the Transfer region, using collision

energies ranging from 1 to 120 V. Prior to the second stage of CID, the tubulin ions were separated from free ligand ions using IMS. For IMS, a wave height of 40 V and a wave velocity between 400 and 700 m s^{-1} were applied along with a helium and nitrogen (IMS gas) gas flow of 80 and 70 mL min^{-1}, respectively. In all cases, data acquisition and processing were performed using MassLynx software ver. 4.1 (Waters, Manchester, UK).

3.3 Result and Discussion

3.3.1 Analysis of tubulin-colchicine binding by ESI-MS

As a starting point for this study, ESI-MS was used to analyze aqueous solutions of tubulin, on its own and in the presence of **L1** (colchicine). Shown in Figure 3.3a is a representative ESI mass spectrum acquired for an aqueous ammonium acetate solution (100 mM, pH 6.8, 22 °C) of αβ-tubulin (14 μM). Abundant ion signal corresponding to tubulin dimer (d^{n+}), at charge states +18 - +22, is evident; low abundance signal corresponding to tubulin tetramer (t^{n+}) ions, at charge states +32 - +29, was also detected. The measured MWs of dimer (101,750 ± 12 Da) and tetramer (203,460 ± 52 Da) from porcine brain (mostly αI and βI)[47,48] are in agreement with theoretical values (UniProt, P02550 for αI and P02554 for βI) (101,677 Da and 203,354 Da, respectively).. The presence of tetramer could be due to self-association of the tubulin dimer; nonspecific binding during the ESI process might also play a role in its formation.[49,50] Because the stock solutions of **L1** – **L8** contain DMSO, ESI mass spectra were also acquired for aqueous solutions of tubulin in the presence of low concentrations of DMSO. Shown in

Figure 3.3b is a representative ESI mass spectrum obtained under the same conditions as those used for Figure 3.3a, but with the presence of 0.05% v/v DMSO. This percentage of DMSO corresponds to amount used in all of the binding measurements carried out in the present study, *vide infra*. It can be seen that, at this concentration, DMSO has little effect on the appearance of the mass spectrum, although there is a slight shift in the charge state distribution, to lower values (+17 to +21), of the tubulin dimer.

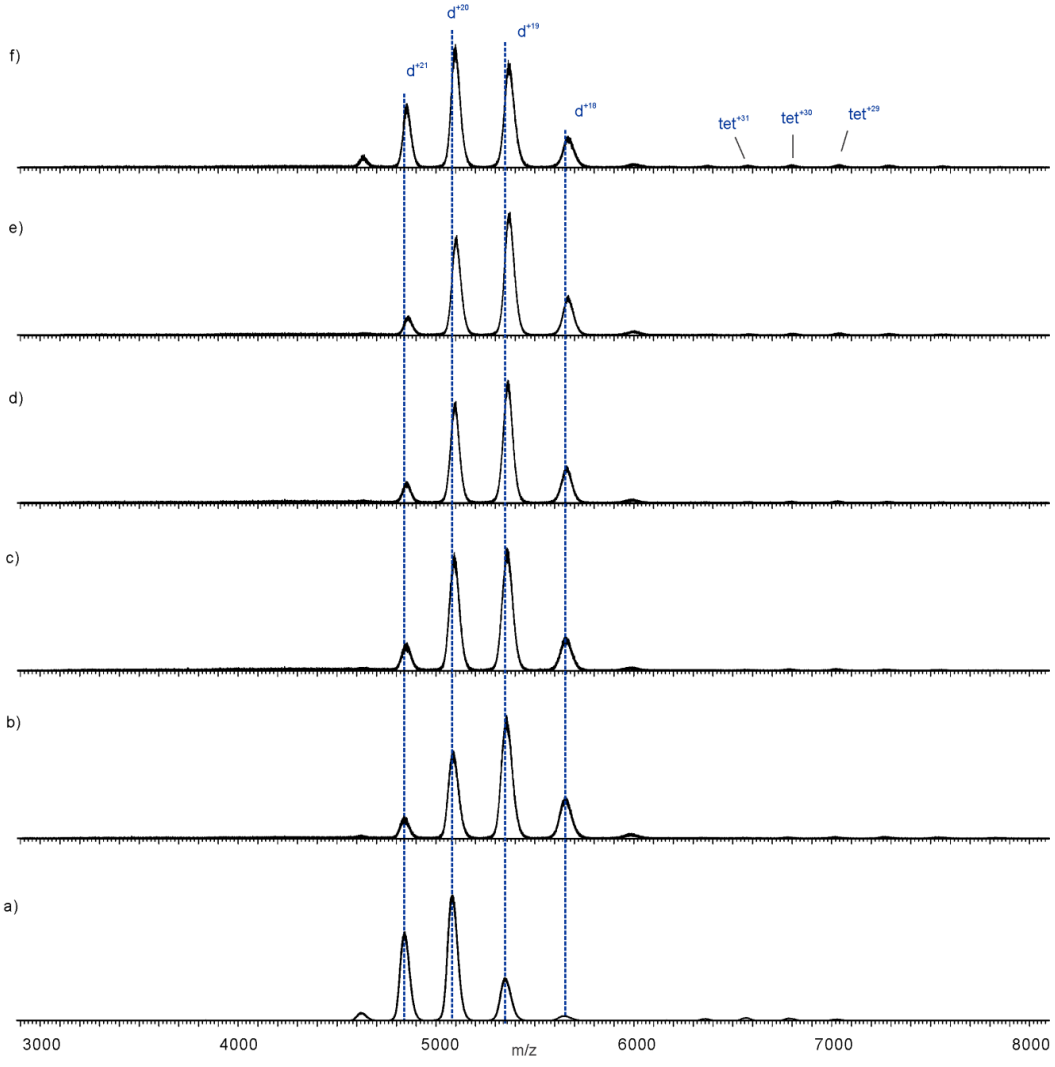

Figure 3.3. ESI mass spectra acquired in positive ion mode for an aqueous ammonium acetate solution (100 mM) of **(a)** tubulin (14 μM), **(b)** DMSO (0.05 %), **L1 (c)** 2, **(d)** 6, **(e)** 14, **(f)** 20.

Shown in Figures 3.3c-f are the ESI mass spectra of aqueous ammonium acetate buffer (100 mM) solutions of αβ-tubulin (14 μM) and a range of colchicine (**L1**) concentrations (2-20 μM) following incubation at 37 °C for 1 h. While it was not possible to directly ascertain the presence of ions corresponding to **L1**-bound tubulin dimer from the mass spectra, the presence of **L1** in solution resulted in a small but measurable increase in the *m/z* of the tubulin dimer ions and the magnitude of the effect increased with increasing **L1** concentration. This observation is consistent with the presence of **L1**-bound tubulin dimer in solution.

To confirm for the presence of bound **L1**, the CaR-ESI-MS assay was employed. As a starting point, the quadrupole mass filter was set to pass all ions, with *m/z* between 4000 and 7000, produced from a solution of αβ-tubulin (14 μM); these were then subjected to CID in Trap region using collision energies ranging from 2 to 140 V (Figure 3.4a). It can be seen that the tubulin ions are stable and do not undergo any fragmentation, even at highest collision energies. In the same way, the Car-ESI-MS assay was applied to tubulin ions produced from a solution of αβ-tubulin (14 μM) and **L1** (14 μM) (Figures 3.4b). It can be seen that CID resulted in the appearance of signal corresponding to protonated **L1** (m/z 400.1) at all of the energies investigated. These results confirm that **L1** was bound to the gaseous tubulin ions.

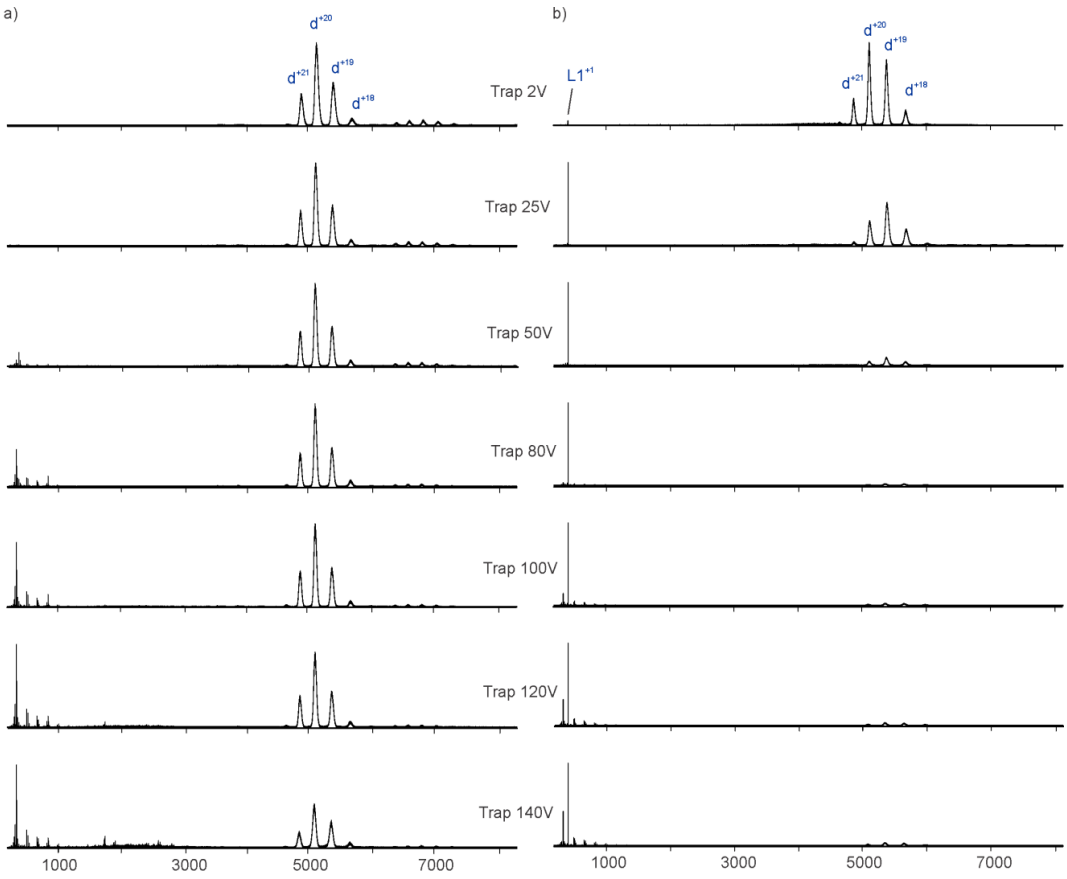

Figure 3.4. CID mass spectra measured for **(a)** tubulin alone (14 μM) and **(b)** tubulin (14 μM) incubated with colchicine **L1** (14 μM) at different Trap voltages of 2, 25, 50, 80, 100, 120, 140 V.

In order to rule out the possibility that the **L1**-tubulin interactions identified by CaR-ESI-MS arose during the ESI process (i.e., due to nonspecific binding), the measurements were repeated using a solution of αβ-tubulin (14 μM), **L1** (14 μM) and BSA (14 μM). To the best of our knowledge BSA does not interact with **L1** in solution and, therefore, served as a reference protein (P_{ref}) to test for nonspecific binding. Isolation of the +18 charge state of the tubulin dimer, followed by CID gave results that are indistinguishable from those shown in

Figure 3.5. In contrast, isolation of the +16 charge state of BSA (B^{+16}), followed by CID failed to produce any signal corresponding to **L1** (Figure 3.5). Taken together, these results suggest that the gaseous **L1**-bound tubulin ions are the result of specific binding in solution, with little or no contribution from non-specific binding during the ESI process.

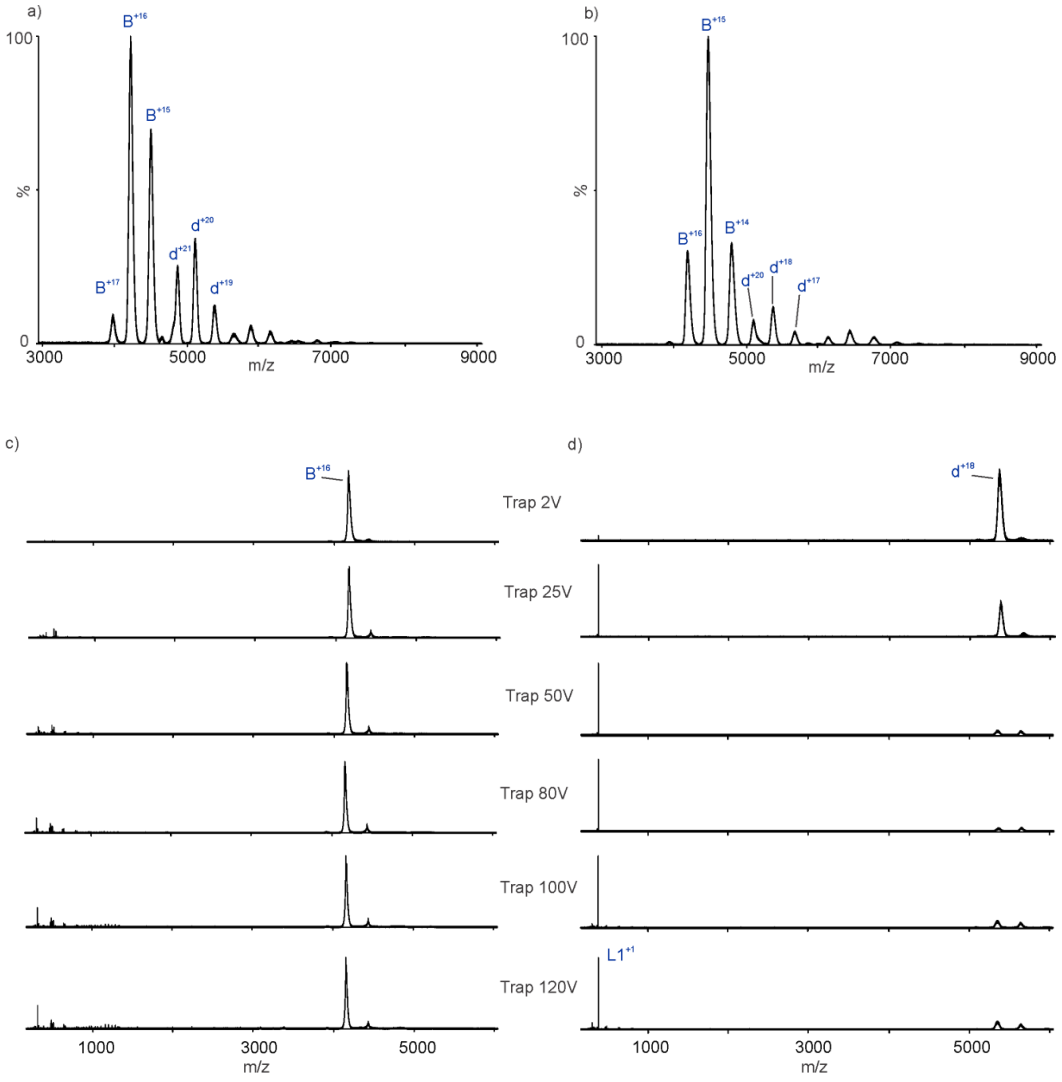

Figure 3.5. ESI mass spectra of **(a)** mixture of tubulin (14 μM) with BSA (14 μM) and **(b)** mixture of tubulin (14 μM) with BSA (14 μM) incubated with colchicine (14 μM) in ammonium acetate buffer (100 mM) at 37 °C for 1h. CID

mass spectra of the mixture of tubulin (14 μM) with BSA (14 μM) incubated with colchicine (14 μM) in ammonium acetate buffer (100 mM) at 37 °C for 1h after isolation of **(c)** +16 charge state of BSA (B^{+16}) and **(d)** +18 charge state of tubulin (d^{+18}) at Trap voltage of 2 to 120 V.

As described above, **L1** binding to tubulin dimer is accompanied by a conformation change. Therefore, it was of interest to investigate whether the binding of **L1** to tubulin could be quantified based on differences in the collision cross sections of the free and ligand-bound tubulin dimer ions. To assess whether the ligand binding-induced conformational changes result in measurable differences in collision cross sections, IMS arrival time distributions (ATDs) were measured for tubulin dimer ions produced from solutions containing αβ-tubulin alone (14 μM) and in the presence of **L1** in ammonium acetate solution (100 mM) at pH 6.8 and 22 °C. (Figure 3.6). Inspection of the ATDs measured for each charge state reveals no measurable differences for tubulin dimers produced in the absence or presence of **L1**, even at the highest concentration (28 μM) of **L1** investigated.

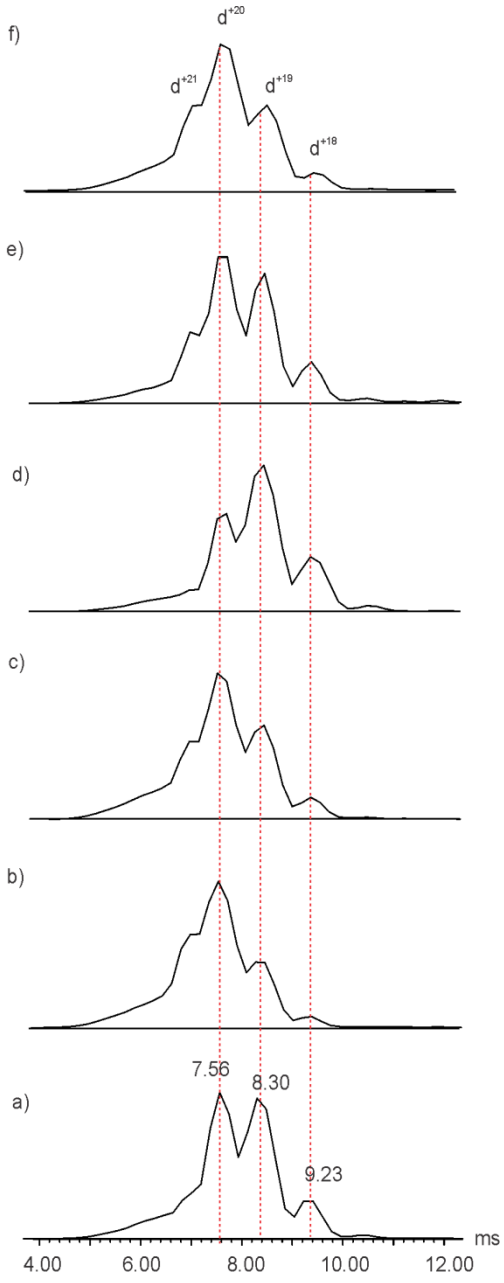

Figure 3.6. Arrival time distributions (ATDs) of **(a)** tubulin (14 μM) mixed with DMSO (% 0.05), and tubulin-colchicine mixture when the concentration ratio are **(b)** 14:2, **(c)** 14:6, **(d)** 14:14, **(e)** 14:20, and **(f)** 14:28 acquired in positive ion mode in ammonium acetate (100 mM, pH 6.8) solution and incubated for 1h at 37 °C.

Taken together, the aforementioned results reveal that, with the current instrumentation, it is not possible to directly quantify tubulin-drug interactions using ESI-MS. Consequently; subsequent efforts were directed towards the possibility of ranking ligand (drug) affinities for tubulin using CaR-ESI-MS. As a starting point, a series of control experiments were carried out to assess the reliability of the approach and to identify optimal instrumental conditions for its implementation. One important requirement when using CaR-ESI-MS to rank affinities based on the relative abundances of the released ligand ions is that the release efficiencies be similar for all of the bound ligands. Because of differences in the nature of the intermolecular interactions for different ligands in the gaseous protein-ligand complex ions, the dissociation (release) rate constants are expected to vary, possibly significantly, between ligands. Consequently, the condition of uniform release efficiencies can only reliably be achieved by fully releasing all bound ligands (i.e., complete dissociation). Based on the changes in the relative abundance of **L1** compared to d^{+19}, the highest abundant charge state of tubulin dimer, versus collision energy (in the Trap region) measured in the mass spectra shown in Figure 3.4b, complete release appears to be achieved at energies ≥120 V. To further support this conclusion, the tubulin ions were subjected to a second stage of CID in the Transfer region. Prior to the second stage of CID, IMS was used to separate the tubulin ions from the **L1** ions released in the Trap region. Shown in Figure 3.7 are the CID (Transfer region) mass spectra acquired for tubulin ions in a solution of tubulin (14 μM) incubated with **L1** (14 μM) tubulin at 37 °C for 1h. From Figure 3.7a, it can be seen L1 is released at the first stage of

CID at Trap 120 V (the maximum release). To confirm that we reached the maximum release at Trap 120 V, second CID was performed at Transfer (60 V) showing no **L1** ions at the same drift time of tubulin were produced (Figure 3.7b), confirming complete release occurred in the Trap region at a collision energy of 120 V. While **L1** is released from ions corresponding to complex at second CID when Trap is less than maximum (e.g. 60 V) and Transfer at 60 V (Figure 3.7d).

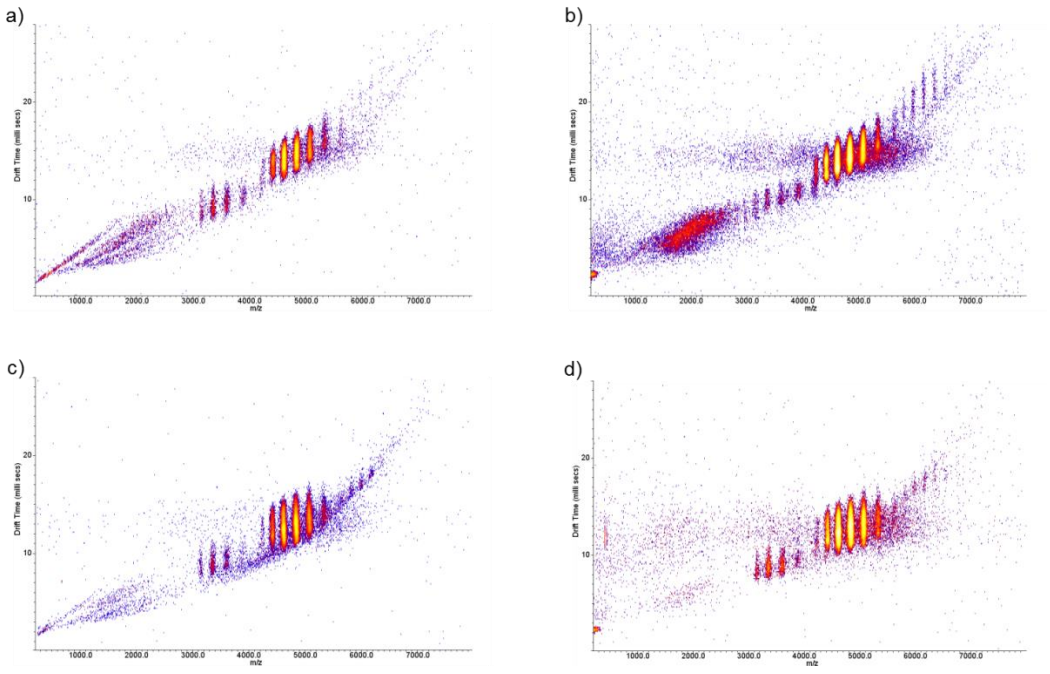

Figure 3.7. IMS mass spectra of tubulin (14 μM) with **L1** (14 μM) incubated at 37 °C for 1 h at pH 6.8 acquired in positive ion mode with parameters set at: **(a)** Trap CID 120 V / Transfer CID 1 V, **(b)** Trap CID 120V / Transfer CID 60 V, **(c)** Trap CID 60 V / Transfer CID 1 V, and **(d)** Trap CID 60 V / Transfer CID 60 V.

To further validate the CaR-ESI-MS assay, it was applied to a solution of a αβ-tubulin (14 μM), **L1** (14 μM) and vincristine (**L9**, 14 μM). These ligands have different binding sites on tubulin and slightly different affinities. As discussed above, the affinity of **L1** for tubulin dimer is reported to be in the 0.5×10^6 to 3×10^6 M^{-1} range, while for **L9** the affinity is slightly lower, 0.1×10^6 to 0.5×10^6 M^{-1}.[5, 32] Shown in Figure 3.7a is a representative ESI mass spectrum acquired for a solution of tubulin (14 μM) with **L1** (14 μM) and **L9** (14 μM); shown in Figures 3.7b-g are CID mass spectra measured in the Trap region at collision energies ranging from 25 to 140 V. Signals corresponding to both protonated **L1** (*m/z* 400.1) and **L9** (*m/z* 825.4) are evident in the CID spectra and their relative abundances (compared to d^{+19}, which is the most abundant charge state of tubulin dimer), increase with collision energy, reaching a maximum at 120 V (Figure 3.8). Notably, measurements performed at different ligand concentrations produced similar agreement with the theoretical ratios (Figure 3.8h).

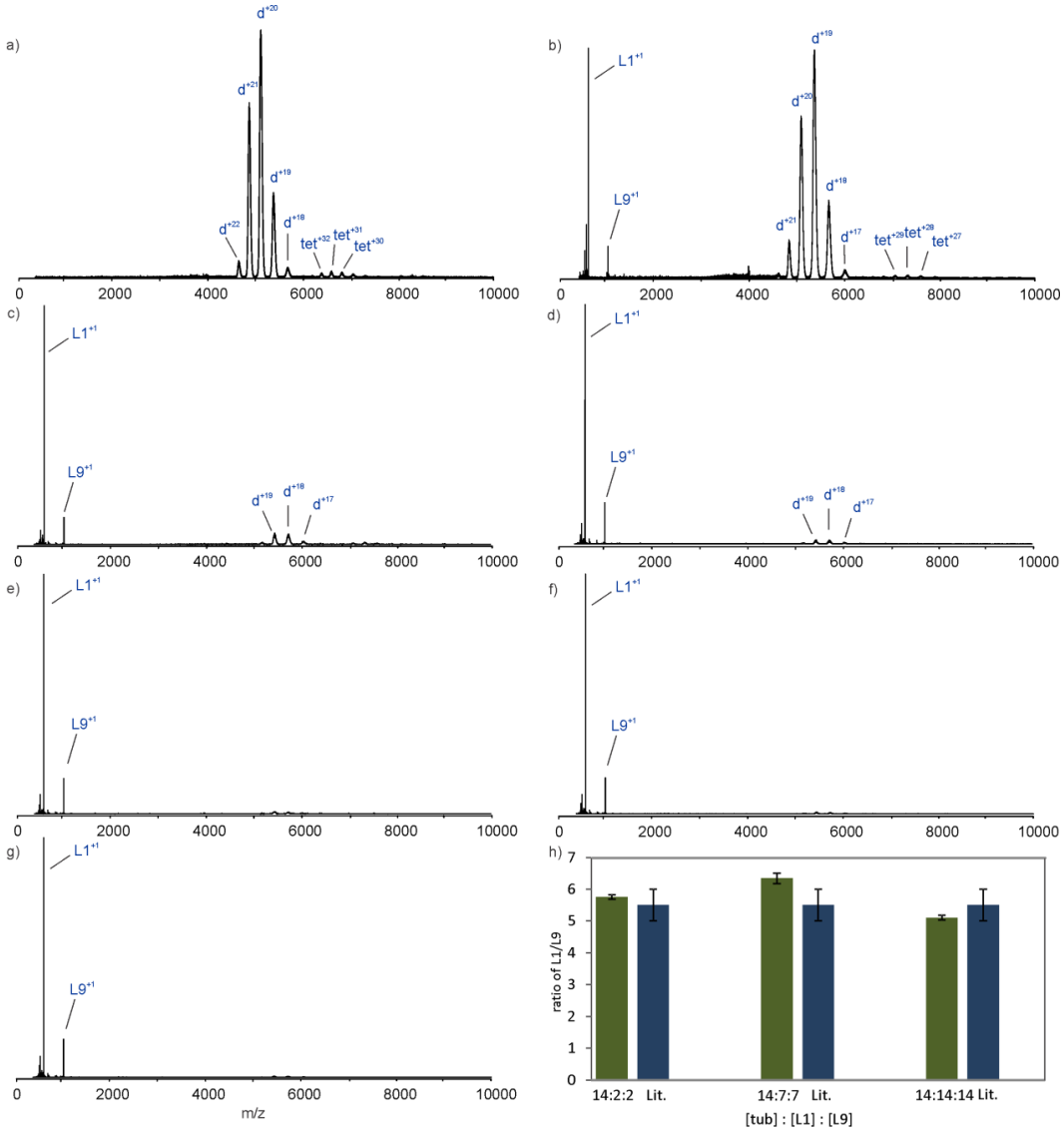

Figure 3.8. (a) Representative ESI mass spectrum acquired in positive ion mode for an aqueous ammonium acetate solution (100 mM) of tubulin (14 μM) at pH 6.8 and 22 °C. CID mass spectra of the tubulin incubated with colchicine and vincristine (14 μM each) at 37 °C for 1 h at Trap voltage 25 **(b)**, 50 **(c)**, 80 **(d)**, 100 **(e)**, 120 **(f)**, and 140 **(g)**. **(h)** Abundance ratio of **L1**/**L9** at three different concentration ratios compared to the binding affinity ratio of **L1**/**L9**.

Analogous measurements were carried out on solutions of αβ-tubulin (14 μM), **L1** (14 μM), vincristine (**L9**) (14 μM) and thiocolchicoside (**L8**) (14 μM). **L8** does not bind to tubulin (microtubule polymerization assay for L8 and L1 was tested by our collaborator to prove that L8 is a non-binder) (data not shown) and served as a negative control. Shown in Figure 3.9a is a representative ESI mass spectrum; the corresponding CID spectrum measured at maximum Trap energy (120 V) is shown in Figure 3.9b. It can be seen that both protonated **L1** and **L9** are released from tubulin. However, signal corresponding to **L8** was not detected under any of the collision energies investigated. Measurements carried out at different concentrations of **L1**, **L8** and **L9** produced similar results (data not shown). The results of these control experiments suggest that the CaR-ESI-MS assay can be used to detect ligand binding to tubulin in solution and, by screening libraries of compounds, to rank their affinities.

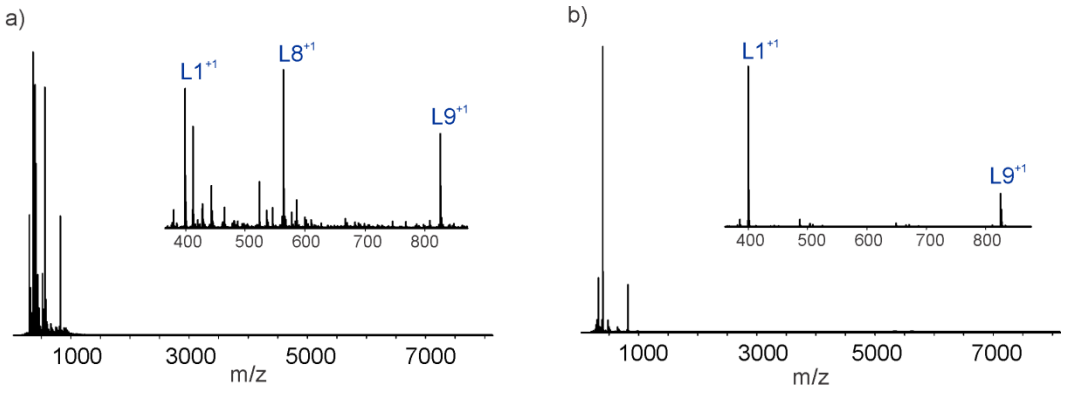

Figure 3.9. (a) ESI mass spectra obtained in positive ion mode for an aqueous ammonium acetate (100 mM) solution of tubulin (14 μM) and **L1**, **L8**, and **L9** (14

μM each), at pH 6.8 and 22 °C. **(b)** CID mass spectrum of the same solution acquired in positive ion mode at Trap voltage of 120 V.

3.3.2 Library screening

Having established the reliability of the CaR-ESI-MS assay for detecting drug binding to tubulin, the assay CaR-ESI-MS was used to screen a small library of colchicinoids (**L1–L7**) against tubulin. Shown in Figure 3.10 are the representative CID mass spectra acquired for an aqueous ammonium acetate (100 mM) solution of αβ-tubulin (14 μM) incubated with the library (**L1–L7**, 2 μM each) at 37 °C for 1 h. Inspection of the mass spectra reveals evidence for the release of all seven ligands as singly protonated ions, **L1** (400.1 *m/z*), **L2** (416.1 *m/z*), **L3** (446.1 *m/z*), **L4** (511.1 *m/z*), **L5** (527.1 *m/z*), **L6** (555.5 *m/z*), **L7** (588.5 *m/z*) (Figure 3.10).

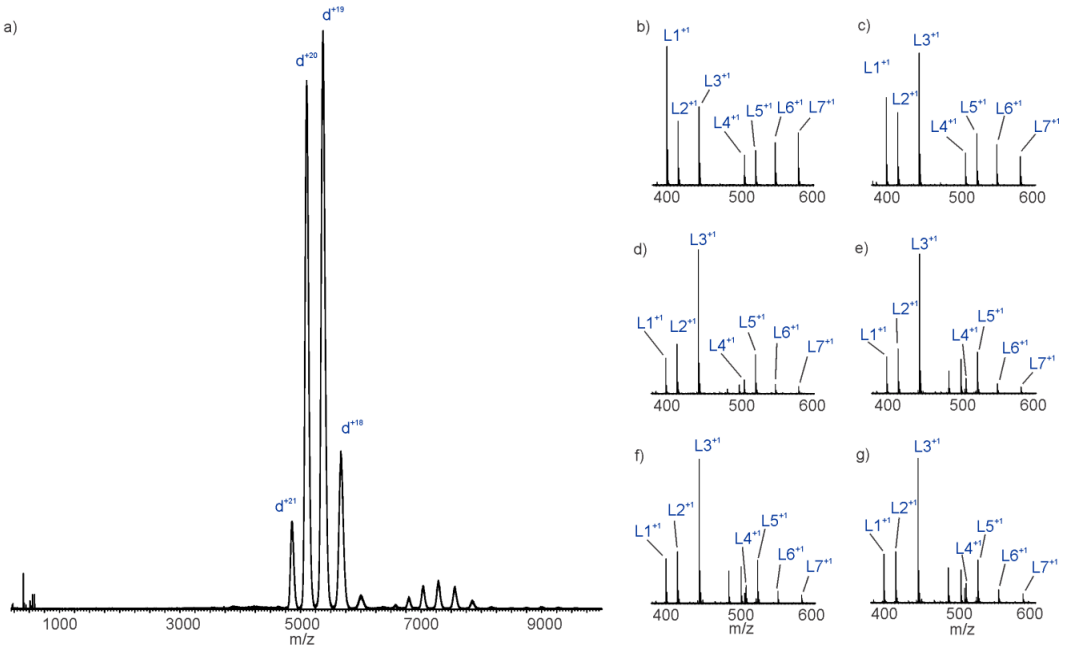

Figure 3.10. ESI-CID mass spectrum of tubulin (14 μM) after incubation with **L1-7** analogues (2 μM each) acquired in positive ion mode (pH 6.8 and 22 °C) at Trap **(a)** 2, **(b)** 25, **(c)** 50, **(d)** 80, **(e)** 100, **(f)** 120, **(g)** 140 V.

Analysis of the relative abundances of the released ligand ions suggests the following trend in affinities: **L3** > **L2** > **L1** ~ **L5** > **L4** > **L6** ~ **L7** (Figure 3.11). To further support these findings, the measurements were repeated at different concentrations of ligands (**L1–L7,** 2 and 7 μM in total) under the same conditions. Notably, similar results were obtained at all of the concentrations investigated.

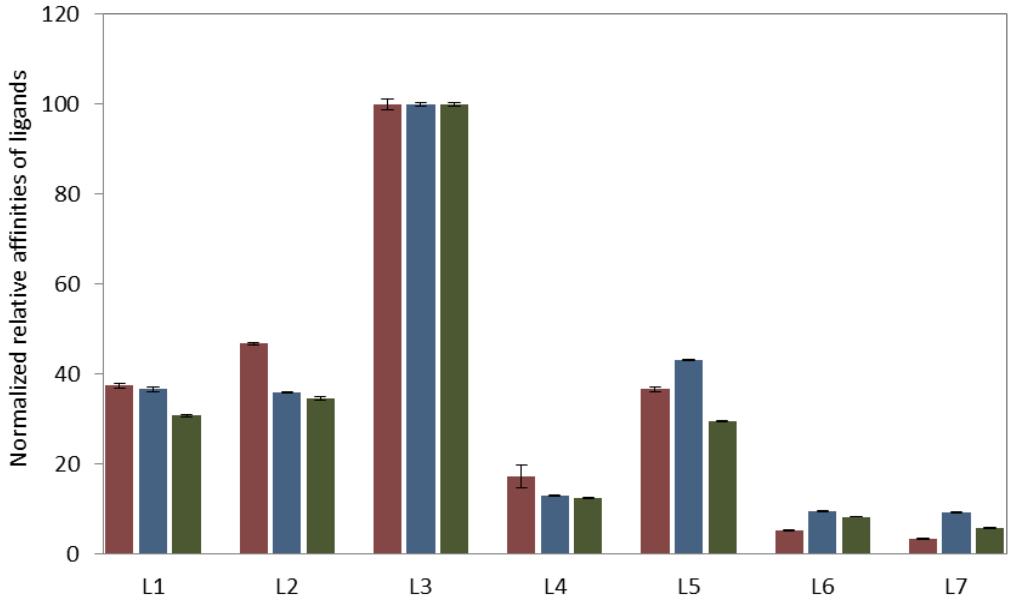

Figure 3.11. Relative affinities of **L1 – L7** for tubulin measured by CaR-ESI-MS acquired in positive ion mode (Trap 120 V) in ammonium acetate (100 mM) solution at pH 6.8 and 22 °C [Tubulin]: [**L1–7**] varies as red represents 14:2, blue 14:7, green 14:14.

3.4 Conclusions

Taken together, the results of this study demonstrate the utility of the CaR-ESI-MS assay for detecting specific drug interactions with tubulin dimers and, when applied to libraries, to rank their affinities. To our knowledge, this is the first reported example of the application of the CaR-ESI-MS assay in the area of anti-cancer drug screening. Proof-of-concept experiments carried out on αβ-tubulin dimers extracted from porcine brain using positive (known ligands) and negative (non-binders) controls were performed to establish the reliability of the assay. The assay was then used to screen a library of seven colchicinoid analogues to test their binding to tubulin and to rank their affinities. Further studies can be performed on each type of β-isotypes to investigate which type of β-tubulin is mainly involved in the binding with colchicinoid analogues.

3.5 Literature cited

1. Nogales, E.; Wolf, S. G.; Downing, K. H. *Nature* **1998,** *391*, 199-203.

2. Bryan, J.; Wilson, L. *Proceedings of the National Academy of Sciences* **1971**, *68*, 1762-1766.

3. Akhmanova, A.; Steinmetz, M. O. *Nature Reviews Molecular Cell Biology* **2008,** *9*, 309-322.

4. Nogales, E.; Wang, H.-W. *Current Opinion in Cell Biology* **2006,** *18*, 179-184.

5. Calligaris, D.; Verdier-Pinard, P.; Devred, F.; Villard, C.; Braguer, D.; Lafitte, D. *Cellular and molecular life sciences* **2010,** *67*, 1089-1104.

6. Lewis, S. A.; Wang, D.; Cowan, N. J. *Science* **1988**, *11*, 936-939.

7. Sullivan, K. F.; Cleveland, D. W. *Proceedings of the National Academy of Sciences* **1986**, *83*, 4327-4331.

8. Ballestrem, C.; Magid, N.; Zonis, J.; Shtutman, M.; Bershadsky, A. In Interplay between the Actin Cytoskeleton, Focal Adhesions and Microtubules, Ridley, A.; Peckham, M.; Clark, P., Eds. Chichester, Wiley: **2004**; pp 75-99.

9. Mane, J. Y.; Semenchenko, V.; Perez-Pineiro, R.; Winter, P.; Wishart, D.; Tuszynski, J. A. *Chemical Biology & Drug Design* **2013,** *82*, 60-70.

10. Kline-Smith, S. L.; Walczak, C. E. *Molecular Cell* **2004,** *15*, 317-327.

11. Wilson, L.; Panda, D.; Ann Jordan, M. *Cell Structure and Function* **1999,** *24*, 329-335.

12. Schiff, P. B.; Fant, J.; Horwitz, S. B. *Nature* **1979,** *277*, 665-667.

13. Bollag, D. M.; McQueney, P. A.; Zhu, J.; Hensens, O.; Koupal, L.; Liesch, J.; Goetz, M.; Lazarides, E.; Woods, C. M. *Cancer Research* **1995,** *55*, 2325-2333.

14. Canales, A.; Rodriguez-Salarichs, J.; Trigili, C.; Nieto, L.; Coderch, C.; Andreu, J. M.; Paterson, I.; Jimenez-Barbero, J.; Diaz, J. F. *American Chemical Society Chemical Biology* **2011,** *6*, 789-799.

15. Wilmes, A.; Bargh, K.; Kelly, C.; Northcote, P. T.; Miller, J. H. *Molecular Pharmaceutics* **2007,** *4*, 269-280.

16. Bhattacharyya, B.; Panda, D.; Gupta, S.; Banerjee, M. *Medicinal research Reviews* **2008,** *28*, 155-183.

17. Gigant, B.; Wang, C.; Ravelli, R. B. G.; Roussi, F.; Steinmetz, M. O.; Curmi, P. A.; Sobel, A.; Knossow, M. *Nature* **2005**, 519-522.

18. Bai, R.; Pettit, G. R.; Hamel, E. *Biochemical Pharmacology* **1990,** *39*, 1941-1949.

19. Anderson, H. J.; Coleman, J. E.; Andersen, R. J.; Roberge, M. *Cancer Chemotherapy And Pharmacology* **1997,** *39*, 223-226.

20. Jordan, M. A.; Wilson, L. *Nature Reviews Cancer* **2004,** *4*, 253-265.

21. Ravelli, R. B. G.; Gigant, B.; Curmi, P. A.; Jourdain, I.; Lachkar, S.; Sobel, A.; Knossow, M. *Nature* **2004,** *428*, 198-202.

22. Schlesinger, N.; Schumacher, R.; Catton, M.; Maxwell, L. *The Cochrane Library* **2006,** 1-16.

23. Richette, P.; Bardin, T. *Expert Openion on Pharmacotheraphy* **2010,** *11*, 2933-2938.

24. Dustin, P., Microtubules. Berlin ; New York : Springer-Verlag, **1978**.: 1978.

25. Sun, L.; Vasilevich, N. I.; Fuselier, J. A.; Coy, D. H. *Anticancer Research* **2004,** *24*, 179-186.

26. Haar, E. T.; Rosenkranz, H. S.; Hamel, E.; Day, B. W. *Bioorganic and Medicinal Chemistry* **1996,** *4*, 1659-1671.

27. Fernando Díaz, J.; Andreu, J. M. *The Journal of Biological Chemistry* **1991,** *266*, 2890-2896.

28. Menéndez, M.; Laynez, J.; Medrano, F. J.; Andreu, J. M. *The Journal Of Biological Chemistry* **1989,** *264*, 16367-16371.

29. Andreu, J. M.; Gorbunoff, M. J.; Medrano, F. J.; Rossi, M.; Timasheff, S. N. *Biochemistry* **1991,** *30*, 3777-3786.

30. Hastie, S. B. *Pharmacology & Therapeutics* **1991,** *51*, 377-401.

31. Banerjee, A.; Luduena, R. F. *The Journal Of Biological Chemistry* **1992,** *267*, 13335-13339.

32. Tahir, S. K.; Kovar, P.; Rosenberg, S. H.; Ng, S. C. *Biotechniques* **2000,** *29*, 156-160.

33. Chabin, R. M.; Hastie, S. B. *Biochemical And Biophysical Research Communications* **1989,** *161*, 544-550.

34. Loo, J. A. *Mass Spectrometry Reviews* **1997,** *16*, 1-23.

35. Daniel, J. M.; Friess, S. D.; Rajagopalan, S.; Wendt, S.; Zenobi, R. *International Journal of Mass Spectrometry* **2002,** *216*, 1-11.

36. Heck, A. J. R.; Van Den Heuvel, R. H. H. *Mass Spectrometry Reviews* **2004,** *23*, 368-389.

37. Gabelica, V.; Rosu, F.; De Pauw, E. *Analytical Chemistry* **2009**, 6708-6715.

38. El-Hawiet, A.; Shoemaker, G. K.; Daneshfar, R.; Kitova, E. N.; Klassen, J. S. *Analytical Chemistry* **2012,** *84*, 50-58.

39. Han, L.; Kitova, E.; Tan, M.; Jiang, X.; Klassen, J. *Journal of the American Society for Mass Spectrometry* **2014,** *25*, 111-119.

40. Leney, A. C.; Fan, X.; Kitova, E. N.; Klassen, J. S. *Analytical Chemistry* **2014,** *86*, 5271-5277.

41. Cheng, X.; Chen, R.; Bruce, J. E.; Schwartz, B. L.; Anderson, G. A.; Hofstadler, S. A.; Gale, D. C.; Smith, R. D.; Gao, J.; Sigal, G. B.; Mammen, M.; Whitesides, G. M. *Journal of the American Chemical Society* **1995**, 8859-8860.

42. Gao, J.; Cheng, X.; Chen, R.; Sigal, G. B.; Bruce, J. E.; Schwartz, B. L.; Hofstadler, S. A.; Anderson, G. A.; Smith, R. D.; Whitesides, G. M. *Journal Of Medicinal Chemistry* **1996,** *39*, 1949-1955.

43. Han, L.; Kitova, E. N.; Tan, M.; Jiang, X.; Klassen, J. S. *Journal Of The American Society for Mass Spectrometry* **2014,** *25*, 111-119.

44. Zhang, Y.; Liu, L.; Daneshfar, R.; Kitova, E. N.; Li, C.; Jia, F.; Cairo, C. W.; Klassen, J. S. *Analytical Chemistry* **2012,** *84*, 7618-7621.

45. El-Hawiet, A.; Kitova, E. N.; Klassen, J. S. *Analytical Chemistry* **2013,** *85*, 7637-7644.

46. Han, L.; Tan, M.; Xia, M.; Kitova, E. N.; Jiang, X.; Klassen, J. S. *Journal Of The American Chemical Society* **2014,** *136*, 12631-12637.

47. Luduena, R. F. *Molecular Biology of the Cell* **1993**, *4*, 445-457.

48. Redeker, V.; Melki, R.; Prome, D.; Le Caer, J-P.; Rossier, J. *Federation of European Biochemical Societies* **1992**, *313*, 185-192.

49. Kitova, E. N.; El-Hawiet, A.; Schnier, P. D.; Klassen, J. S. *Journal Of The American Society for Mass Spectrometry* **2012,** *23*, 431-441.

50. Wang, W. J.; Kitova, E. N.; Klassen, J. S. *Analytical Chemistry* **2005,** *77*, 3060-3071.

Chapter 4

Conclusions and Future Work

This work describes the development and application of ESI-MS methods to study the kinetic of enzymatic reactions of glycolipids in different soluble lipid environments in the first research project. The second research project highlights the potential of ESI-MS to distinguish the relative affinities of new anti-cancer drugs against target protein.

In chapter 2, the application of the direct ESI-MS assay for studying the enzyme kinetics of glycolipids was described. In addition to conventional spectroscopic assays for enzyme kinetic studies, ESI-MS assay could benefit from several advantages including not requiring of labeling or modification, the ability to detect substrates as well as products simultaneously, and low sample consumption. To validate our ESI-MS kinetic assay, the relative rates of hydrolysis of soluble synthesized glycolipids obtained from ESI-MS assay were compared with fluorescence-based assay. Due to the insolubility of glycolipids, the enzymatic studies of glycolipids was performed in three soluble lipid platforms including micelles, nanodiscs (incorporation of glycolipids into synthetic phospholipid bilayers), and picodiscs (a novel presentation of glycolipids in a natural lysosomal sphingolipid activator protein). To compare the enzyme kinetics of each platform, the formation of sialic acid (SIA) was monitored over time. ESI-CID-MS was also used to induce the dissociation of discs to be able to track the substrates depletion. The finding from both

monitoring methods demonstrates that picodiscs provide a better presentation for the hydrolysis of glycolipids.

There are several possible extensions of the enzyme kinetic assay. As mentioned in chapter 2, the linkage in soluble substrates **S1**, **S2**, and **S3** is α(2,3) and these substrates with α(2,6) linkage are also synthesized. The kinetic of hydrolysis of α(2,6)-substrates can also be studied by ESI-MS assay in addition to fluorescence-based assay. Similar studies have been tested the characteristic substrate preferences of neuraminidases (NEU1-4) by Pshezhetsky et al.[1] Therefore, the kinetic assay findings on α(2,3)- and α(2,6)-substrates can provide useful information about the hNEU3 mechanism of interaction, and how the linkage (steric hindrance) affects the enzymatic reactions.[2] Moreover, there is a possibility of testing all six substrates with hNEU2 and hNEU4 to observe which one is a better substrate for which enzyme.

Another extension to the enzyme kinetic chapter is investigating the reasons of observing fast kinetic in picodiscs compared to micelles and nanodiscs. The initial thoughts to answer this question are measuring the binding of mutant-inactive hNEU3 with glycolipids in PDs, NDs, or micelles. The binding results could show whether the fast kinetics of picodiscs is due to higher binding affinity of glycolipids in picodiscs with enzyme or not.

In chapter 3, catch-and-release (CaR)-ESI-MS approach was employed for the first time to screen new anti-cancer drugs against tubulin for specific interactions. In this study, we demonstrated the applicability of the CaR-ESI-MS in cases where the distinguishing the complex from free protein is not feasible.

Proof-of-concept experiments have been performed to test the reliability of our assay to detect specific interactions of tubulin. The relative affinities of bound ligands were obtained using collision-induced dissociation (CID) of ions corresponding to complex. The use of ion mobility separation (IMS) apart from applying a range of voltages to the complex in Trap and Transfer region allowed for the maximum release of ligands. As a result, **L3** out of **L1-7** colchicine analogues demonstrated higher release and consequently, higher relative affinity.

The relevant future work to chapter 3 is to use the CaR-ESI-MS assay to study the binding of colchicine analogues with different isotypes of αβ-tubulin. These investigations can be performed on recombinant monomer (αI, αII, βI, βII, and etc.) and dimer forms (αIβI, αIβII, αIIβI, αIIβII, and etc.) of α- and β-tubulin to figure out the relative affinities of drugs to each isotype. Similar studies have been performed on αβII- and αβIII-tubulin using fluorescence-based assay,[3] therefore, the findings could give us more information about the role of each isotype in the area of drug development.

Since our CaR-ESI-MS is a general method for screening the ligands against the target protein, this assay could also be used for screening other libraries of anti-cancer drugs such as noscapine and combretastatin A-4 against αβ-tubuin.

4.1 Literature cited

1. Smutova, V.; Albohy, A.; Pan, X. F.; Korchagina, E.; Miyagi, T.; Bovin, N.; Cairo, C. W.; Pshezhetsky, A. V. *Public Library of Science One* **2014,** *9,* 1-10.

2. Cairo, C. W. *Medchemcomm* **2014,** *5*, 1067-1074.

3. Mane, J. Y.; Semenchenko, V.; Perez-Pineiro, R.; Winter, P.; Wishart, D.; Tuszynski, J. A. *Chemical Biology and Drug Design* **2013,** *82*, 60-70.

Literature cited

Chapter 1

1. Cleveland, D. W.; Mao, Y.; Sullivan, K. F. *Cell* **2003**, *112*, 407-421.

2. Igakura, T.; Stinchcombe, J. C.; Goon, P. K. C.; Taylor, G. P.; Weber, J. N.; Griffiths, G. M.; Tanaka, Y.; Osame, M.; Bangham, C. R. M. *Science* **2003**, 1713-1715.

3. Waldron, K. J.; Robinson, N. J. *Nature Reviews Microbiology* **2009**, *7*, 25-35.

4. Berg, J. M. *Annual Review of Biophysics and Biophysical Chemistry* **1990**, *19*, 405-421.

5. Anderson, B. F.; Baker, H. M.; Dodson, E. J.; Norris, G. E.; Rumball, S. V.; Waters, J. M.; Baker, E. N., *Proceedings of the National Academy of Sciences* **1987**, *84*, 1769-1773.

6. Saboury, A. A. *Journal of the Iranian Chemical Society* **2006**, *3*, 1-21.

7. Wilcox, D. E. *Inorganica Chimica Acta* **2008**, *361*, 857-867.

8. Velázquez Campoy, A.; Freire, E. *Biophysical Chemistry* **2005**, *115*, 115-124.

9. Utsuno, K.; UludaA, H. *Biophysical Journal* **2010**, *99*, 201-207.

10. Daghestani, H. N.; Day, B. W. *Sensors* **2010**, *10*, 9630-9646.

11. De Crescenzo, G.; Boucher, C.; Durocher, Y.; Jolicoeur, M. *Cellular and Molecular Bioengineering* **2008**, *1*, 204-215.

12. Karlsson, R. *Journal of Molecular Recognition* **2004**, *17*, 151-161.

13. Schuck, P. *Annual Review of Biophysics And Biomolecular Structure* **1997**, *26*, 541-566.

14. Homola, J. *Analytical & Bioanalytical Chemistry* **2003**, *377*, 528-539.

15. Loo, J. A. *Mass Spectrometry Reviews* **1997**, *16*, 1-23.

16. Fangel, J. U.; Pedersen, H. L.; Vidal-Melgosa, S.; Ahl, L. I.; Salmean, A. A.; Egelund, J.; Rydahl, M. G.; Clausen, M. H.; Willats, W. G. T. *Methods In Molecular Biology* **2012**, *918*, 351-362.

17. Wishart, D. *Current Pharmaceutical Biotechnology* **2005**, *6*, 105-120.

18. Angulo, J.; Rademacher, C.; Biet, T.; Benie, A. J.; Blume, A.; Peters, H.; Palcic, M.; Parra, F.; Peters, T. *Methods in Enzymology* **2006**, *416*, 12-30.

19. Shuker, S. B.; Hajduk, P. J.; Meadows, R. P.; Fesik, S. W., *Science* **1996**, 274, 1531-1534.

20. Zech, S. G.; Olejniczak, E.; Hajduk, P.; Mack, J.; McDermot, A. E. *Journal of the American Chemical Society* **2004**, *126*, 13948-13953.

21. Gizachew, D.; Dratz, E. *Chemical Biology and Drug Design* **2011**, *78*, 14-24.

22. Mayer, M.; Meyer, B. *Angewandte Chemie-International edition* **1999**, *38*, 1784-1788.

23. Mayer, M.; Meyer, B. *Journal of the American Chemical Society* **2001**, *123*, 6108-6117.

24. Haselhorst, T.; Lamerz, A.-C.; Itzstein, M. v. Methods in Molecular Biology, Glycomics: Methods and Protocols **2009**, *534*, pp 375-386.

25. Viegas, A.; Manso, J.; Nobrega, F. L.; Cabrita, E. J. *Journal of Chemical Education* **2011**, *88*, 990-994.

26. Palmer, R. A.; Niwa, H. *Biochemical Society Transactions* **2003**, *31*, 973-979.

27. Greco, A.; Ho, J. G. S.; Lin, S.-J.; Palcic, M. M.; Rupnik, M.; Ng, K. K. S. *Nature Structural and Molecular Biology* **2006**, *13*, 460-461.

28. Jason, G. S. H.; Antonio, G.; Maja, R.; Kenneth, K. S. N.; Levitt, M., *Proceeding of the National Academy of Sciences* **2005**, 18373-18378.

29. Staunton, D.; Owen, J.; Campbell, I. D. *Accounts of Chemical Research* **2003**, *36*, 207-214.

30. Bizzarri, A. R.; Cannistraro, S. *Journal of Physical Chemistry B* **2009**, *113*, 16449-16464.

31. Hill, J. J.; Royer, C. A. *Methods In Enzymology* **1997**, *278*, 390-416.

32. Malnasi-Csizmadia, A.; Pearson, D. S.; Kovacs, M.; Woolley, R. J.; Geeves, M. A.; Bagshaw, C. R. *Biochemistry* **2001**, 12727-12737.

33. Srisa-Art, M.; Dyson, E. C.; deMello, A. J.; Edel, J. B. *Analytical Chemistry* **2008**, 7063-7069.

34. Bao, J.; Krylova, S. M.; Wilson, D. J.; Reinstein, O.; Johnson, P. E.; Krylov, S. N. *Chembiochem: A European Journal Of Chemical Biology* **2011**, *12*, 2551-2554.

35. Kitova, E. N.; Bundle, D. R.; Klassen, J. S. *Journal of the American Chemical Society* **2002**, 5902-5913.

36. Wang, W. J.; Kitova, E. N.; Klassen, J. S. *Analytical Chemistry* **2005**, *77*, 3060-3071.

37. Sun, J.; Kitova, E. N.; Wang, W.; Klassen, J. S. *Analytical Chemistry* **2006**, *78*, 3010-3018.

38. Liu, L.; Bagal, D.; Kitova, E. N.; Schnier, P. D.; Klassen, J. S. *Journal of the American Chemical Society* **2009**, *131*, 15980-15981.

39. Kitova, E. N.; El-Hawiet, A.; Schnier, P. D.; Klassen, J. S. *Journal of the American Society for Mass Spectrometry* **2012**, *23*, 431-441.

40. Konermann, L.; Collings, B. A.; Douglas, D. J. *Biochemistry* **1997**, *36*, 5554-5559.

41. Lee, V. W.; Chen, Y. L.; Konermann, L. *Analytical Chemistry* **1999**, *71*, 4154-4159.

42. Sobott, F.; Benesch, J. L. P.; Vierling, E.; Robinson, C. V. *Journal of Biological Chemistry* **2002**, *277*, 38921-38929.

43. Simmons, D. A.; Wilson, D. J.; Lajoie, G. A.; Doherty-Kirby, A.; Konermann, L. *Biochemistry* **2004**, *43*, 14792-14801.

44. Deng, G.; Sanyal, G. *Journal of Pharmaceutical And Biomedical Analysis* **2006**, *40*, 528-538.

45. Pan, J.; Rintala-Dempsey, A. C.; Li, Y.; Shaw, G. S.; Konermann, L. *Biochemistry* **2006**, *45*, 3005-3013.

46. Sharon, M.; Robinson, C. V. *Annual Review of Biochemistry* **2007**, *76*, 167-193.

47. Clarke, D. J.; Stokes, A. A.; Langridge-Smith, P.; Mackay, C. L. *Analytical Chemistry* **2010**, *82*, 1897-1904.

48. Robbins, M. D.; Yoon, O. K.; Barbula, G. K.; Zare, R. N. *Analytical Chemistry* **2010**, *82*, 8650-8657.

49. Miao, Z.; Chen, H.; Liu, P.; Liu, Y. *Analytical Chemistry* **2011**, *83*, 3994-3997.

50. Pacholarz, K. J.; Garlish, R. A.; Taylor, R. J.; Barran, P. E. *Chemical Society Reviews* **2012**, *41*, 4335-4355.

51. Kitova, E. N.; Bundle, D. R.; Klassen, J. S. *Angewandte Chemie-International Edition* **2004**, *43*, 4183-4186.

52. Shoemaker, G. K.; Kitova, E. N.; Palcic, M. M.; Klassen, J. S. *Journal Of The American Chemical Society* **2007**, *129*, 8674-8675.

53. Kitova, E. N.; Mikyung, S.; Roy, P.-N.; Klassen, J. S. *Journal of the American Chemical Society* **2008**, *130*, 1214-1226.

54. Liu, L.; Michelsen, K.; Kitova, E. N.; Schnier, P. D.; Klassen, J. S. *Journal Of The American Chemical Society* **2010**, *132*, 17658-17660.

55. Liesener, A.; Karst, U. *Analytical & Bioanalytical Chemistry* **2005**, *382*, 1451-1464.

56. Eisenthal, R.; Danson, M. J., Enzyme assays: a practical approach. Oxford, OX ; New York : Oxford University Press, **2002**. 2nd ed.: **2002**.

57. Harris, T. K.; Keshwani, M. M. Guide to Protein Purification, 2nd ed.: **2009**, *463*, 57-71.

58. Wallenfels, K. *Methods in Enzymology* **1962**, *5*, 212-219.

59. Zechel, D. L.; Konermann, L.; Withers, S. G.; Douglas, D. J. *Biochemistry* **1998**, *37*, 7664-7669.

60. Bothner, B.; Chavez, R.; Wei, J.; Strupp, C.; Phung, Q.; Schneemann, A.; Siuzdak, G. *The Journal of Biological Chemistry* **2000**, *275*, 13455-13459.

61. Ge, X.; Sirich, T. L.; Beyer, M. K.; Desaire, H.; Leary, J. A. *Analytical Chemistry* **2001**, *73*, 5078-5082.

62. Gao, H.; Petzold, C. J.; Leavell, M. D.; Leary, J. A. *Journal of the American Society for Mass Spectrometry* **2003**, *14*, 916-924.

63. Gao, H.; Leary, J. A. *Analytical Biochemistry* **2004**, *329*, 269-275.

64. Pi, N.; Hoang, M. B.; Gao, H.; Mougous, J. D.; Bertozzi, C. R.; Leary, J. A. *Analytical Biochemistry* **2005**, *341*, 94-104.

65. Danan, L. M.; Yu, Z.; Ludden, P. J.; Jia, W.; Moore, K. L.; Leary, J. A. *Journal of the American Society for Mass Spectrometry* **2010**, *21*, 1633-1642.

66. Soya, N.; Fang, Y.; Palcic, M. M.; Klassen, J. S. *Glycobiology* **2011**, *21*, 547-552.

67. Rob, T.; Wilson, D. J. *European Journal of Mass Spectrometry* **2012**, *18*, 205-214.

68. Covey, T. R.; Thomson, B. A.; Schneider, B. B. *Mass spectrometry reviews* **2009,** *28*, 870-897.

69. Ganem, B.; Li, Y. T.; Henion, J. D. *Journal of the American Chemical Society* **1991**, *113*, 6294-6296.

70. Drummond, J. T.; Loo, R. R. O.; Matthews, R. G. *Biochemistry* **1993**, 9282.

71. Deroo, S.; Hyung, S. J.; Marcoux, J.; Gordiyenko, Y.; Koripella, R. K.; Sanyal, S.; Robinson, C. V. *Chemical Biology* **2012**, *7*, 1120-1127.

72. Rosu, F.; Gabelica, V.; Shin-ya, K.; De Pauw, E. *Chemical Communications* **2003**, 2702-2703.

73. Gabelica, V.; Rosu, F.; De Pauw, E. *Analytical Chemistry* **2009**, *81*, 6708-6715.

74. Kebarle, P.; Verkerk, U. H. *Mass spectrometry reviews* **2009**, *28*, 898-917.

75. Wu, X. Y.; Oleschuk, R. D.; Cann, N. M. *Analyst* **2012**, *137*, 4150-4161.

76. Rayleigh, L. *Philosophical Magazine Series 5* **1882**, *14*, 184-187.

77. Fenn, J. B. *Angewandte Chemie-International Edition* **2003**, *42*, 3871-3894.

78. Cech, N. B.; Enke, C. G. *Mass Spectrometry Reviews* **2001**, *20*, 362-387.

79. Nguyen, S.; Fenn, J. B., *Proceedings of the National Academy of Sciences* **2007**, *23*, 1111-1117.

80. Konermann, L.; Ahadi, E.; Rodriguez, A. D.; Vahidi, S. *Analytical Chemistry* **2013**, *85*, 2-9.

81. Hogan, C. J., Jr.; Carroll, J. A.; Rohrs, H. W.; Biswas, P.; Gross, M. L. *Journal of the American Chemical Society* **2009,** *81*, 369-377.

82. Ahadi, E.; Konermann, L. *Journal of Physical Chemistry B* **2012**, *116*, 104-112.

83. Konermann, L.; Rodriguez, A. D.; Jiangjiang, L. *Analytical Chemistry* **2012**, *84*, 6798-6804.

84. Wilm, M.; Mann, M. *Analytical Chemistry* **1996**, 1-10.

85. Karas, M.; Bahr, U.; Dülcks, T. *Analytical Chemistry* **2000**, *366*, 669-676.

86. Juraschek, R.; Dulcks, T.; Karas, M. *Journal of the American Chemical Society for Mass Spectrometry* **1999**, *10*, 300-308.

87. Hoffmann, E. d.; Stroobant, V., Mass spectrometry: Principles and Applications. Chichester, England; Hoboken, NJ : J. Wiley, **2007**. 3rd ed. Edmond de Hoffmann, Vincent Stroobant.: **2007**.

88. Pringle, S. D.; Giles, K.; Wildgoose, J. L.; Williams, J. P.; Slade, S. E.; Thalassinos, K.; Bateman, R. H.; Bowers, M. T.; Scrivens, J. H. *International Journal of Mass Spectrometry* **2007**, *261*, 1-12.

89. Karasek, F. W. *Analytical Chemistry* **1974**, *46*, 710-710.

90. McCullough, B. J.; Kalapothakis, J.; Eastwood, H.; Kemper, P.; MacMillan, D.; Taylor, K.; Dorin, J.; Barran, P. E. *Analytical Chemistry* **2008**, *80*, 6336-6344.

91. Armenta, S.; Alcala, M.; Blanco, M. *Analytica Chimica Acta* **2011**, *703*, 114-123.

92. Cohen, M. J.; Karasek, F. W. *Journal of Chromatographic Science* **1970**, *8*, 330-337.

93. Buryakov, I. A.; Krylov, E. V.; Nazarov, E. G.; Rasulev, U. K. *International Journal of Mass Spectrometry and Ion Processes* **1993**, *128*, 143-148.

94. Shvartsburg, A. A.; Smith, R. D. *Analytical Chemistry* **2008**, 9689-9697.

95. Wildgoose, J.; McKenna, T.; Hughes, C.; Giles, K.; Pringle, S.; Campuzano, I.; Langridge, J.; Bateman, R. H. *Molecular and Cellular Proteomics* **2006**, *5*, S14-S14.

96. Ruotolo, B. T.; Benesch, J. L. P.; Sandercock, A. M.; Hyung, S.-J.; Robinson, C. V. *Nature Protocols* **2008**, *3*, 1139-1152.

97. Wang, W.; Kitova, E. N.; Klassen, J. S. *Methods In Enzymology* **2003**, *362*, 376-397.

98. Wortmann, A.; Rossi, F.; Lelais, G.; Zenobi, R. *Journal of Mass Spectrometry* **2005**, *40*, 777-784.

99. Abzalimov, R. R.; Dubin, P. L.; Kaltashov, I. A. *Analytical Chemistry* **2007**, *97*, 6055-6063.

100. Cederkvist, F.; Zamfir, A. D.; Bahrke, S.; Eijsink, V. G. H.; Sorlie, M.; Peter-Katalinic, J.; Peter, M. G. *Angewandte Chemie-International Edition* **2006,** *45*, 2429-2434.

101. El-Hawiet, A.; Shoemaker, G. K.; Daneshfar, R.; Kitova, E. N.; Klassen, J. S. *Analytical Chemistry* **2012,** *84*, 50-58.

102. Wyttenbach, T.; Bowers, M. T. *Annual Review of Physical Chemistry* **2007**, *58*, 511-33.

103. Sun, N.; Sun, J.; Kitova, E. N.; Klassen, J. S. *Journal Of The American Society For Mass Spectrometry* **2009**, *20*, 1242-1250.

104. Kitova, E. N.; Soya, N.; Klassen, J. S. *Analytical Chemistry* **2011**, *83*, 5160-5167.

Chapter 2

1. Hakomori, S. I. *Annual Review of Biochemistry* **1981,** *50*, 733-764.

2. Hakomori, S. I. *Journal of Biological Chemistry* **1990,** *265*, 18713-18716.

3. Cohen, M.; Varki, A. *Omics-a Journal of Integrative Biology* **2010,** *14*, 455-464.

4. Byrne, B.; Donohoe, G. G.; O'Kennedy, R. *Drug Discovery Today* **2007,** *12*, 319-326.

5. Bieberich, E.; Liour, S. S.; Yu, R. K. *Sphingolipid Metabolism and Cell Signaling, Pt B* **2000,** *312*, 339-358.

6. Schauer, R. *Current Opinion in Structural Biology* **2009,** *19*, 507-514.

7. Lopez, P. H. H.; Schnaar, R. L. *Current Opinion in Structural Biology* **2009,** *19*, 549-557.

8. Sakarya, S.; Oncu, S. *Medical Science Monitor : International Medical Journal of Experimental and Clinical Research* **2003,** *9*, 76-82.

9. Suzuki, Y.; Ito, T.; Suzuki, T.; Holland, R. E.; Chambers, T. M.; Kiso, M.; Ishida, H.; Kawaoka, Y. *Journal of Virology* **2000,** *74*, 11825-11831.

10. Viswanathan, K.; Chandrasekaran, A.; Srinivasan, A.; Raman, R.; Sasisekharan, V.; Sasisekharan, R. *Glycoconjugate Journal* **2010,** *27*, 561-570.

11. Lasky, L. A. *Science* **1992,** *258*, 964-969.

12. Lowe, J. B. *Current Opinion in Cell Biology* **2003,** *15*, 531-538.

13. Mabry, E. W.; Carubelli, R. *Experientia* **1972,** *28*, 182-183.

14. Hakomori, S. *Proceedings of the National Academy of Sciences* **2002,** *99*, 10231-10233.

15. Rual, J. F.; Venkatesan, K.; Hao, T.; Hirozane-Kishikawa, T.; Dricot, A.; Li, N.; Berriz, G. F.; Gibbons, F. D.; Dreze, M.; Ayivi-Guedehoussou, N.; Klitgord, N.; Simon, C.; Boxem, M.; Milstein, S.; Rosenberg, J.; Goldberg, D. S.; Zhang, L. V.; Wong, S. L.; Franklin, G.; Li, S. M.; Albala, J. S.; Lim, J. H.; Fraughton, C.; Llamosas, E.; Cevik, S.; Bex, C.; Lamesch, P.; Sikorski, R. S.; Vandenhaute, J.; Zoghbi, H. Y.; Smolyar, A.; Bosak, S.; Sequerra, R.; Doucette-Stamm, L.; Cusick, M. E.; Hill, D. E.; Roth, F. P.; Vidal, M. *Nature* **2005,** *437*, 1173-1178.

16. Yanagisawa, K.; Odaka, A.; Suzuki, N.; Ihara, Y. *Nature Medicine* **1995,** *1*, 1062-1066.

17. Maglione, V.; Marchi, P.; Di Pardo, A.; Lingrell, S.; Horkey, M.; Tidmarsh, E.; Sipione, S. *Journal of Neuroscience* **2010,** *30*, 4072-4080.

18. Bembi, B.; Marsala, S. Z.; Sidransky, E.; Ciana, G.; Carrozzi, M.; Zorzon, M.; Martini, C.; Gioulis, M.; Pittis, M. G.; Capus, L. *Neurology* **2003,** *61*, 99-101.

19. Battula, V. L.; Shi, Y.; Evans, K. W.; Wang, R.-Y.; Spaeth, E. L.; Jacamo, R. O.; Guerra, R.; Sahin, A. A.; Marini, F. C.; Hortobagyi, G.; Mani, S. A.; Andreeff, M. *Journal of Clinical Investigation* **2012,** *122*, 2066-2078.

20. Marquina, G.; Waki, H.; Fernandez, L. E.; Kon, K.; Carr, A.; Valiente, O.; Perez, R.; Ando, S. *Cancer Research* **1996,** *56*, 5165-5171.

21. Pender, M. P.; Greer, J. M. *Current Allergy and Asthma Reports* **2007,** *7*, 285-292.

22. Miyagi, T.; Yamaguchi, K. *Glycobiology* **2012,** *22*, 880-896.

23. Taeko, M. *Trends in Glycoscience and Glycotechnology* **2010,** *22*, 162-172.

24. Cairo, C. W. *Medchemcomm* **2014,** *5*, 1067-1074.

25. Kakugawa, Y.; Wada, T.; Yamaguchi, K.; Yamanami, H.; Ouchi, K.; Sato, I.; Miyagi, T. *Proceedings of the National Academy of Sciences* **2002,** *99*, 10718-10723.

26. Miyagi, T.; Wada, T.; Yamaguchi, K.; Hata, K. *Glycoconjugate Journal* **2004,** *20*, 189-98.

27. Kato, K.; Shiga, K.; Yamaguchi, K.; Hata, K.; Kobayashi, T.; Miyazaki, K.; Saijo, S.; Miyagi, T. *Biochemical Journal* **2006,** *394*, 647-656.

28. Miyagi, T. *Proceedings of the Japan Academy Series B-Physical and Biological Sciences* **2008,** *84*, 407-418.

29. Wada, T.; Yoshikawa, Y.; Tokuyama, S.; Kuwabara, M.; Akita, H.; Miyagi, T. *Biochemical and Biophysical Research Communications* **1999,** *261*, 21-27.

30. Ha, K. T.; Lee, Y. C.; Cho, S. H.; Kim, J. K.; Kim, C. H. *Molecules and Cells* **2004,** *17*, 267-273.

31. Azuma, Y.; Sato, H.; Higai, K.; Matsumoto, K. *Biological & Pharmaceutical Bulletin* **2007,** *30*, 1680-1684.

32. Miyagi, T.; Wada, T.; Iwamatsu, A.; Hata, K.; Yoshikawa, Y.; Tokuyama, S.; Sawada, M. *Journal of Biological Chemistry* **1999,** *274*, 5004-5011.

33. Wang, Y.; Yamaguchi, K.; Shimada, Y.; Zhao, X. J.; Miyagi, T. *European Journal of Biochemistry* **2001,** *268*, 2201-2208.

34. Lopez, P. H. H.; Schnaar, R. L. *Methods in Enzymology* **2006,** *417*, 205-220.

35. Song, X.; Heimburg-Molinaro, J.; Cummings, R. D.; Smith, D. F. *Current Opinion in Chemical Biology* **2014,** *18*, 70-77.

36. Feizi, T. *Annals of the New York Academy of Sciences* **2013,** *1292*, 33-44.

37. Palma, A. S.; Feizi, T.; Childs, R. A.; Chai, W.; Liu, Y. *Current Opinion in Chemical Biology* **2014,** *18*, 87-94.

38. Rinaldi, S.; Schiavo, G.; Crocker, P. R.; Willison, H. J.; Brennan, K. M.; Goodyear, C. S.; O'Leary, C. *Glycobiology* **2009,** *19*, 789-796.

39. Arigi, E.; Blixt, O.; Buschard, K.; Clausen, H.; Levery, S. B. *Glycoconjugate Journal* **2012,** *29*, 1-12.

40. Grant, O. C.; Smith, H. M. K.; Firsova, D.; Fadda, E.; Woods, R. J. *Glycobiology* **2014,** *24*, 17-25.

41. Campanero-Rhodes, M. A.; Smith, A.; Wengang, C.; Sonnino, S.; Mauri, L.; Childs, R. A.; Yibing, Z.; Ewers, H.; Helenius, A.; Imberty, A.; Feizi, T. *Journal of Virology* **2007,** *81*, 3-3.

42. Stowell, S. R.; Leffler, H.; Smith, D. F.; Cummings, R. D.; Blixt, O.; Arthur, C. M.; Mehta, P.; Slanina, K. A. *Journal of Biological Chemistry* **2008,** *283*, 10109-10123.

43. Czogalla, A.; Grzybek, M.; Jones, W.; Coskun, Ü. *BBA - Molecular & Cell Biology of Lipids* **2014,** *1841*, 1049-1059.

44. Cho, H.; Wu, M.; Bilgin, B.; Walton, S. P.; Chan, C. *Proteomics* **2012,** *12*, 3273-3282.

45. Sanghera, N.; Correia, Bruno E. F. S.; Correia, Joana R. S.; Ludwig, C.; Agarwal, S.; Nakamura, Hironori K.; Kuwata, K.; Samain, E.; Gill, Andrew C.; Bonev, Boyan B.; Pinheiro, Teresa J. T. *Chemistry and Biology* **2011,** *18*, 1422-1431.

46. Shi, J.; Yang, T.; Kataoka, S.; Zhang, Y.; Diaz, A. J.; Cremer, P. S. *Journal of the American Chemical Society* **2007,** *129*, 5954-5961.

47. Rao, C. S.; Lin, X.; Pike, H. M.; Molotkovsky, J. G.; Brown, R. E. *Biochemistry* **2004,** *43*, 13805-13815.

48. Chen, W. C.; Kawasaki, N.; Nycholat, C. M.; Han, S.; Pilotte, J.; Crocker, P. R.; Paulson, J. C. *Public Library of Science One* **2012,** *7,* 1-9.

49. Jayaraman, N.; Maiti, K.; Naresh, K. *Chemical Society Reviews* **2013,** *42*, 4640-4656.

50. Nath, A.; Atkins, W. M.; Sligar, S. G. *Biochemistry* **2007,** *46*, 2059-2069.

51. Bayburt, T. H.; Sligar, S. G. *Febs Letters* **2010,** *584*, 1721-1727.

52. Denisov, I. G.; Grinkova, Y. V.; Lazarides, A. A.; Sligar, S. G. *Journal of the American Chemical Society* **2004,** *126*, 3477-3487.

53. Borch, J.; Torta, F.; Sligar, S. G.; Roepstorff, P. *Analytical Chemistry* **2008,** *80*, 6245-6252.

54. Zhang, Y.; Liu, L.; Daneshfar, R.; Kitova, E. N.; Li, C.; Jia, F.; Cairo, C. W.; Klassen, J. S. *Analytical Chemistry* **2012,** *84*, 7618-7621.

55. Leney, A. C.; Fan, X.; Kitova, E. N.; Klassen, J. S. *Analytical Chemistry* **2014,** *86*, 5271-5277.

56. Sloan, C. D. K.; Marty, M. T.; Sligar, S. G.; Bailey, R. C. *Analytical Chemistry* **2013,** *85*, 2970-2976.

57. Locatelli-Hoops, S.; Remmel, N.; Klingenstein, R.; Breiden, B.; Rossocha, M.; Schoeniger, M.; Koenigs, C.; Saenger, W.; Sandhoff, K. *Journal of Biological Chemistry* **2006,** *281*, 32451-32460.

58. Popovic, K.; Holyoake, J.; Pomes, R.; Prive, G. G. *Proceedings of the National Academy of Sciences of the United States of America* **2012,** *109*, 2908-2912.

59. Schulze, H.; Sandhoff, K. *Biochimica Et Biophysica Acta-Molecular and Cell Biology of Lipids* **2014,** *1841*, 799-810.

60. Albohy, A.; Li, M. D.; Zheng, R. B.; Zou, C.; Cairo, C. W. *Glycobiology* **2010,** *20*, 1127-1138.

61. Sandbhor, M. S.; Soya, N.; Albohy, A.; Zheng, R. B.; Cartmell, J.; Bundle, D. R.; Klassen, J. S.; Cairo, C. W. *Biochemistry* **2011,** *50*, 6753-6762.

62. Mehrotra, K. N.; Dauterman, W. C. *Journal of Neurochemistry* **1963,** *10*, 119-129.

63. Roberts, M. F.; Adamich, M.; Robson, R. J.; Dennis, E. A. *Biochemistry* **1979,** *18*, 3301-3308.

64. Sato, K.; Hanagata, G.; Kiso, M.; Hasegawa, A.; Suzuki, Y. *Glycobiology* **1998,** *8*, 527-532.

65. Li, S. C.; Li, Y. T.; Moriya, S.; Miyagi, T. *Biochemical Journal* **2001,** *360*, 233-237.

Chapter 3

1. Nogales, E.; Wolf, S. G.; Downing, K. H. *Nature* **1998,** *391*, 199-203.

2. Bryan, J.; Wilson, L. *Proceedings of the National Academy of Sciences* **1971**, *68*, 1762-1766.

3. Akhmanova, A.; Steinmetz, M. O. *Nature Reviews Molecular Cell Biology* **2008,** *9*, 309-322.

4. Nogales, E.; Wang, H.-W. *Current Opinion in Cell Biology* **2006,** *18*, 179-184.

5. Calligaris, D.; Verdier-Pinard, P.; Devred, F.; Villard, C.; Braguer, D.; Lafitte, D. *Cellular and molecular life sciences* **2010,** *67*, 1089-1104.

6. Lewis, S. A.; Wang, D.; Cowan, N. J. *Science* **1988**, *11*, 936-939.

7. Sullivan, K. F.; Cleveland, D. W. *Proceedings of the National Academy of Sciences* **1986**, *83*, 4327-4331.

8. Ballestrem, C.; Magid, N.; Zonis, J.; Shtutman, M.; Bershadsky, A. In Interplay between the Actin Cytoskeleton, Focal Adhesions and Microtubules, Ridley, A.; Peckham, M.; Clark, P., Eds. Chichester, Wiley: **2004**; pp 75-99.

9. Mane, J. Y.; Semenchenko, V.; Perez-Pineiro, R.; Winter, P.; Wishart, D.; Tuszynski, J. A. *Chemical Biology & Drug Design* **2013,** *82*, 60-70.

10. Kline-Smith, S. L.; Walczak, C. E. *Molecular Cell* **2004,** *15*, 317-327.

11. Wilson, L.; Panda, D.; Ann Jordan, M. *Cell Structure and Function* **1999,** *24*, 329-335.

12. Schiff, P. B.; Fant, J.; Horwitz, S. B. *Nature* **1979,** *277*, 665-667.

13. Bollag, D. M.; McQueney, P. A.; Zhu, J.; Hensens, O.; Koupal, L.; Liesch, J.; Goetz, M.; Lazarides, E.; Woods, C. M. *Cancer Research* **1995,** *55*, 2325-2333.

14. Canales, A.; Rodriguez-Salarichs, J.; Trigili, C.; Nieto, L.; Coderch, C.; Andreu, J. M.; Paterson, I.; Jimenez-Barbero, J.; Diaz, J. F. *American Chemical Society Chemical Biology* **2011,** *6*, 789-799.

15. Wilmes, A.; Bargh, K.; Kelly, C.; Northcote, P. T.; Miller, J. H. *Molecular Pharmaceutics* **2007,** *4*, 269-280.

16. Bhattacharyya, B.; Panda, D.; Gupta, S.; Banerjee, M. *Medicinal research Reviews* **2008,** *28*, 155-183.

17. Gigant, B.; Wang, C.; Ravelli, R. B. G.; Roussi, F.; Steinmetz, M. O.; Curmi, P. A.; Sobel, A.; Knossow, M. *Nature* **2005**, 519-522.

18. Bai, R.; Pettit, G. R.; Hamel, E. *Biochemical Pharmacology* **1990,** *39*, 1941-1949.

19. Anderson, H. J.; Coleman, J. E.; Andersen, R. J.; Roberge, M. *Cancer Chemotherapy And Pharmacology* **1997,** *39*, 223-226.

20. Jordan, M. A.; Wilson, L. *Nature Reviews Cancer* **2004,** *4*, 253-265.

21. Ravelli, R. B. G.; Gigant, B.; Curmi, P. A.; Jourdain, I.; Lachkar, S.; Sobel, A.; Knossow, M. *Nature* **2004,** *428*, 198-202.

22. Schlesinger, N.; Schumacher, R.; Catton, M.; Maxwell, L. *The Cochrane Library* **2006,** 1-16.

23. Richette, P.; Bardin, T. *Expert Openion on Pharmacotheraphy* **2010,** *11*, 2933-2938.

24. Dustin, P., Microtubules. Berlin ; New York : Springer-Verlag, **1978**.: 1978.

25. Sun, L.; Vasilevich, N. I.; Fuselier, J. A.; Coy, D. H. *Anticancer Research* **2004,** *24*, 179-186.

26. Haar, E. T.; Rosenkranz, H. S.; Hamel, E.; Day, B. W. *Bioorganic and Medicinal Chemistry* **1996,** *4*, 1659-1671.

27. Fernando Díaz, J.; Andreu, J. M. *The Journal of Biological Chemistry* **1991,** *266*, 2890-2896.

28. Menéndez, M.; Laynez, J.; Medrano, F. J.; Andreu, J. M. *The Journal Of Biological Chemistry* **1989,** *264*, 16367-16371.

29. Andreu, J. M.; Gorbunoff, M. J.; Medrano, F. J.; Rossi, M.; Timasheff, S. N. *Biochemistry* **1991,** *30*, 3777-3786.

30. Hastie, S. B. *Pharmacology & Therapeutics* **1991,** *51*, 377-401.

31. Banerjee, A.; Luduena, R. F. *The Journal Of Biological Chemistry* **1992,** *267*, 13335-13339.

32. Tahir, S. K.; Kovar, P.; Rosenberg, S. H.; Ng, S. C. *Biotechniques* **2000,** *29*, 156-160.

33. Chabin, R. M.; Hastie, S. B. *Biochemical And Biophysical Research Communications* **1989,** *161*, 544-550.

34. Loo, J. A. *Mass Spectrometry Reviews* **1997,** *16*, 1-23.

35. Daniel, J. M.; Friess, S. D.; Rajagopalan, S.; Wendt, S.; Zenobi, R. *International Journal of Mass Spectrometry* **2002,** *216*, 1-11.

36. Heck, A. J. R.; Van Den Heuvel, R. H. H. *Mass Spectrometry Reviews* **2004,** *23*, 368-389.

37. Gabelica, V.; Rosu, F.; De Pauw, E. *Analytical Chemistry* **2009**, 6708-6715.

38. El-Hawiet, A.; Shoemaker, G. K.; Daneshfar, R.; Kitova, E. N.; Klassen, J. S. *Analytical Chemistry* **2012,** *84*, 50-58.

39. Han, L.; Kitova, E.; Tan, M.; Jiang, X.; Klassen, J. *Journal of the American Society for Mass Spectrometry* **2014,** *25*, 111-119.

40. Leney, A. C.; Fan, X.; Kitova, E. N.; Klassen, J. S. *Analytical Chemistry* **2014,** *86*, 5271-5277.

41. Cheng, X.; Chen, R.; Bruce, J. E.; Schwartz, B. L.; Anderson, G. A.; Hofstadler, S. A.; Gale, D. C.; Smith, R. D.; Gao, J.; Sigal, G. B.; Mammen, M.; Whitesides, G. M. *Journal of the American Chemical Society* **1995**, 8859-8860.

42. Gao, J.; Cheng, X.; Chen, R.; Sigal, G. B.; Bruce, J. E.; Schwartz, B. L.; Hofstadler, S. A.; Anderson, G. A.; Smith, R. D.; Whitesides, G. M. *Journal Of Medicinal Chemistry* **1996,** *39*, 1949-1955.

43. Han, L.; Kitova, E. N.; Tan, M.; Jiang, X.; Klassen, J. S. *Journal Of The American Society for Mass Spectrometry* **2014,** *25*, 111-119.

44. Zhang, Y.; Liu, L.; Daneshfar, R.; Kitova, E. N.; Li, C.; Jia, F.; Cairo, C. W.; Klassen, J. S. *Analytical Chemistry* **2012,** *84*, 7618-7621.

45. El-Hawiet, A.; Kitova, E. N.; Klassen, J. S. *Analytical Chemistry* **2013,** *85*, 7637-7644.

46. Han, L.; Tan, M.; Xia, M.; Kitova, E. N.; Jiang, X.; Klassen, J. S. *Journal Of The American Chemical Society* **2014,** *136*, 12631-12637.

47. Luduena, R. F. *Molecular Biology of the Cell* **1993**, *4*, 445-457.

48. Redeker, V.; Melki, R.; Prome, D.; Le Caer, J-P.; Rossier, J. *Federation of European Biochemical Societies* **1992**, *313*, 185-192.

49. Kitova, E. N.; El-Hawiet, A.; Schnier, P. D.; Klassen, J. S. *Journal Of The American Society for Mass Spectrometry* **2012,** *23*, 431-441.

50. Wang, W. J.; Kitova, E. N.; Klassen, J. S. *Analytical Chemistry* **2005,** *77*, 3060-3071.

Chapter 4

1. Smutova, V.; Albohy, A.; Pan, X. F.; Korchagina, E.; Miyagi, T.; Bovin, N.; Cairo, C. W.; Pshezhetsky, A. V. *Public Library of Science One* **2014,** *9,* 1-10.

2. Cairo, C. W. *Medchemcomm* **2014,** *5*, 1067-1074.

3. Mane, J. Y.; Semenchenko, V.; Perez-Pineiro, R.; Winter, P.; Wishart, D.; Tuszynski, J. A. *Chemical Biology and Drug Design* **2013,** *82*, 60-70.